

Evaluating and Understanding of Bridge Scour Calculation

by

Sudan Pokharel

A thesis submitted to the Graduate Faculty of

Auburn University

in partial fulfillment of the

requirements for the Degree of

Master of Science

Auburn, Alabama

December 16, 2017

Keywords: Bridge, Hydraulics, flow

Scour, WSPRO, HEC-RAS

Approved by

Xing Fang, Chair, Arthur H. Feagin Chair Professor of Civil Engineering

Jose G. Vasconcelos, Associate Professor of Civil Engineering

J. Brian Anderson, Associate Professor of Civil Engineering

ABSTRACT

Channel scour and channel instability at bridges are the major cause of bridge collapse caused by flooding. Currently, Departments of Transportation (DOTs) in the USA use the HEC-18 procedure and associated software, which was developed for the scour depth calculation of non-cohesive soil, for scour calculation of any soil. Scour in non-cohesive soil is well known but scour in the cohesive soil is not. HEC-18 provides a deterministic procedure to calculate the scour depth near a bridge site, but the procedure and the input parameter determination have various uncertainties, calculated scour depth could be quite different in some cases. This type of uncertainty of HEC-18, i.e., the variability of both the input parameters and calculated scour depth, is dealt with in this study. The critical shear stress for scour in HEC-18 is linked with median particle-size (D_{50}) but actually related to many other factors especially for cohesive soils. HEC-18 critical shear stress and critical velocities of six clay soil samples are compared to the critical shear stress and critical velocity previously obtained from Erosion Function Apparatus (EFA) for studying the uncertainty of HEC-18 due to the soil property. The multilayer method was proposed and tested to determine the total feasible scour depth calculated using layer by layer D_{50} along the depth. Comparing with the scour depth determined using average D_{50} , which is the current normal practice by DOTs, the multilayer method can give a more reasonable prediction of scour depth but requires D_{50} values below the estimated scour depth. HEC-18 lacks clear instructions in

determining hydraulic parameters for the scour calculation in different parts of the channel cross sections. Various one-dimensional models such as WSPRO and HEC-RAS can be used to determine the hydraulics of bridges. Although these models use the standard step method to solve the energy equation for gradually varied flow, these models have their own processes to solve the energy equation that are different from each other in many ways. The HEC-RAS models for four bridge sites in Alabama were developed by using the input data of the WSPRO models to calculate the hydraulic parameters needed for HEC-18 to calculate the scour depth. The differences in the hydraulic parameters and eventual scour depths were discussed and analyzed for understanding and evaluating the uncertainty of hydraulic parameters. A step by step procedure was developed using Pugger mixer to mix the different soil components and create non-slaking soil samples for EFA testing in order to study critical shear velocity and erosion rate of cohesive soils in the future. This study confirmed that there exists certain uncertainty in HEC-18 which should be addressed, and it is better suited for calculating scour depth for non-cohesive soil. The uncertainty of predicting and estimating the scour depth comes from various sources such as soil properties (D_{50} , critical velocity and scour rate) and hydraulic parameters. EFA testing results could help to reduce uncertainty of scour calculations.

ACKNOWLEDGEMENTS

I would first like to thank my thesis advisor Dr. Xing Fang of the Samuel Ginn College of Engineering at Auburn University, for his patience and persistent support throughout this study. The door to professor Fang was always open whenever I ran into a trouble spot or had a question about my research or writing. Without him, this research wouldn't have been possible.

I would also like to thank and extend my sincere gratitude to my committee members Dr. Jose Vasconcelos and Dr. J. Brian Anderson for their valuable insights, comments, and suggestions to the study and thesis. Also, I would like to express my appreciation to Tom Flournoy, Bridge Hydraulic Engineer, for help regarding the WSPRO model and the report provided by ALDOT. I want to extend my regards to the members of HEC-RAS Users Group for providing their views on this study

Finally, I must express my very profound gratitude to my parents for providing me with unfailing support and continuous encouragement throughout my years of study. Also, I would like to thank all the colleagues in my department, who have contributed immensely to my professional and personal life at Auburn. Sincere thanks to this great source of knowledge and friendship.

TABLE OF CONTENTS

ABSTRACT.....	ii
ACKNOWLEDGEMENTS.....	iv
LIST OF TABLES.....	viii
LIST OF FIGURES.....	xi
Chapter 1 INTRODUCTION.....	1
1.1 BACKGROUND.....	1
1.2 BRIDGE SCOUR.....	5
1.3 SCOPE AND OBJECTIVE.....	13
1.4 THESIS ORGANIZATION.....	16
Chapter 2 LITERATURE REVIEW.....	18
2.1 LITERATURE REVIEW.....	18
2.2 SOIL TYPES.....	24
2.3 EROSION FUNCTION APPARATUS.....	26
2.3.1 METHODS.....	27
2.3.2 EFA RESULTS.....	28
2.1 CLEAR-WATER SCOUR IN 25 ALABAMA BRIDGES.....	29

Chapter 3 EVALUATING UNCERTAINTY IN BRIDGE SCOUR USING HEC-18 AND MEAN PARTICEL SIZE	31
3.1 INTRODUCTION	31
3.2 COMPARISON OF CRITICAL VELOCITY AND SHEAR STRESS.....	33
3.3 DISCUSSION	40
Chapter 4 MULTILAYER METHOD AND COMPARISION of SCOUR DEPTHS FROM HEC-18	42
4.1 INTRODUCTION	42
4.2 STUDY AREA	44
4.3 SITE AND SOIL INFORMATION OF SPEAR CREEK.....	50
4.4 MULTILAYER METHOD	56
4.5 RESULTS FROM MULTILAYER METHOD.....	57
4.6 SCOUR DEPTHS USING AVERAGE D_{50} WITH AND WITHOUT OUTLIERS	67
4.7 DISCUSSION.....	69
Chapter 5 COMPARISION OF HYDRAULIC PARAMETERS AND SCOUR DEPTH OBTAINED FROM WSPRO AND HEC-RAS MODEL	73
5.1 INTRODUCTION	73
5.2 METHODOLOGY	75
5.3 WSPRO INPUTS FOR HEC-RAS MODEL DEVELOPMENT	78
5.3.1 CROSS-SECTIONAL GEOMETRY	85

5.3.2 MANNING’S N VALUES	86
5.3.3 CHANNEL BANK STATIONS AND REACH LENGTHS	86
5.3.4 EFFECTIVE FLOW AREA	87
5.3.5 BRIDGE CROSSING GEOMETRY.....	87
5.3.6 CONTRACTION AND EXPANSION COEFFICIENTS.....	88
5.3.7 FINAL MODEL DEVELOPMENT	89
5.4 OUTPUT OF WSPRO	89
5.5 RESULTS OF HYDRAULIC PARAMETERS AND SCOUR DEPTHS.....	93
Chapter 6 SUMMARY AND CONCLUSIONs	111
6.1 SUMMARY	111
6.2 CONCLUSION.....	113
6.3 FUTURE STUDIES.....	117
Appendix A HEC-RAS AND WSPRO MODEL PROCEDURE AND DEVELOPMENT OF HEC-RAS MODEL FOR THE STUDY	125
Appendix B USING PUGGER MIXER TO DEVELOP SOIL SAMPLES FOR EFA TESTING	146

LIST OF TABLES

Table 1.1 Bridge failure modes.....	2
Table 1.2 Value of K_1 (after Richardson and Davis, 2001).....	10
Table 2.1 Different soil types with D_{50} value.....	24
Table 3.1: Summary of data taken from EFA.....	32
Table 3.2 Comparison of critical shear stress from EFA and HEC-18.....	35
Table 3.3 Comparison of critical velocities from EFA data and from HEC-18 ($Y = 4m$)	37
Table 3.4 Hydraulic parameters in Spear Creek from WSPRO method.....	39
Table 4.1 Boring location with station number.	52
Table 4.2 D_{50} value along depth of boring B-1, B-2, B-3, B-5	54
Table 4.3 D_{50} value along depth of boring B-1, B-2, B-3, B-5 continued	54
Table 4.4 Output from HEC-RAS	55
Table 4.5 Calculation of scour depth using multilayer method (Spear Creek).....	60
Table 4.6 Differences in scour depth using average D_{50} and the multilayer method (Spear Creek)	61
Table 4.7 Calculation of scour depth using multilayer method (Valley Creek).....	64
Table 4.8 Calculation of scour depth using multilayer method (Alamuchee Creek).....	66
Table 4.9 Calculation of scour depth at LOB using multilayer method (Pintalla Creek).....	67
Table 4.10 Comparison of scour depths in Spear Creek determined from average D_{50} without and with outliers	68

Table 4.11 Comparison of scour depth in Valley Creek determined from average D_{50} without and with outliers	68
Table 4.12 Comparison of scour depth in Alamuchee Creek determined from average D_{50} without and with outliers	69
Table 5.1 Definition of each column of XS header and its content (after WSPRO manual)	80
Table 5.2 Definition of each column of GR header and its content (after WSPRO manual)	81
Table 5.3 Definition of each column of SA header and its content (after WSPRO manual)	82
Table 5.4 Definition of each column of BR header and its content (after WSPRO manual)	83
Table 5.5 Definition of each column of CD header and its content (after WSPRO manual)	83
Table 5.6 Different bridge types	84
Table 5.7 Definition of each column of HP header and its content (after WSPRO manual)	85
Table 5.8 Expansion and contraction coefficients in WSPRO and HEC-RAS	89
Table 5.9 Comparison of the hydraulic parameters from WSPRO's and HEC-RAS's energy methods	95
Table 5.10 Comparison of ratios of the hydraulic parameters and scour depths from WSPRO and HEC-RAS's energy method at overbank areas (LOB and ROB)	98
Table 5.11 Comparison of ratios of the hydraulic parameters and scour depths from WSPRO's and HEC-RAS's energy method at channel	100
Table 5.12 Comparison of the hydraulic parameters and scour depth from Energy method and WSPRO method of HEC-RAS model using same contraction and expansion coefficient as HEC-RAS methodology	102
Table 5.13 Comparison of the hydraulic parameters and scour depth from HEC-RAS WSPRO method using different contraction and expansion coefficient	103
Table 5.14 Ranges of expansion ratio	104
Table 5.15 Change in scour depth with the change in minimum expansion and contraction length using HEC-RAS model	106

Table 5.16 Change in scour depth with the change in maximum expansion and contraction length using HEC-RAS model.....	107
Table 5.17 Change in scour depth with and without including ineffective flow area using HEC-RAS model with WSPRO method.....	108
Table 5.18 Comparison of simulated water surface elevations between WSPRO and HEC-RAS models.....	110
Table A.1 Velocity indexes (Pintalla Creek)	145
Table A.2 Channel contraction ratio (Pintalla Creek)	145
Table B.1 Percentage mixture of two soil samples.....	154
Table B.2 Properties of soil samples prepared by the pugger mixer	154
Table B.3 Calculation of shear stress and scour rate for sample 1	159
Table B.4 Calculation of shear stress and scour rate for the sample 2	161
Table B.5 Critical velocity and shear stress of two soil samples determined using EFA.....	164
Table B.6 Comparison of critical shear stress from EFA and HEC-18	165
Table B.7 Comparison of critical velocities for two soil sample from EFA and HEC-18	165

LIST OF FIGURES

Figure 1.1 Bridge failure in Schoharie Creek	3
Figure 1.2 Bridge failure in Hatchie River	3
Figure 1.3 Sketch of different scour types (Briaud et al. 2009).....	6
Figure 1.4 Layout of cross-section for modeling bridges (after US Army Corps of Engineers, 2002)	9
Figure 1.5 Step by step procedure of calculation of contraction scour in HEC-18.	12
Figure 2.1 Erosion Function Apparatus to measure erodibility (Briaud et al. 1999).....	27
Figure 2.2 Comparison of observed and theoretical scour depth (Lee and Hedgecock 2008)	30
Figure 3.1 Hypothetical particle size distributions with the same D_{50}	41
Figure 4.1 Location of Spear Creek and bridge site characteristics.	46
Figure 4.2 Location of Valley Creek and bridge site characteristics.....	47
Figure 4.3 Location of Pintalla Creek and bridge site characteristics.	48
Figure 4.4 Location of Alamuchee Creek and bridge site characteristics.	49
Figure 4.5 Cross-section of the bridge at Spear Creek with station number.	50
Figure 4.6 Plan view of the bridge side with boring location (Spear Creek).....	51
Figure 4.7 D_{50} values along depth of boring stations (also tabulated in Table 4.2 and Table 4.3)	53
Figure 4.8 Flow chart for multilayer method.....	57
Figure 4.9 Bar diagram showing difference in scour depth using average D_{50} and the multilayer method.....	62

Figure 4.10 Bar diagram showing the difference in scour depth from using average D_{50} and multilayer.	65
Figure 5.1 Input data format of WSPRO	79
Figure 5.2 Bridge geometry of Spear Creek in HEC-RAS.....	88
Figure 5.3 Cross-sectional properties output from WSPRO (Spear Creek)	91
Figure 5.4 Comparison of scour depth from WSPRO and HEC-RAS (energy method).....	100
Figure A.1 Definition sketch of cross-section locations used in WSPRO for a single opening bridge	127
Figure A.2 Cross-section location at bridge (HEC-RAS).....	132
Figure A.3 Representation of terms of energy equation	133
Figure A.4 Envelope curve of observed clear-water contraction-scour depths based on the velocity index at selected sites in the Black Prairie Belt of the Coastal Plain of Alabama (Lee and Hedgecock 2008)	138
Figure A.5 Location of physiographic provinces in Alabama (Lee and Hedgecock 2008)	139
Figure A.6 Definition sketch of variable used (Velocity Index)	140
Figure A.7 Envelope curve of observed clear-water contraction-scour depths based on the channel-contraction ratio at selected sites in the Black Prairie Belt of the Coastal Plain of Alabama (Lee and Hedgecock 2008).....	142
Figure A.8 Definition sketch of variable used (Channel-contraction ratio)	143
Figure B.1 Peter pugger mixer.....	150
Figure B.2 Assembly of Peter pugger.....	150
Figure B.3 Particle size distribution of Ottawa sand	153
Figure B.4 Particle size distribution of two soil samples.....	154
Figure B.5 Holding Shelby tube to transfer soil from pugger	155
Figure B.6 Auburn University EFA.....	156

Figure B.7 Uneven scour of the soil sample	158
Figure B.8 Velocity-based erosion function for sample 1	160
Figure B.9 Shear stress based erosion function for sample 1	160
Figure B.10 Velocity based erosion function	162
Figure B.11 Shear stress based erosion function	162
Figure B.12 Example of data recorded by computer during an EFA test.....	163

Chapter 1 INTRODUCTION

1.1 BACKGROUND

A bridge is a structure that is built over a railroad, water body, or road so that people or vehicles can cross from one side to the other. In the context of civil engineering, a bridge is defined as a structure built to span physical obstacles without closing the way underneath such as a body of water, valley, or road, for providing passage over the obstacle. Per the Merriam Webster dictionary, hydraulics is a branch of science that deals with practical application (such as the transmission of energy or the effects of flow) of liquid such as water in motion. At many locations, either a bridge or a culvert will fulfill both the structural and hydraulic requirements for the stream crossing. A hydrologic and hydraulic analysis is required for designing all new bridges over waterways, bridge widening, bridge replacement, and roadway profile modification that may adversely affect the floodplain even if no structural modification are necessary.

According to the Federal Highway Administration (FHWA), in 2009, there are approximately 603,000 bridges in the national bridge inventory. Out of 603,000 bridges, roughly 83 percent are over water (Lagasse 2007). Water when flows in its path is not a disaster but when it overflows from its path it causes a disaster called flooding. Flooding can be defined as an overflowing of a large amount of water beyond its normal confines, especially over what is normally a dry land. Flooding is the most common natural disaster. The Federal Emergency Management Agency (FEMA) states that about 90 percent of presidential disaster declarations involves flooding as a major component (FEMA, 1996).

Scour is a phenomenon which is caused due to the high flow of water in and around the water bodies; in this study, the scour around the bridge area was evaluated. Therefore, it can be defined as removal of sediments such as sand and rock from around bridge abutments or piers. With 83 percent of the bridges crossing over the water, scour is a major concern with a high flow of water. More than half of all bridge failures were caused by hydraulic factors (Shirole and Holt 1991). Modes of hydraulic factors include scour, channel movement, debris or ice jam buildup, and embankment erosion due to overtopping. There doesn't appear to be a central data base anywhere in the U.S. that can provide comprehensive information about bridge failure. The New York Department of Transportation (DOT) compiled a nationwide list of bridge failures and reported them by categories since 1950 for a time period of 41 years (Shirole and Holt 1991) as shown in Table 1.1.

Table 1.1 Bridge failure modes.

Failure Type	Number of failures	Percentages (%)
Hydraulics	494	60
Collision	108	13
Overload	84	10
Fire	24	3
Earthquake	14	2
Other	99	12
Total	823	100

In past, history shows that there were many bridge failures due to scour. Some examples of bridge failure are, the bridge in Schoharie Creek (Figure 1.1) which is in the northwest of Albany, New York. The bridge was constructed in 1954 and was collapsed on 1987 due to scour underneath pier 3. This bridge failure caused 10 fatalities with the loss of property. A bridge

located in Covington, Tennessee over Hatchie River was constructed in 1936. It collapsed in 1989 due to scour (Figure 1.2). There were 8 fatalities. From Table 1.1 and the histories of bridge failure, it is well known that scour is a major cause of bridge failure.



Figure 1.1 Bridge failure in Schoharie Creek

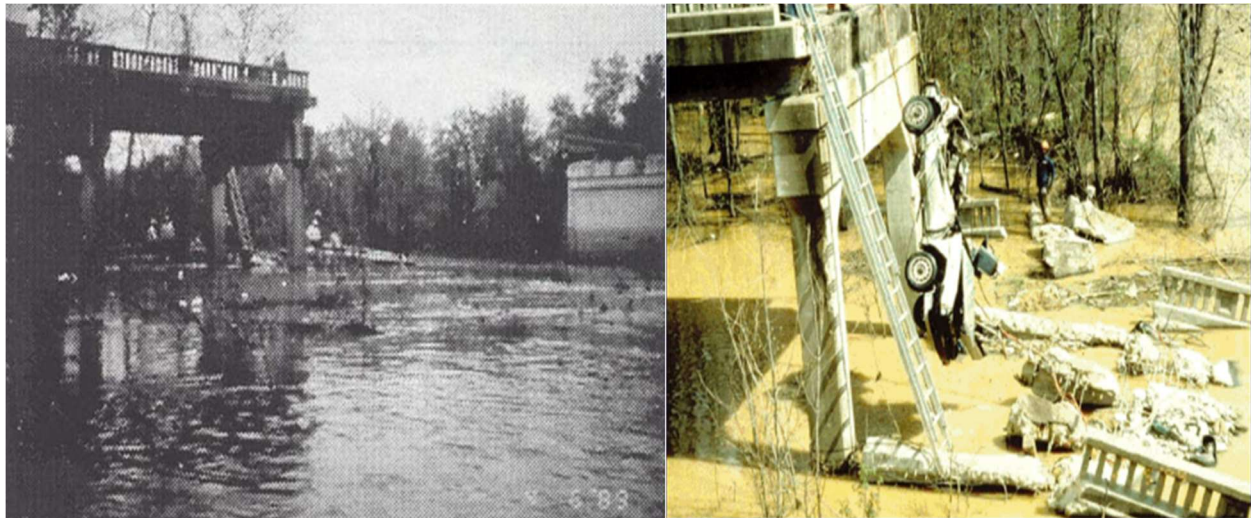


Figure 1.2 Bridge failure in Hatchie River¹

¹ The above figures and data were taken from Ms. Alacyia Hall, ALDOT, Presented at the 53rd annual transportation conference, February 23, 2010

Currently, DOTs are using the procedures presented in Hydraulic Engineering Circular 18 (Arneson et al. 2012) abbreviated as HEC-18, and Hydraulic Engineering Circular 20 or HEC-20 (Lagasse et al. 2012) to calculate the bridge scour. These reports were published by the Federal Highway Administration (FHWA). These reports recommend estimating the scour depth based on four major variables: channel configuration, stream velocity, soil grain size, and underlying bed material. FHWA developed a Hydraulic Toolbox (current version 4.2 released in 2014, <https://www.fhwa.dot.gov/engineering/hydraulics/software/toolbox404.cfm>) for DOT engineers to perform various hydraulic calculations. The Hydraulic Toolbox has scour calculators that follow the HEC-18 procedures. In this thesis, FHWA's scour calculators were used to calculate the scour depth. Since the scour calculators just mathematically implement the HEC-18 procedures, in this study the scour calculators are also simply called as HEC-18. In professional practices, actually, DOT engineers use HEC-18 to mean for the HEC-18 procedure, report and associated software (scour calculators). Hydraulic parameters required for HEC-18 were calculated or modeled using either the Water Surface Profile (WSPRO) computer program (Arneson and Shearman 1998) or the Hydrologic Engineering Center-River Analysis System (HEC-RAS) program (Brunner 2001) and then manually inputted to HEC-18 for calculating the scour depth. From the version 3.0.1 (current version is 5.03) of HEC-RAS, the HEC-18 procedures were also implemented in HEC-RAS as one of the Hydraulic Design Functions – Bridge Scour, which automatically takes hydraulic parameters modeled by HEC-RAS for calculating the scour depth.

1.2 BRIDGE SCOUR

There are two major components of the bridge scour. One is general scour, and another is local scour. General scour is the accumulation (aggradation) or degradation (removal) of the riverbed material and is not related to the bridge or the presence of the local obstacles. Aggradation can be defined as the gradual accumulation of the sediments on the river bed. In contrast, degradation is the gradual removal of the sediments from the riverbed. Local scour is the erosion of soil around obstacles to the water flow, such as those imposed by a bridge (Akan 2011). Local scour can be divided into three components as shown in Figure 1.3

- Contraction scour
- Pier scour
- Abutment scour

Contraction scour can be defined as the removal of sediment from the riverbed due to the contraction of stream channel either naturally or created by the bridge approach embankment and bridge piers. Pier scour is the removal of the soil around the foundation of a pier. Abutment scour is the removal of soil around an abutment at the junction between a bridge and embankment.

There are two types of contraction scour: the clear-water and live-bed scour. When there is no movement of bed materials in the flow upstream of the bridge or when the upstream flow velocity is less than the critical velocity, the clear-water scour occurs. In contrast, when there is a movement of bed materials from the upstream reach to the bridge section at a significant rate and the flow velocity is greater than critical velocity, the live-bed scour occurs (Arneson et al. 2012).

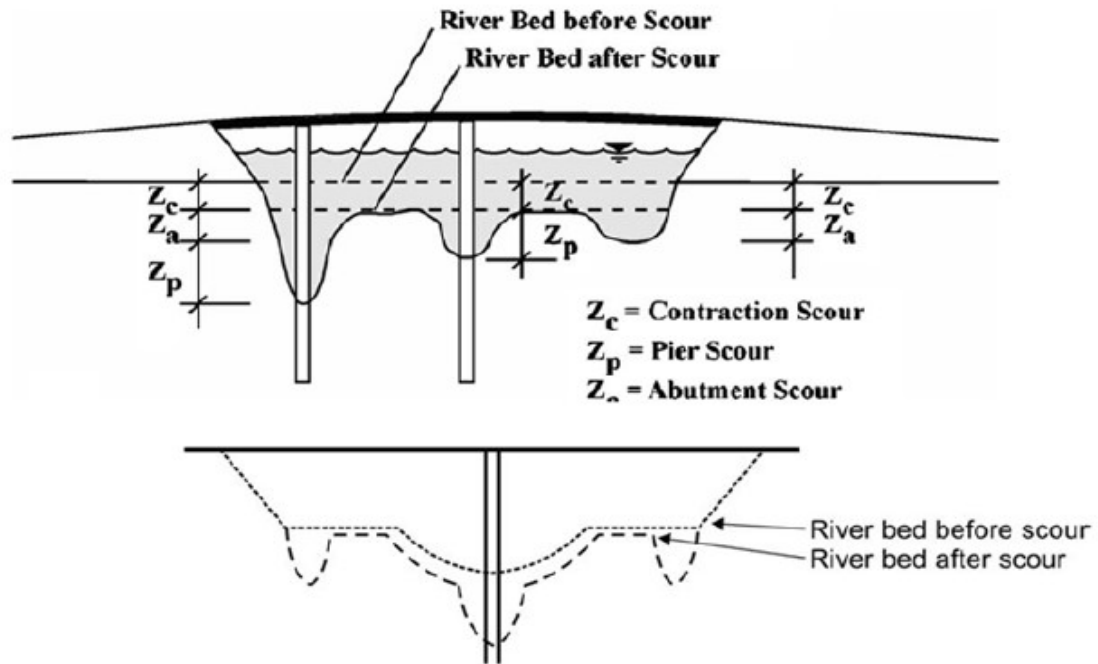


Figure 1.3 Sketch of different scour types (Briaud et al. 2009)

Critical velocity can be defined as the velocity above which the bed material of a specified size and smaller will be transported. Critical velocity is one of the criteria to determine either the scour is a livebed or clear-water scour. Equation (1.1) is used to calculate the critical velocity in HEC-18.

$$V_c = K_u y^{1/6} D_{50}^{1/3} \quad (1.1)$$

where y = average depth upstream of the bridge, D_{50} = mean particle size, K_u = correction factor = 6.19 $m^{1/2}/s$ or 11.17 $ft^{1/2}/s$

Most of the current literature has mostly focused on local scour, which is divided into the three components as mentioned above. An overview of the scour evaluation process for contraction scour and pier or abutment scour is given below.

The literature presents various methods for estimating the contraction scour including regime equations, hydraulic-geometry equations, numerical sediment-transport models, and contraction scours equations (Zhang et al. 2013).

Regime and hydraulic-geometry equations are empirical equations that are used to assess changes in channel geometry for given hydraulic conditions. Numerical sediment-transport models combine various sediment-transport equations with numerical hydraulic models to simulate scour process in streams. The literature shows that the various sediment-transport equations provide significantly different estimates of sediments discharge for the same site. To assure that the results from the numerical models are reasonable, the model should be calibrated and verified with observed field data. However, sediment transport models are rarely used to estimate the contraction scour because of the time and cost associated with data collection necessary to construct, calibrate and verify these models. Also, the literature describes a number of semi-empirical contraction scour equations that were developed using laboratory tests (Zhang et al. 2013).

Similarly, many analytical equations have been primarily derived for pier and abutment scours from the observation obtained from small-scale physical model studies conducted in laboratory flumes (Zhang et al. 2013). The empirical equations were developed from envelope curves or a regression analysis of dimensionless variables obtained from laboratory investigations. Several other equations were derived from field observations which were not valid or may not be applicable to other sites.

There are different existing methods which are developed to predict the scour depth (Zhang et al. 2013). In past decades, significant efforts and resources have been devoted by the FHWA, state DOTs, and academic institutions to study bridge scour. Many research has been done to figure out the scour in the bridge, but all DOTs are not using the same design method for determining the scour depth. Scour depths at a bridge cross sections are the function of stream hydraulic conditions, sediment transport by flowing water, streambed sediment properties, bridge structure dimensions and time. Numerous models and equations were developed from numerous studies. But none of the equations/models developed can accurately predict the scour depth without the aid of engineering judgment.

The most widely used model is HEC-18 recommended by FHWA for calculation of the scour depth. HEC-18 was developed by assuming a uniform, unstratified, non-cohesive sediments that are representative of the most severe scour condition. But on contrary, the soils found at different bridge sites could be the combination of stratified soils with varying degree of cohesiveness.

HEC-18 method uses a peak discharge during a flood event to calculate the hydraulic parameters needed to calculate the scour. Mainly, 100-year discharge is used but also 500-year discharge can be used with a factory of safety. These discharge data can be obtained from the US Geological Survey (USGS) or calculated using regression equations developed by USGS. After getting the flood discharge data hydraulic analysis is performed by using USGS or FHWA' s WSPRO computer program or U.S Army Corps of Engineer (USACE) HEC-RAS program. The equations that are used in HEC-18 were primarily developed based on laboratory small-scale flume studies on a uniform non-cohesive soil. Thus, it can be said that HEC-18 method tends to

overestimate the scour depth as there is the presence of stratified soil with varying cohesion in real bridge site. This uncertainty of HEC-18 is further discussed in a later chapter in details.

Contraction scour as described earlier can be a live-bed or clear-water contraction scour. The live-bed contraction scour occurs when the bed material is being transported from the upstream section of the bridge (Laursen 1962). In Figure 1.4, BU and BD are the automatically created cross-sections inside the bridge by HEC-RAS after a simulation is run. BU is the cross-section passing through the upstream edge of the bridge deck but below the cross-section 3. BD is the cross-section passing through the downstream edge of the bridge deck but just above cross-section 2.

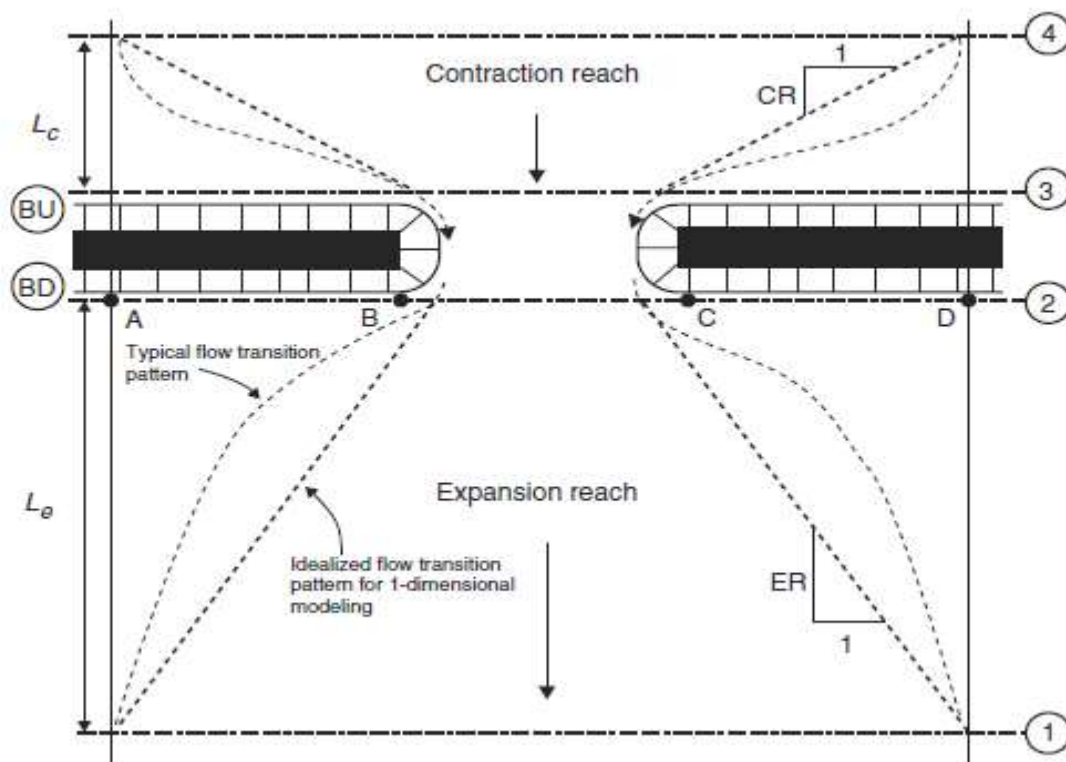


Figure 1.4 Layout of cross-section for modeling bridges (after US Army Corps of Engineers, 2002)

Equation (1.2) is used by HEC-18 to calculate the live-bed contraction scour.

$$y_s = y_4 \left(\frac{Q_{BU}}{Q_4} \right)^{6/7} \left(\frac{W_4}{W_{BU}} \right)^{K_1} - y_{BU} \quad (1.2)$$

where

y_s = Scour depth

y_4 = Average depth upstream of the bridge (at the approach section 4 in Figure 1.4)

Q_{BU} = Discharge at contraction section (section BU in Figure 1.4)

Q_4 = Discharge at the upstream section

W_4 = Width upstream of the bridge

W_{BU} = Width at the contraction section

y_{BU} = Average depth prior to scour at the contraction section

K_1 = exponential coefficient (Table 1.2)

The value of K_1 depends upon the ratio of shear velocity (V^*) to sediment settling velocity also known as fall velocity (w). The shear velocity, calculated as $(gY_4S_{f4})^{1/2}$ (g is the acceleration due to gravity), depends upon the slope of energy grade line (S_{f4}). The fall velocity depends on the D_{50} value of the bed material and water temperature

Table 1.2 Value of K_1 (after Richardson and Davis, 2001)

$\frac{V^*}{w}$	K_1	Mode of bed material transport
<0.50	0.59	Mostly contact bed material discharge
0.50 to 2.0	0.64	Some suspended bed material discharge
>2.0	0.69	Mostly suspended bed material discharge

The clear-water scour equation (1.3) used in HEC-18 is derived from the bed shear stress concept by Laursen (1962).

$$y_s = \left(\frac{Q_{BU}^2}{C_u D_m^{2/3} W_{BU}^2} \right)^{3/7} - y_{BU} \quad (1.3)$$

where

y_s = Scour depth

Q_{BU} = Discharge at the contraction section (bridge crossing, i.e., BU and BD)

W_{BU} = Width at the contraction section

y_{BU} = Average depth prior to scour at the contraction section

$D_m = 1.25D_{50}$

$C_u = 40 \text{ m/s}^2$ or 130 ft/s^2

Figure 1.5 shows the step by step procedure of calculation of contraction scour in HEC-18. In the flow chart, V_4 is the upstream cross-section velocity. The upstream velocity (V_4) is compared with the critical velocity (V_c) to determine the scour either as live bed or clear-water contraction scour.

The local scour at piers is caused by horseshoe vortices forming at the base of the pier. The local scour at piers is a function of bed material characteristics, bed configuration, flow characteristics, fluid properties, and the geometry of the pier and footing. The local scour at pier was not studied here and more information is provided by Richardson and Davis (2001).

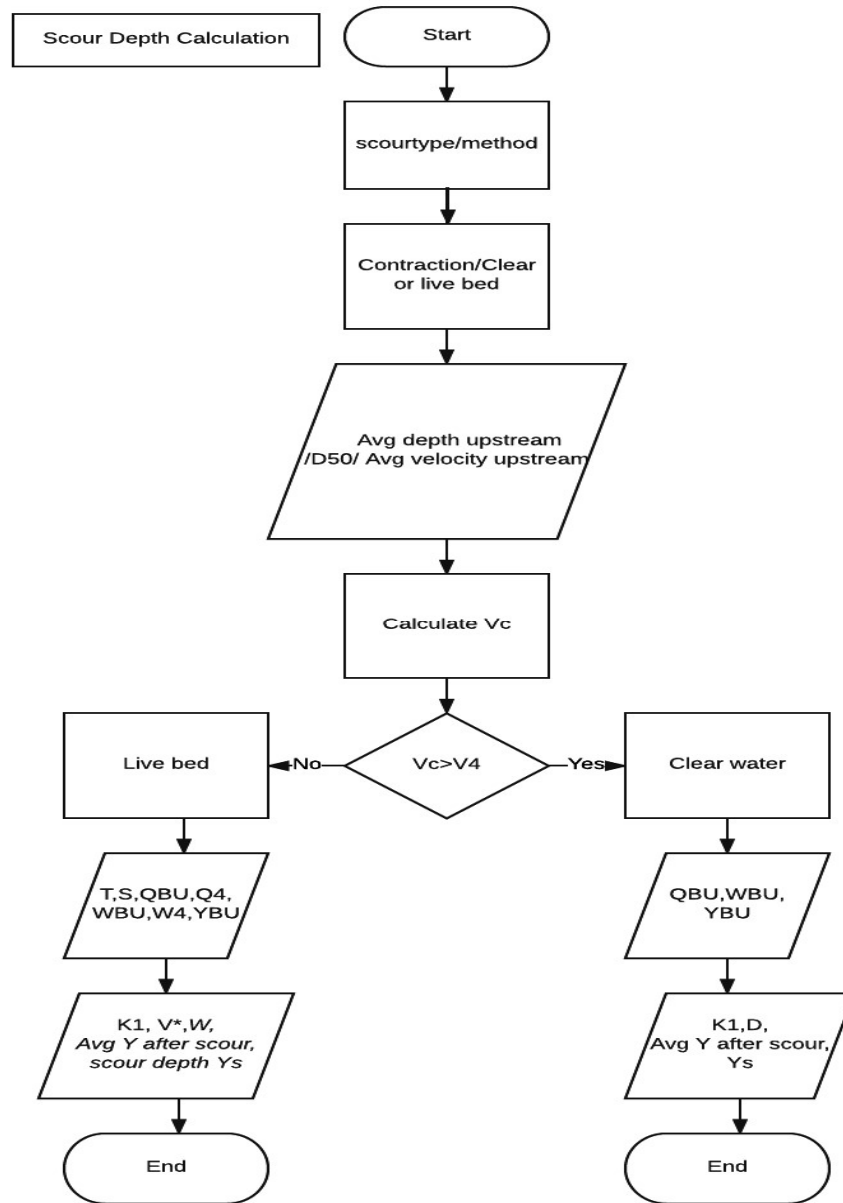


Figure 1.5 Step by step procedure of calculation of contraction scour in HEC-18.

1.3 SCOPE AND OBJECTIVE

The goal of this study was to understand, evaluate and confirm some uncertainties in HEC-18 procedures and recommend a better method (multilayer method) to determine the scour depth at bridge sites. Alabama Department of Transportation (ALDOT) is using HEC-18 to calculate the scour depth for both cohesive and non-cohesive soils which are different in many ways. ALDOT provided four bridge cases for the study. For all the bridge cases, the scour depth was calculated using HEC-18 which uses average D_{50} to determine the scour type. Also, ALDOT provided the input and output files of WSPRO models for these bridge sites. To calculate the scour depth from HEC-18 different hydraulic parameters were needed. The input and output files of WSPRO were used to build HEC-RAS models of four bridges sites. The hydraulic parameters using two computer models WSPRO and HEC-RAS were calculated, compared and evaluated.

In today's world, there are several hydraulic tools available in use for bridge hydraulic modeling. Each of the various methods provides its own set of guidelines and assumptions for operation. Each of the methods may give a different output depending upon the way of calculation and the set of guidelines. The objective of the study was to suggest and assist bridge engineers to use the better method from many methods available by illustrating the uncertainties in HEC-18. Since RAS is newest and seemingly popular in hydraulic modeling most of the calculation in this study was done using RAS model. RAS provides six different methods to calculate the water surface profiles through a bridge reach. Some of the methods are compared as it is directly related to calculating the hydraulic parameters which at last can alter the scour depth. Also, to get the same output as provided by ALDOT, WSPRO is also used in this study.

HEC-18 provides a deterministic (not stochastic) procedure to calculate the scour depth near a bridge site. Therefore, one should expect the same prediction on the scour depth at the same

bridge site by different designers and engineers. If the procedure and the input parameter determination have various uncertainties, calculated scour depth could be quite different in some cases. This is the uncertainty that this study deals with. Specifically, the study examines the variability of input parameters and calculated scour depth. These modeling choices and resulting parameters have an impact on the range of possible results (e.g., anticipated variability in calculated scour depth) from the applications of the HEC-18 procedure. This is not a sensitivity analysis on model inputs even the study does examine impacts of input parameters on the scour depth prediction/estimation. Scour depth for bridge design is unknown so that it is impossible to quantify uncertainty by comparing calculated with observed scour depth. For 25 Alabama bridge sites studied by USGS (Lee and Hedgecock 2008), even we have both observed and theoretically calculated scour depths, the information cannot be directly used to compare with scour depths in this study (six soil samples collected in the field presented in Chapter 3 and four bridge study sites presented in Chapters 4 and 5).

The specific objectives of this study are listed as follows:

1. To understand and evaluate some uncertainties in HEC-18 using the median particle size (D_{50}) for calculation of scour depth (contraction scour only).
2. To propose and test a multilayer method for determining total feasible scour depth and compare with the scour depths determined from HEC-18 (using average D_{50}).
3. To understand the process of calculation of water surface profiles and associated hydraulic parameters using WSPRO and HEC-RAS model and develop HEC-RAS models of four bridge sites for the study.

4. To compare the different hydraulic parameters obtained from the WSPRO model and the HEC-RAS model and then corresponding scour depths using HEC-18 to evaluate the uncertainty of HEC-18 in scour calculation from hydraulic parameters

To accomplish the objective 1 the following tasks were completed:

1. Critical shear stresses from HEC-18 and determined using EFA for six soil samples were compared.
2. Critical velocity was calculated from the critical shear stress determined from EFA and then compared with the critical velocity from HEC-18.

To accomplish the objective 2, the following tasks were completed:

1. Mean particle sizes at different layers along the depth at four bridge sites were figured out and tabulated accordingly
2. The HEC-18 simulations were performed, and scour depth was figured out using D_{50} in each layer.
3. A multilayer method was proposed and comparisons of scour depths were made between HEC-18(using average D_{50} value) and multilayer method (using layer by layer D_{50} values).

To accomplish the objective 3 following work was done:

1. An in-depth literature review was done for both WSPRO and HEC-RAS model (a part of the information is summarized in Appendix A).
2. Prepare necessary input data, such as geometry data, reach lengths, contraction and expansion coefficients, bridge geometry form the WSPRO input to develop HEC-RAS model for each bridge site

3. Simulate flow distribution and water surface profile, obtain hydraulic parameters needed to calculate scour depth

To accomplish the objective 4, the following tasks were completed:

1. Hydraulic simulation at bridge sites was done using WSPRO and HEC-RAS
2. Different hydraulic parameters needed for scour depth calculation were extracted and compared
3. Scour depths from WSPRO and RAS's hydraulic parameters were calculated using HEC-18 procedure and compared.

1.4 THESIS ORGANIZATION

This thesis is divided into six chapters and two appendixes. Chapter 1 covers background, scope, objectives, and overall thesis organization. Chapter 2 covers literature review on bridge scour.

Chapter 3 describes the study of the uncertainty in bridge scour that could result from the HEC-18 methods when the median particle size D_{50} is used. Chapter 4 presents proposed multilayer method for determining the scour depth considering characteristics of the soil sizes in different depths. It compares the scour depth obtained using the average D_{50} value (traditional HEC-18 method) and the multilayer method. Chapter 5 presents the comparisons of the hydraulic parameters from both WSPRO and HEC-RAS models. In addition, the differences in corresponding scour depths are also tabulated and discussed to understand and evaluate the uncertainty due to hydraulic parameters.

Chapter 6 documents the overall summary, conclusion, and scope of future studies. Appendix A documents the procedure involved in WSPRO and HEC-RAS model. Also, it includes

the use of USGS envelope curves to a bridge site (Pintalla Creek). Appendix B documents the use/procedure of Pugger Mixer to develop soil sample and test in EFA.

Chapter 2 LITERATURE REVIEW

2.1 LITERATURE REVIEW

An extensive literature review was conducted to study the bridge scour its types and issues related to bridge scour, including the concepts of bridge scour, the underlying theories, and the current design methods recommended by FHWA, and other agencies. The United States is a leading country in the research field and billions of dollars are invested in different sectors. One of the sector, where research was carried out, was the highway. The 1950's had a boom in federal transportation funding with the beginning of the interstate system. The research carried over into all the areas of highway design including bridge hydraulics. FHWA is one of the organizations which is heavily involved in the bridge and hydraulic research. The WSPRO computer program was developed by FHWA in contract with USGS.

Many methods were developed in past years to predict the scour of bridges. FHWA has developed design manuals, including HEC-18, HEC-20, and HEC-23 for the state DOTs to evaluate the scour potential of existing bridges and estimate the scour depths for new bridges. Florida Department of Transportation developed a new method based on the HEC-20 method. Maryland State Highway Administration developed the ABSCOUR program based on the research of Chang and Davis(1998), which differs slightly from the HEC-18 method

Texas Department of Transportation also developed a scour rate based method and Texas A&M University developed the SRICOS-EFA method which basically focuses on pier and contraction scour in cohesive soil. Many of the states use HEC-18 procedure (Arneson et al. 2012) to measure the bridge scour. The HEC-18 manual was extensively reviewed for this research project.

The U.S Army Corps of Engineers is responsible for flood controls in most of the watersheds throughout the country. The Corps has conducted a lot of research in the area of flood control and flood plain management. This led to the development of HEC-2, HEC-RAS, and other several related hydraulics programs. The HEC-2 and HEC-RAS programs have been used extensively by many institutions, research agencies to gather the data needed to perform the scour depth calculation.

Since 1950 the FHWA and the U.S Army Corps of Engineers have been the major sponsors of hydraulic research. The final output of the research by both the agencies, which are used for hydraulic modeling, are used and accepted by engineers throughout the country. The programs used in this study are WSPRO by the FHWA and HEC-RAS by the U.S Army Corps of Engineers.

For the calculation of the scour depth by HEC-18, a number of hydraulic input parameters are needed. These hydraulic parameters or variables can be calculated by using either the FHWA program or U.S Army Corps Program. A plethora of documents concerning the theories and equations used by RAS are available. The HEC-RAS users can use HEC-RAS user's manual (Brunner 2001) and Hydraulic Reference manual (Brunner 1995) for complete knowledge of RAS. The user manual of WSPRO (Arneson and Shearman 1998) is a great help to understand and prepare the input data in a proper format. Without that manual, it would have been very difficult for users to know the exact meaning of data in different columns. Also, several researchers (Angel and Huff 1997; Shearman et al. 1986) have discussed the WSPRO methodology in detail.

Shearman and others (1986) provide theoretical background and data requirements for using the WSPRO method for bridge analysis. Also, they provided charts and tables for calculating the coefficient of discharge which is one of the important parameters in WSPRO for the calculation of the hydraulic parameters, eventually scour depth.

Different research studies were carried out to compare the outputs of HEC-RAS, WSPRO, and HEC-2. Brunner and Hunt (1995) compared the one-dimensional bridge hydraulics routines from HEC-RAS, HEC-2 and WSPRO models using the same bridge sites. Their report discusses the similarities and differences of the fundamental computational methods of each of these models. Also, these report compares the observed water surface elevation with the computed water surface elevation from HEC-RAS, HEC-2, and WSPRO. Out of 22 bridge sites obtained from the USGS, 13 were used for the study. Also, some of them were omitted because of sparse water surface measurement in the vicinity of the bridge. A few sites were omitted due to the inadequate bridge geometry and layout information. Almost all of the events were the class A low flow (i.e., open channel, subcritical flow through the bridge opening), while three of the events had water surfaces higher than the bridge low cord on the upstream side of the bridge.

There are lots of literature which describe the bridge reach, transition length, cross-section spacing, and contraction and expansion coefficients (Brunner and Hunt 1995). For the one-dimensional hydraulic modeling using HEC-RAS, a bridge reach is a river segment defined by a minimum of four cross sections (Figure 1.4). The most downstream cross section (the section 1 in Figure 1.4) is located at the point where the active flow area has expanded to the full, unconstructed floodplain width, which is called the exit section in WSPRO. The most upstream cross section is located at the point where the active flow just begins to contract from the full floodplain width, i.e., the section 4 in Figure 1.4, and it is called the approach section in WSPRO. It is suggested to

use one cross section just upstream and downstream of the bridge, i.e., the sections 2 and 3 (Figure 1.4) used in HEC-RAS, so that all the influences on the local water surface elevation are included. There are many conflicting recommendations about placing exit and approach section in relation to the bridge. Different models use a different convention in selecting the exit and approach section in relation to the bridge. Chow (1959) recommends the approach section be located at the upstream end point of the backwater curve, but he did not provide specific guidance as to where the point is. Matthai (1967) and Shearman et. al (1986) recommend locating the approach section one bridge length above the upstream bridge face. Shearman suggests having the exit section one bridge length below the downstream face while Matthai did not require and use the exit section in his procedure. Also, HEC has different approaches which are based on the obstruction length.

The document of HEC-2 provides recommendations for locating the approach section and the exit section. The approach section should be located at a distance upstream equal to the obstruction length and the exit section should be located downstream at a distance four time the obstruction length (the average of the distances A to B and C to D from Figure 1.4). The average obstruction length is half of the total reduction in floodplain width caused by the two bridge approach embankment. More recent study discards this approach and declared this method to be inaccurate. The cross-section spacing is also an issue in hydraulic modeling. Both FHWA and HEC recommend that the cross section should be placed where there is a significant change in the channel like certain contraction or expansion. Some researchers have discussed the cross-section spacing. Brunner and Hunt (1995) figure out that the location of the cross-section to be more important than the type of model used. However, they do not provide guidance for this. Gates et al. (1998) provided guidance for this issues. HEC-RAS has the ability to interpolate the cross-section by itself.

The soil in nature is present in different layers. Different layers have different particle sizes. The mean particle size is one of the important factors to determine the scour depth. Also, the scour depth at different flood events would be different. Briaud et al. (2001) proposed SRICOS method. This document shows the importance of considering the multi-layer soil and multi-flood events. This method is now limited to cylindrical piers and water depths larger than two times the pier width.

One thousand bridges have collapsed over the last 30 years in the United States and 60% of the failure are due to scour (Shirole and Holt 1991). Therefore, scour is considered as one of the major causes of bridge failure. In the report conducted by Chang (1998) for the Federal Highway Administration reported that 25 percent of the 383 bridges failures due to catastrophic floods involving pier damage; whereas, 72 percent involved abutment damage. During the 1993 flood in the upper Mississippi and lower Missouri river basin, at least 22 of the 28 bridges that failed were due to scour at an estimated cost of more than \$ 8,000,000. In 1994, flooding from Storm Alberto in Georgia (GA) damaged over 500 bridges. Thirty-one state-owned bridges experienced 15-20 ft. of scour and thus had to be replaced. The total damage to the Georgia Department of Transportation (GADOT) highway system was approximate \$130 million (Zhang et al. 2013)

Bridge scour is a major cause of bridge failure. Bridge and hydraulic engineers are trying to design and maintain bridge foundations that are safe from scour. Bridge scour is a major factor that contributes to the total construction and maintenance cost of the bridge in the United States. Scour depth predicted using adapted methods by DOTs are crucial. Underprediction of the bridge scour depth can cause bridge failure and result in loss of lives and property. Overprediction of the bridge scour depth can cause loss of millions of dollars on a single bridge. From this viewpoint,

we can say that bridge scour evaluation should be done as accurately as possible and consider a reasonable safety factor.

Different methods over the past years (Johnson et al. 2015) were developed to predict the scour depth. Federal Highway Administration developed several design manuals including HEC-18, HEC-20, and HEC-23, for state DOTs, to evaluate the scour potential of existing bridge and estimate the scour depths for new bridges. Although various methods have been developed to predict the scour depth, most of the DOTs in the USA are using the equations and methods given in FHWA HEC-18, which were developed for non-cohesive soils. The EFA has been built and tested to measure the erosion rate of the cohesive soil. This method can also be used to predict the erosion rate of the non-cohesive soil.

It is well-known that significant uncertainty exists in the use of HEC-18 equations (Johnson et al. 2015). These equations were developed based on flume tests performed on fine sand and later compared with field measurement. Those equations used in HEC-18 do not include soil parameters except the particle size D_{50} and make the basic assumption that all soils behave like a fine sand (Yao et al. 2014). Many research studies (Johnson et al. 2015) were carried out in the past to understand and quantify/determine the uncertainty of the HEC-18 for calculation of the scour depth. Many researchers (Breusers et al. 1977; Melville and Coleman 2000; Sturm et al. 2011) have acknowledged the uncertainty of the laboratory-derived equations. Several studies have been performed to highlight the uncertainty of HEC-18 equations by various field investigation of bridge scour. Mueller and Wagner (2005) checked the performance of 26 different pier-scour equations using 266 field measurements and concluded that none have accurately and conservatively predicted the scour observed in the field. Benedict and Caldwell (2006) assessed the performance of the HEC-18 clear water contraction scour equation using 174 field

measurements and concluded that the equation was conservative with frequent overprediction and significant numbers of under predictions. Benedict et al. (2006) assessed the performance of 6 abutment-scour equations using 209 field measurements and concluded that most of those equations were conservative with several under prediction.

Richardson and Davis (2001) note that engineers must, “Evaluate whether the computed scour depths are reasonable and consistent with the design engineer’s previous experience and engineering judgment.” If the scour depth calculated is unreasonable design engineer can modify the obtained value by giving the sound engineering judgment.

2.2 SOIL TYPES

The soil is a mixture of sand, gravel, silts, clay, water, and air. Different types of soil layer are present in earth surface with different D50 values (Table 2.1). Depending upon the amount of these ingredients we can determine the cohesiveness of the soil. Cohesiveness can be defined as how well the soil holds together. Cohesive soil doesn’t crumble. It can be molded easily when it is wet and becomes hard when it is dry. Clay is an example of cohesive soil and is a fine-grained soil. Sand and gravel are course grained soil and has little cohesion or bonding, so it is often called as non-cohesive soil.

Table 2.1 Different soil types with D50 value.

Soil Types	D ₅₀ (mm)
Clay	< 0.002
Silt	0.002-0.06
Sand	0.06-2
Gravel	2-60
Cobbles and Boulders	60-200

One of the parameters involved in the erodibility of a soil is the critical shear stress. The critical shear stress (τ_c) is the threshold shear stress at which erosion is initiated. It is assumed that if the eroding shear stress exceeds τ_c , the soil will experience an erosion. In this framework, τ_c is considered as a soil property which can be compared between cohesive and non-cohesive soil. The eroding mechanism of soil is different for cohesive and non-cohesive soil. In sands and gravels, which are non-cohesive, the main soil parameter influencing τ_c is the particle grain size D_{50} . In fact, in this case, gravity forces applied to soil is related to the particle size and then links or correlates to τ_c based on experimental studies of non-cohesive soils. But in the fine-grained soil which is cohesive, the size of the particle only is not the good predictor of τ_c (Briaud et al. 2001a). The reason for this is that the gravity force will no longer be the only control of the soil behavior and electromagnetic and electrostatic forces become significant. Electrostatic force, also called as Coulomb force, can be defined as the attraction or repulsion of particles because of their electric charges. The electromagnetic force is a type of physical interaction that occurs between electrically charged particles. In fine-grained soil, many other factors can influence the critical shear stress τ_c . Briaud et al. (1999a) notify some of the influencing factors including soil water content (w), the soil unit weight (γ), soil plasticity (PI), the soil mean grain size (D_{50}), the soil percent passing the no. 200 sieve (%200), the soil clay mineral, the soil temperature (T), the water temperature (T_w), the soil cation exchange capacity (CEC), the soil sodium absorption ratio (SAR), and the water chemical composition. At this point, we can say that many differences lie in between the cohesive and non-cohesive soil and using the same equations suggested by HEC-18, which were derived based on lab experiments of non-cohesive soil, for cohesive soil will not accurately predict the scour depth.

2.3 EROSION FUNCTION APPARATUS

Calculation of scour depth around a bridge pier is a major design consideration for bridge design. All the bridge foundation design is based upon the scour of soil caused by the flow of water. The deeper the foundation the more expensive the bridge. It is, therefore, necessary to predict the scour depth accurately so that the foundation design could be done accurately and effectively.

Scour in the non-cohesive soil like sand and gravel is well-understood (Briaud et al. 2001a). It is easy to calculate the scour rate in the non-cohesive soil as a single flood event can cause maximum scour depth. Clean sands and gravels erode particle by particle (Briaud et al. 2001a). Non-cohesive soils can be eroded quickly and very evenly because the only force that resists erosion is the frictional force between the grains (Briaud et al. 2001a). Unlike non-cohesive soil, the scour in cohesive soil is difficult to find out because of the electromagnetic and electrostatic forces between the particles (Briaud et al. 1999b). It increases the scour resistance in cohesive soil. Due to this force, the cohesive soil can be eroded very irregularly and its erosion is slower than non-cohesive soil. Because of the soil slow erosion, it is necessary to understand and predict the scour rate accurately so that the bridge design could be done effectively. An apparatus measuring the scour rate of the cohesive soil was developed by Briaud et al. in the early 1990s called Erosion Function Apparatus (EFA).

The EFA is a closed channel flume equipped with a pump and a stepping motor. A circular opening at the bottom of the flume is for testing the samples collected in the tube. The cross-section of the flume is 101.6 mm × 50.8 mm with a total length of 1.22 meters. The tubes are placed into

the device and one millimeter of soil is protruded into the flume (Figure 2.1). The velocity of the waters ranges between 0.1 to 6 m/s. The velocity is increased incrementally.

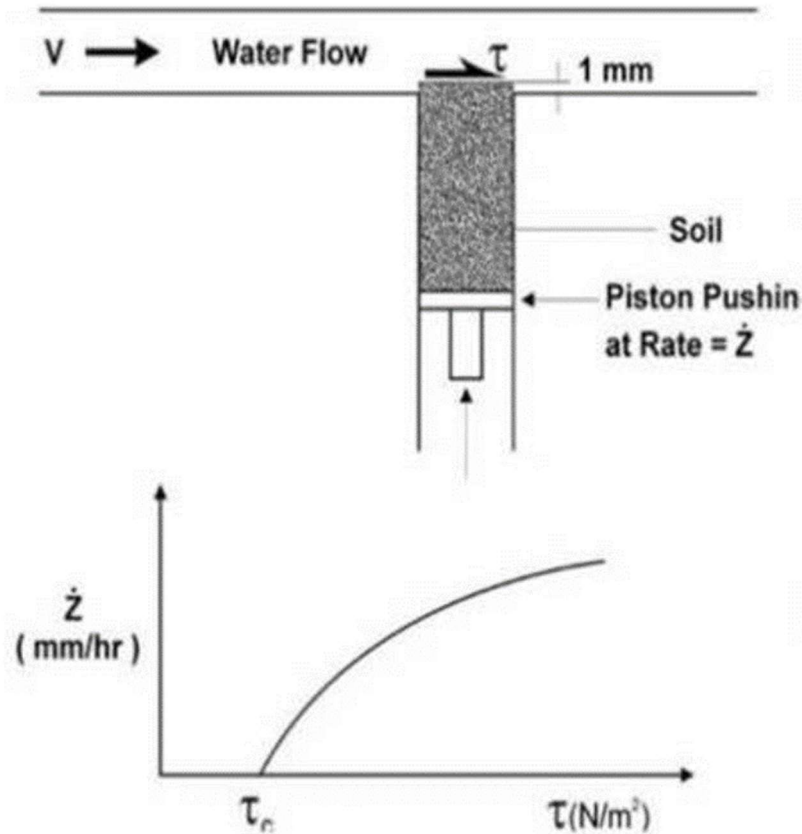


Figure 2.1 Erosion Function Apparatus to measure erodibility (Briaud et al. 1999)

2.3.1 METHODS

The first step in performing an EFA test is to place the soil sample in the bottom of the flume. The flume is filled with water. After one hour, the flow velocity is set to 0.3 m/s and the sample is protruded 1 mm into the flume. There is a viewing glass in EFA from which technician will view the erosion rate with respect to time. After 1 mm of soil sample eroded, or after one hour of testing whichever comes first, the sample is trimmed off and again 1mm of the soil sample is

advanced. The velocity is increased to 0.6 m/s. The erosion of the soil sample is again recorded and this process is repeated with an increase in velocity of 1 m/s, 1.5 m/s, 2 m/s, 3m/s, 4.5m/s, and 6 m/s (Briaud et al. 2001a).

2.3.2 EFA RESULTS

The test result consists of erosion rate (mm/hr.) and shear stress (Pa). The erosion rate is obtained by simply dividing the length of the soil sample eroded by the time required to do so for each velocity.

$$z = \frac{h}{t} \quad (2.1)$$

where h is the length of the sample eroded in time t .

A different test was done for the calculation of the shear stress. After several attempts at measuring the shear stress, it was found that the best way to calculate shear stress τ for the EFA was by using the Moody's chart (Briaud et al. 2001a).

$$\tau = \frac{1}{8} f \rho v^2 \quad (2.2)$$

where τ is the shear stress on the wall of the pipe, f is the friction factor obtained from the moody chart, ρ is the mass density of the water (1,000 kg/m³), and v is the mean flow velocity in the pipe. The friction factor f is the function of the Reynolds number R and roughness \mathcal{E}/D . The Reynolds number is a dimensionless value that measure the ratio of inertial force to viscous forces and describe the degree of laminar or turbulent flow. The relative roughness is the ratio of the average height of the roughness elements on the pipe surface over the pipe diameter D . The average height of the roughness element \mathcal{E} is taken equal to 0.5 D_{50} . It is used because it is assumed that the top

half of the particle protrudes into the flow while the bottom half is buried into the soil mass (Briaud et al. 2001a).

2.1 CLEAR-WATER SCOUR IN 25 ALABAMA BRIDGES

The U.S Geological Survey, in cooperation with the ALDOT, measured clear-water contraction scour at 25 bridge sites in the Black Prairie Belt of the Coastal Plain of Alabama (Lee and Hedgecock 2008). The theoretical clear-water contraction scour depths calculated using HEC-18 were compared with the observed scour depths (Figure 2.2). The observed scour depths ranged from 1.4 to 10.4 ft. The bridge sites which were studied have a mixture of grassland and wooded areas in the floodplain. In USGS study, two assumptions were made: (1) the data collected were reflective of unaltered, clear-water scour; (2) the measured scour hole has reached its maximum depth and is at equilibrium. The observed scour depths were neither measured during or directly after a flood event. The observed scour depths were measured using an electronic total station. At first, several representative ground shots of the unscoured floodplain on both the upstream and downstream sides of the bridge opening were taken. A regression technique was used to develop a best fit ground line on either side of the bridge opening. The maximum scour depth for a particular site was determined by finding the maximum difference between the estimated unscoured ground line and ground points surveyed in the bottom of the scour hole. A common level rod was used to figure out the maximum deepest areas of the scour hole. The theoretical clear water contraction scours were computed for the 50-years recurrence interval flood with the assumption that every bridge site selected have once experienced a 50-year flood flow.

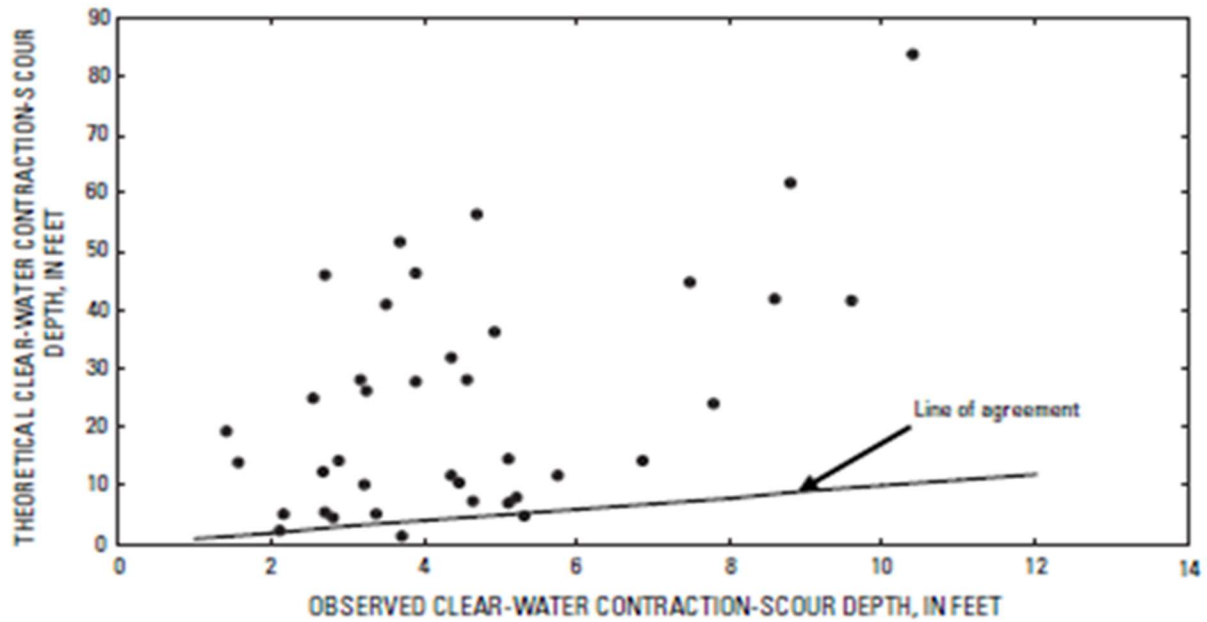


Figure 2.2 Comparison of observed and theoretical scour depth (Lee and Hedgercock 2008)

The comparison of the theoretical and observed scour depths showed the difference ranging from 73 ft to -2.5 ft with an average difference of ~20 ft. The comparison between theoretical and observed scour depth indicates that the theoretical clear-water scour depth was, on average, about 475 percent higher than the actual observed scour depths in the overbank areas.

Chapter 3 **EVALUATING UNCERTAINTY IN BRIDGE SCOUR USING HEC-18 AND MEAN PARTICEL SIZE**

3.1 INTRODUCTION

Uncertainty simple means lack of certainty, a state of limited knowledge where it is impossible to exactly describe the existing state, a future outcome, or more than one possible outcome. HEC-18 needs soil parameter D_{50} and hydraulic parameters for the calculation of the scour depth. The input variables for HEC-18 are not precisely known since they are not typically measured/observed or can be obtained/selected in various ways due to lack of guidance. There is usually an uncertainty in determining and specifying their values. The degree of uncertainty may vary from one variable to another. The HEC-18 equations were derived based on the lab experiments done on non-cohesive soils and is being used for calculation of scour depth for cohesive soils too. The soil parameter such as critical velocity for cohesive and non-cohesive soil is different and plays an important role in predicting the scour depth. However, HEC-18 equations are only using D_{50} solely as the representation of the soil parameter.

This part of the study was carried out to identify and illustrate some uncertainty existing in HEC-18 by comparing the critical velocity and shear stress obtained from HEC-18 (using D_{50}) and EFA. Even we got some basic soil data (e.g., D_{50}) for the four bridge sites from ALDOT where the scour depths were previously determined using HEC-18, the research team and ALDOT did not have specific funds to obtain soil samples from these four bridge sites for determining critical velocity and shear stresses using EFA. Therefore, an alternate approach was used in this study

using six soil samples obtained from a previous ALDOT project (Anderson et al. 2015) from or near Alabama bridge sites.

The EFA data were taken from a published report by Anderson et al. (2015) named as “Evaluation of Scour Potential of Cohesive Soil- Phase 2” submitted to the Alabama Department of Transportation on January 2015. In that study, ten cohesive soil formations were sampled and tested in an updated EFA. Several geotechnical properties of the soil sample were determined experimentally and were correlated to measured scour rate determined using EFA. Velocity and shear based erosion function were generated for the seven erodible soil samples (other three soil samples were classified as scour-resisted). Shear stress is related to velocity by using the geometry of the flume, density of water, and friction factor obtained from a Moody chart. The median grain particle size, critical velocity, and shear stress obtained from EFA for six soil types are shown in Table 3.1.

Table 3.1: Summary of data taken from EFA.

Soil Type	D ₅₀ (mm)	Critical velocity V_c (m/s)	EFA’s Critical Shear Stress τ_{c-EFA} (N/m ²)
Naheola-Dark	0.016	0.59	1.15
Naheola-Yellow	0.028	0.65	0.41
Bucatumna	0.033	0.39	0.53
Nanafalia	0.080	0.42	0.63
Porter’s Creek	0.082	0.20	0.16
Yazoo	0.088	0.47	0.79

3.2 COMPARISON OF CRITICAL VELOCITY AND SHEAR STRESS

In this study, the critical shear stresses and critical velocities for six soil samples obtained from EFA tests and HEC-18 were compared. In HEC-18, the critical velocity plays a vital role in determining the depth of the scour. If the velocity of the flow is above the critical velocity, then scour occurs. The critical velocity should be determined accurately otherwise scour depth could be overestimated or underestimated. The critical velocity in the scour related studies is defined as the velocity above which the bed material of a specified size and smaller will be transported.

In HEC-18 the critical velocity is determined from the equation developed by Laursen (1963). The derivation of the critical velocity equation is given below. The average bed shear stress on the channel bed is expressed as (Chow 1959)

$$\tau_0 = \gamma R S_f \quad (3.1)$$

where, τ_0 is the average shear stress, R is the hydraulic radius, S_f is the friction slope, and γ is the specific weight of water (~ 62.4 lbf/ft³ or 9.81 kN/m³).

Using Manning formula to evaluate the frictional slope and approximating the hydraulics radius by flow depth (e.g., wide rectangular channels), Equation (3.1) can be written as,

$$\tau_0 = \frac{\gamma n^2 V^2}{k_n^2 y^{1/3}} \quad (3.2)$$

where n is Manning's roughness coefficient, k_n is 1.0 m^{1/3}/s for SI units or 1.49 ft^{1/3}/s for engineering units, y is the flow depth and V is the velocity of the flow.

Shields (1936) conducted experiments of incipient motion to determine the relationship between the Reynolds number $\frac{VD_s}{\nu}$ and $\frac{\tau_0}{(\gamma_s - \gamma)D_s}$, known as the shield relation. The study has four parts of which the second part considers primary the conditions at the beginning of bed-load

movement. The study considered the grains of uniform sizes and investigated: when the grain be dislodge from the bed and set in motion. From the Shield relation (Shields 1936), the critical bed shear stress can be expressed as,

$$\tau_c = k_s(\gamma_s - \gamma)D_s \quad (3.3)$$

where, τ_c = critical shear stress, k_s = Shield's coefficient, D_s = particle size, γ_s = specific weight of the sediment particle. The motion of the sediment particle is initiated when $\tau_0 = \tau_c$, so that the critical velocity can be determined by equating right hand sides of both equations (3.2) and (3.3) and solving for $V = V_c$

$$V_c = \frac{k_n}{n} \sqrt{k_s(s - 1)} y^{1/6} D_s^{1/2} \quad (3.4)$$

where $s = \gamma_s / \gamma$ = specific gravity of the soil particles. Substituting D_{50} for D_s and using Strickler equation (Chow 1959) $n = 0.034(k_v D_{50})^{1/6}$ with $k_v = 3.28 \text{ m}^{-1} = 1.0 \text{ ft}^{-1}$

$$V_c = K_u y^{1/6} D_{50}^{1/3} \quad (3.5)$$

where $k_u = k_n \{k_s(s - 1)\}^{1/2} / (0.034 k_v)^{1/6}$ is a constant equal to $6.19 \text{ m}^{1/2}/\text{s}$ or $11.17 \text{ ft}^{1/2}/\text{s}$ when the Shield's coefficient is 0.039 (Akan 2011), the specific gravity is assumed as 2.65, D_{50} is the mean particle size, and y is the average water depth upstream of the bridge contraction. Equation (3.5) is used in HEC-18 for the calculation of the critical velocity using necessary inputs: D_{50} and y .

In Table 3.2, the critical shear stress obtained from EFA (τ_{c2}) is compared to the critical shear stress obtained from the HEC-18 (τ_{c1}) using D_{50} as input. The ratio of τ_{c2}/τ_{c1} ranges from 3.2 to 115 with an average of 31.8 and standard deviation of 37.9; therefore, it means for these clay

soils the critical shear stress from HEC-18 is significantly smaller than the critical shear stress determined using EFA tests.

Table 3.2 Comparison of critical shear stress from EFA and HEC-18

Soil Type	D ₅₀ (mm)	Critical Shear Stress for HEC-18 (N/m ²) (τ _{c1})	EFA's Critical Shear Stress τ _{c-EFA} (N/m ²) (τ _{c2})	Ratio (τ _{c2} / τ _{c1})
Naheola-Dark	0.016	0.01	1.15	115
Naheola-Yellow	0.028	0.02	0.41	20.5
Bucatumna	0.033	0.02	0.53	26.5
Nanafalia	0.080	0.05	0.63	12.6
Porter's Creek	0.082	0.05	0.16	3.2
Yazoo	0.088	0.06	0.79	13.2

Note: critical shear stress from HEC-18: $\tau_c = k_s \gamma(s-1) D_{50}$ and $k_s = 0.039$, $S = 2.65$

The critical velocity for an EFA test is determined by changing the conduit or test velocity and then visually identifying whether the soil sample erosion starts or not. For modified EFA, the soil erosion was determined by distance measurement using ultrasonic sensors (Walker 2013). The critical velocity in HEC-18 is linked with D₅₀ and water depth (y) in the channel where the bridge locates. Therefore, comparing the critical velocity from EFA (flow velocity in the conduit) with the critical velocity obtained from the HEC-18 is not considered feasible. To compare the critical velocities obtained from EFA and HEC-18 equation, the above derivation was modified. Substituting the critical bed shear stress into equation (3.4), one can get the relation of V_c and τ_c:

$$V_c = \frac{k_n}{n} * \sqrt{\frac{\tau_c}{\gamma}} * y^{\frac{1}{6}} \quad (3.6)$$

Manning roughness factor n can be determined from Strickler's equation as a function of D₅₀ (Akan 2011). Equation (3.6) was used to calculate the critical velocity by using the shear stress and D₅₀ values obtained in EFA tests.

The critical velocity calculated from HEC-18 and the critical velocity using τ_{c-EFA} and D_{50} (Table 2.3) are compared when the upstream water depth (y) is taken as constant equal to 4 m (close to water depth in Spear Creek main channel, Table 3.4) and 1.5 m (close to water depths in Spear Creek overbank areas, Table 3.4) for all calculations. The ratio of V_{c2}/V_{c1} ranges from 1.7 to 10.4 with an average of 4.8 and standard deviation of 2.7. This means for the clay soil samples the critical velocities calculated from HEC-18 are significantly smaller than critical velocities calculated using τ_c determined using EFA and D_{50} . From Table 3.3 it can be seen that the critical velocities calculated from the HEC-18 equation using same D_{50} value and different average depths upstream (4 m for channel and 1.5 m for overbank areas) are somewhat different since it is proportion to $y^{1/6}$. When the particle size D_{50} ranges from 0.016 to 0.088 mm, the critical velocity from HEC-18 equation (2.5) changes from 0.2 to 0.35 m/s (proportion to $D_{50}^{1/3}$) and shows an impact of D_{50} on calculating the critical velocity and then the scour depth. For example, for the bridge site in Spear Creek, the velocity at the upstream approach section (V_I) calculated using WSPRO is 0.72 or 0.97 ft/s (0.22 or 0.29 m/s) in the overbank areas and 3.35 ft/s (1.02 m/s) in the main channel (Table 3.4).

Based on Table 3.3 for six soil samples, V_C from Equation (2.6) is always greater than upstream velocity V_I in overbank areas, but V_C from Equation (2.5) could be greater or less than V_I . When overbank areas are heavily vegetated, current DOT practices force or always use the clear-water scour to compute the scour depths in overbank areas. Therefore, the critical velocity linked to the particle size does not play a role to determine which type of the scours occurs in the overbank areas, but the particle size D_{50} directly affects the scour depth calculation based on Equation (1.3).

For the main channel, V_C obtained from HEC-18 Equation 2.5 is less than V_I which would make it a live-bed scour. Table 3.4 shows the scour depth of 7.74 ft calculated using default method from HEC-18, which allows HEC-18 to determine whether or not the clear-water or live-bed scour would occur. HEC-18 results show the live-bed scour would occur. However, V_C obtained from Equation 2.6 is greater than V_I for same channel section which would make it as a clear-water scour. The particle size D_{50} has a direct impact on calculating the clear-water scour depth after the scour (Equation 1.3), i.e., proportion to $1/D_{50}^{2/7}$. The scour depth calculated using the clear-water scour would result in 47.76 ft of scour depth in the main channel. This is a huge difference in calculated scour depth that illustrates the uncertainty in the HEC-18 equation.

Table 3.3 Comparison of critical velocities from EFA data and from HEC-18 (Y = 4m)

Soil Type	D_{50} (mm)	V_{c1} (HEC-18) Eqn. (3.5) (m/s)	V_{c2} using τ_{c-EFA} and D_{50} Eqn. (3.6) (m/s)	Ratio V_{c2}/V_{c1}
Naheola-Dark	0.016	0.20 (0.17)	2.07 (1.76)	10.4
Naheola-Yellow	0.028	0.24 (0.20)	1.13 (0.96)	4.7
Bucatumna	0.033	0.25 (0.21)	1.25 (1.06)	5.70
Nanafalia	0.080	0.34 (0.29)	1.17 (1.0)	3.4
Porter's Creek	0.082	0.34 (0.29)	0.59 (0.5)	1.7
Yazoo	0.088	0.35 (0.30)	1.29 (1.1)	3.7

Note: ⁻¹ the water depth y in Equations (2.5) and (2.6) was assumed as 4.0 m for the comparison purpose. The critical velocity inside brackets was computed using $y = 1.5$ m.

Why is the scour depth calculated by the clear-water scour much different from the scour depth calculated by the live-bed scour? For the live-bed scour hydraulic parameters at upstream approach section and the contraction section (bridge crossing) play a role in calculating the scour depth at the bridge site. If $V_I > V_c$ at the upstream approach section for the live-bed scour, V_2 is definitely greater than V_c at the bridge contraction section (Table 3.4); it means the scour occur at

both approach and contraction sections, which is why both hydraulic parameters at both sections will be used for the scour computation. The soil scoured from the approach section becomes the supply of soil for the contraction section; therefore, the total or over scour at the bridge site is smaller, e.g., 7.74 ft at Spear Creek under the 100-year flood. The ratio of hydraulic parameters between two sections would be small such as $Q_2/Q_1=1.59$ and $W_1/W_2=1.10$, when these ratios are multiplied it will give a small value for determining water depth after the live-bed scour (Equation 1.2). Subtracting Y_0 the depth at the contraction section prior to scour would give the final scour depth of a live-bed scour; therefore, the scour depth for the live-bed scour is much smaller. For clear-water scour only the ratio of Q_2 and W_2 at the contraction section is used which gives the greater value of the water depth after the scour (Equation 1.3). The ratio of the hydraulic parameter, i.e., $(Q_2^2/W_2^2)^{6/7}$ is greater and equals to 43.37 in Spear Creek. The ratio of other parameters, i.e., $(1/C_u * D_m^{2/3})^{3/7}$ is just 1.44. When this ratio is multiplied by the ratio of hydraulic parameters the result would be 62.04 which when deducted from Y_0 (14.28 ft) would give a scour depth of 47.76 ft. This calculation and comparison to the live-bed scour depth clearly shows the uncertainty of HEC-18 equations.

From the comparison in Table 3.4, a firm conclusion can be drawn regarding the use of the HEC-18 equation in calculating the scour depth of cohesive soil. The critical velocity and critical shear stress obtained from the HEC-18 is far less than those obtained from EFA. The critical velocity is used in HEC-18 to determine the types of contraction scour (live-bed and clear-water). The possible change in the type of contraction scours would cause a change in scour depth estimate as the equation used in calculating the scour depth would be different (Arneson et al. 2012). The meaning of smaller critical velocity is that the scour will occur earlier than it should be which will overestimate the scour depth. The effect of the change in the type of equations used has a huge

effect on the scour depth. The difference in the scour depth using two different equations is 35.63 ft for the main channel in Spear Creek, which is a huge difference. It is well-known that determination of accurate scour depth is imperative to designing safe, economic and efficient bridge foundation. HEC-18 compared to EFA predicts higher scour depth which leads to extra cost and not efficient bridge foundation. It can also be concluded that HEC-18 equations which are developed based on the experiments done on non-cohesive soil don't account well for cohesive soil. This information is very important in scour calculation because, if cohesive soils are encountered at a bridge site, scour will occur at a much lower rate than that is given by the HEC-18 equation.

Table 3.4 Hydraulic parameters in Spear Creek from WSPRO method.

Hydraulic Parameters	LOB	CH	ROB
Y_1 (ft)	3.56	13.75	5.38
V_1 (ft/s) ¹	0.72	3.35	0.97
Y_o (ft) ²	4.02	14.28	5.14
Q_2 (cfs)	514.12	2357.13	948.75
W_2 (ft)	41.00	29.00	50.00
V_2 (ft)	3.12	5.69	3.69
D_{50} (mm)	0.03	0.047	0.055
<i>Scour Eqn.</i>	Clear-water	Default	Clear-water
Q_1 (cfs)	1347.64	1473.89	998.48
W_1 (ft)	290.00	32.00	100.00
Scour (ft)	10.25	7.74 (47.76) ³	11.97

Note: ¹ – the subscript 1 for the upstream approach section, 2 for the contraction section at the bridge crossing, ² - Y_o is the average depth prior to scour at contraction section, i.e., Y_{BU} in Equations (1.2) and (1.3); ³ – the number in the bracket is for the scour depth calculated using the clear-water scour equation (1.3).

3.3 DISCUSSION

The equations for the HEC-18 to calculate critical velocity were derived from the laboratory experiments using non-cohesive soil and only should be used for non-cohesive soil for calculation of scour depth. For the cohesive soil, other methods like using EFA data should be considered/used which give more reliable values. For the calculation of the scour depth, HEC-18 use the average D_{50} value of the bed material. Only taking D_{50} of a bed material in the calculation of scour depth could either underestimate or overestimate the scour depth. Two different soil samples which have a different percentage of sand, clay, and silt could have same D_{50} value as illustrated in Figure 3.1. The critical shear stress and velocity for initiating scour on those two samples could be different and could result in different scour depths under the same flood. Sample 2 has more fine-grained soil (30% clay, $D_{50} \leq 0.002$ mm) compared to the sample 1, which has less-fine-grained soil as shown in Figure 3.1. Sample 2 having more clay would erode slowly compared to sample 1. However, if HEC-18 is used for the calculation of the scour depth it would only consider the D_{50} , which is same for both soil samples, and give same scour depth. This hypothetical example further illustrates the uncertainty of HEC-18 equations.

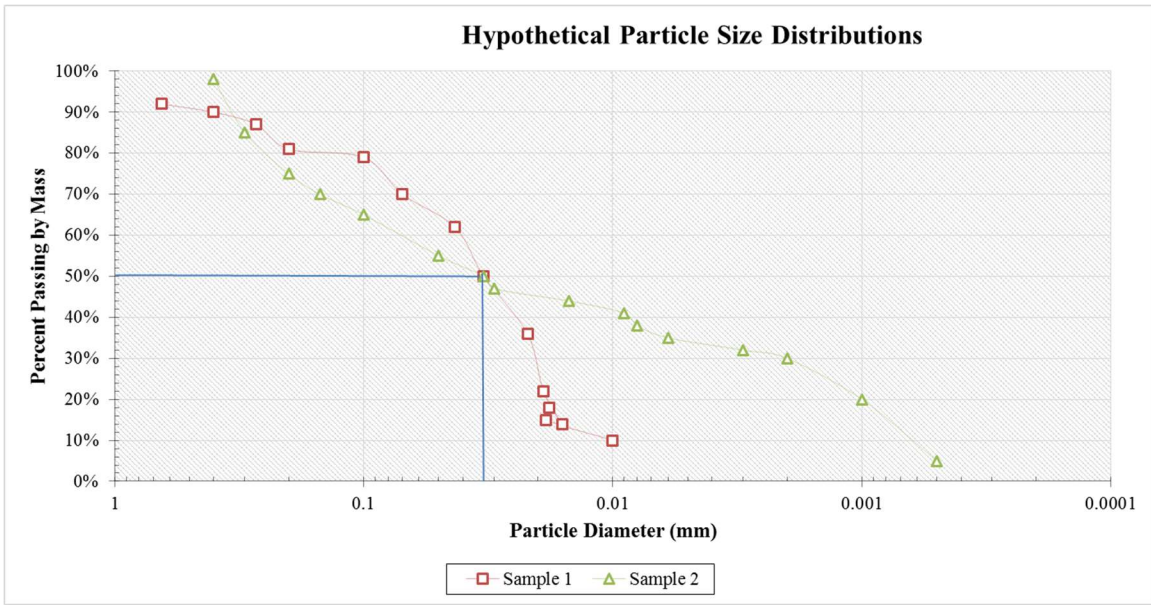


Figure 3.1 Hypothetical particle size distributions with the same D₅₀.

The HEC-18 manual should give clear instruction and meaning about the parameters used. This could help the new engineers to clearly know about the parameter data they should acquire to calculate the scour depth. EFA as one of the most reliable method could be used to determine critical velocities and shear stresses for both cohesive and non-cohesive soil. EFA results can be used to calculate the scour depth based on the relationship between the erosion rate and the hydraulic shear stress applied. EFA can be a very useful tool for designing bridges. It is used to determine the critical velocity and shear stress using a relatively undisturbed, site-specific soil sample. This apparatus should be part of a complete procedure to predict the scour depth versus time curve at bridges.

Chapter 4 **MULTILAYER METHOD AND COMPARISON OF SCOUR DEPTHS FROM HEC-18**

4.1 INTRODUCTION

Scour is crucial in designing bridge foundation. The bridge foundation is the pillars where the heavy mass of bridge deck resists on. The bridge foundation is constructed on the earth surface and penetrated to a certain depth. There are different soil types on earth surface with different D_{50} values (Table 2.1). At a bridge site, different soil layers along depth may exist with different D_{50} . D_{50} is the grain diameter for which half the sample (by weight) is smaller and another half is larger.

D_{50} is one of the important parameters to calculate the scour depth using HEC-18. One of the reasons for bridge failure is the stratification of the river bed. Stratification of soils means the arrangement of soils in different layers with different D_{50} values at different depths. In the same zone (e.g., left or right overbank area or main channel) where the soil samples are taken, there are several D_{50} values from different sample sites. At the same sample site, there could be clay layers, which have smaller D_{50} , or sand or gravel layers having higher D_{50} . HEC-18 lacks to notify whether average surface D_{50} or average D_{50} at certain depths to be used to calculate the scour depth. This uncertainty could result in either overprediction or underprediction of the scour depth.

From the literature analysis, it is known that either the topsoil layer data or the average of the soil data in the river bed is considered while calculating the scour depth. In the complex geological structure of the river bed with different soil layers, calculated depth of scour may increase or decrease, depending on the thickness and sequence of the layers.

Using the top layer D_{50} or the average of them along the layers could result in wrong scour depth and possible structures destruction. For example, the depth of scour is always greater when a fine sand layer is under a coarse-sand layer(s), compared with the depth of scour obtained with mean grain size diameter of the coarse-sand layer, which is on the top (Gjunsburgs et al. 2013). When a fine sand layer is under a coarse-sand layer, critical conditions can occur. When the coarse-sand layer is scoured, the depth of scour is rapidly developing in the next fine-sand layer. In this case, the dominant grain size for computing the depth of scour at foundations under stratified bed conditions is the mean diameter of the second layer or of the next one, where scour stops (Gjunsburgs et al. 2014). Thus, the calculation of scour depth taking only one-grain size diameter of the soil can lead to unbearable damage to the structure under floods.

The aim of the following study is to elucidate the influence of the river bed stratification on the scour depth calculation by comparing the scour depth obtained from the HEC-18 model (using average D_{50} value) with the scour depth using a layer by layer D_{50} value, i.e., multilayer method proposed and tested through this study. The average D_{50} used for HEC-18 in this study was determined by doing the average of D_{50} in all layers provided in the bridge cases from ALDOT. For the ALDOT practice, average D_{50} is determined after removing some outliers from D_{50} in all layers based on engineer's experience. Due to not enough information on which D_{50} value ALDOT took as outliers, all the given D_{50} values were averaged and used for the calculation of scour depth. The comparison of scour depths calculated using with or without outliers was also made to illustrate the uncertainty of the scour depth calculation due to using the average D_{50} .

In this part of the study, soil data (D_{50}) at different depth layers collected by ALDOT from four bridge sites were used to test and evaluate the multilayer method proposed in this study. For bridge design projects, it typically does not have any observed scour depth from any previous flood

for comparison. Therefore, scour depths obtained from the HEC-18 model and the multilayer method were compared, but it is impossible to conclude which scour depth is more accurate. However, this analysis and discussion can still infer which scour depth could be more reasonable or a better estimate.

4.2 STUDY AREA

In this study, reports and related information for four bridge sites that had scour estimations were provided by ALDOT along with the input and output files of the WSPRO model. The bridge site provided were of Spear Creek located in Choctaw County, Valley Creek located at Dallas County, Pintalla Creek located at Cantelous County, and Alamuchee Creek located in Sumter County. The location of the site of all four bridge is shown in Figure 4.1 to Figure 4.4.

Spear Creek is a small perennial stream located in the city of Butler on SR-10, Choctaw County. Spear Creek has a narrow floodplain with a drainage area of 9.4 square miles upstream the bridge. The channel is roughly thirty feet wide and ten to twelve feet deep. There is thick tree undergrowth line in the channel banks. The channel is sinuous through this reach and appears entrenched. The channel boundaries are semi-alluvial with little or no natural levees through this reach of the stream.

Valley Creek is a small perennial stream with a narrow floodplain which is located in the city of Selma, Dallas County with a drainage area of 63.5 square miles. The channel is roughly eighty feet wide and six to eight feet deep. There are trees and thick undergrowth in the channel banks.

Pintalla Creek is a medium perennial creek with a wider floodplain which is located in the line of Montgomery and Lowndes County with a drainage area of 250 square miles at the bridge

crossing. The channel is roughly ninety-one feet wide and eighteen to nineteen feet deep. The channel boundaries are alluvial. There is thick tree undergrowth line in the channel banks and cover the floodplain. The stream is highly meandering.

Alamuchee Creek is a small perennial stream with a wide floodplain with a drainage area of 62.3 square miles which is located in Sumter County. The channel is approximately seventy feet wide and eight to ten feet deep. There is thick tree undergrowth line in the channel banks and cover the floodplain. The stream is meandering.



Figure 4.1 Location of Spear Creek and bridge site characteristics.



Figure 4.2 Location of Valley Creek and bridge site characteristics.

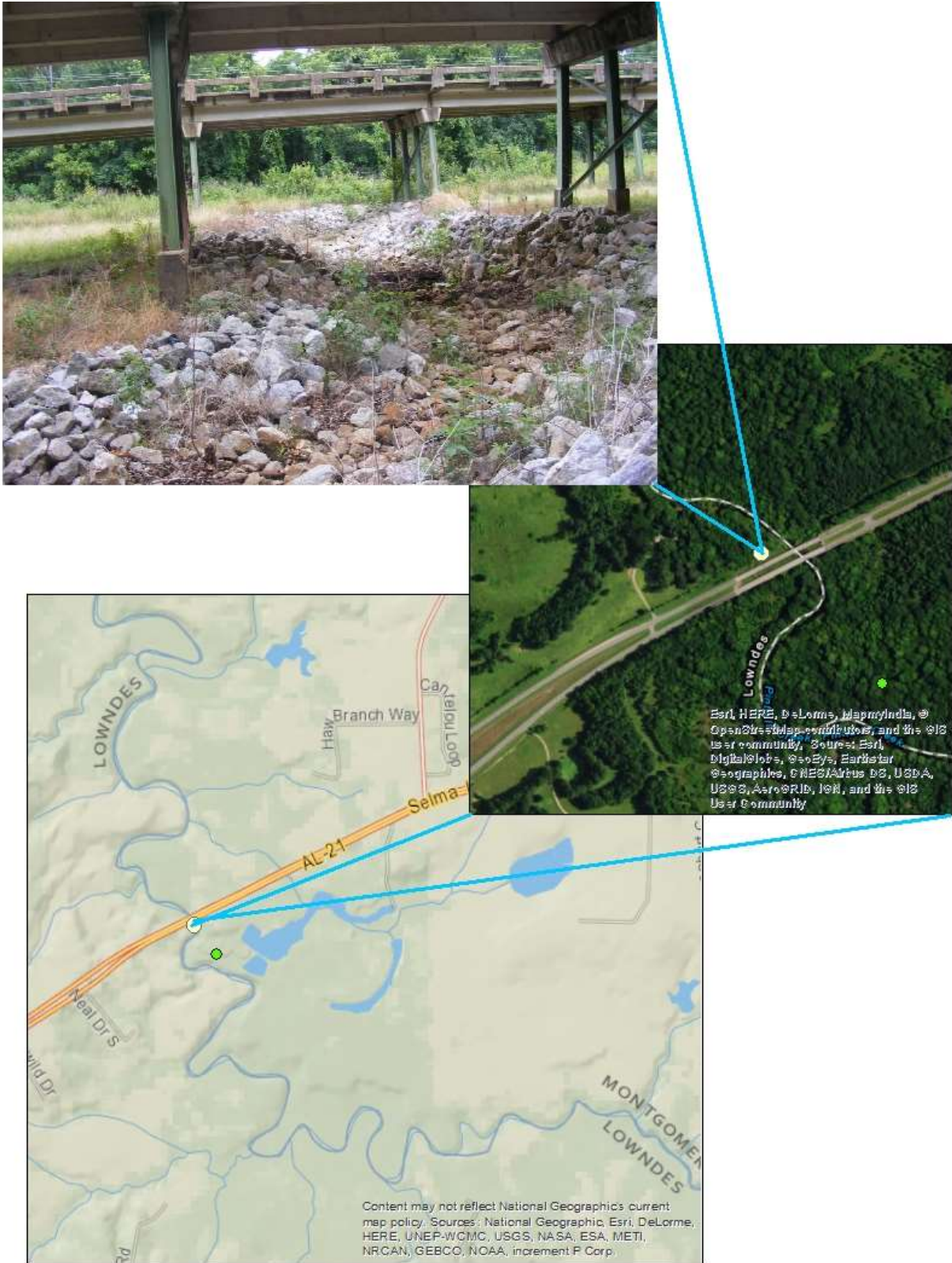


Figure 4.3 Location of Pintalla Creek and bridge site characteristics.

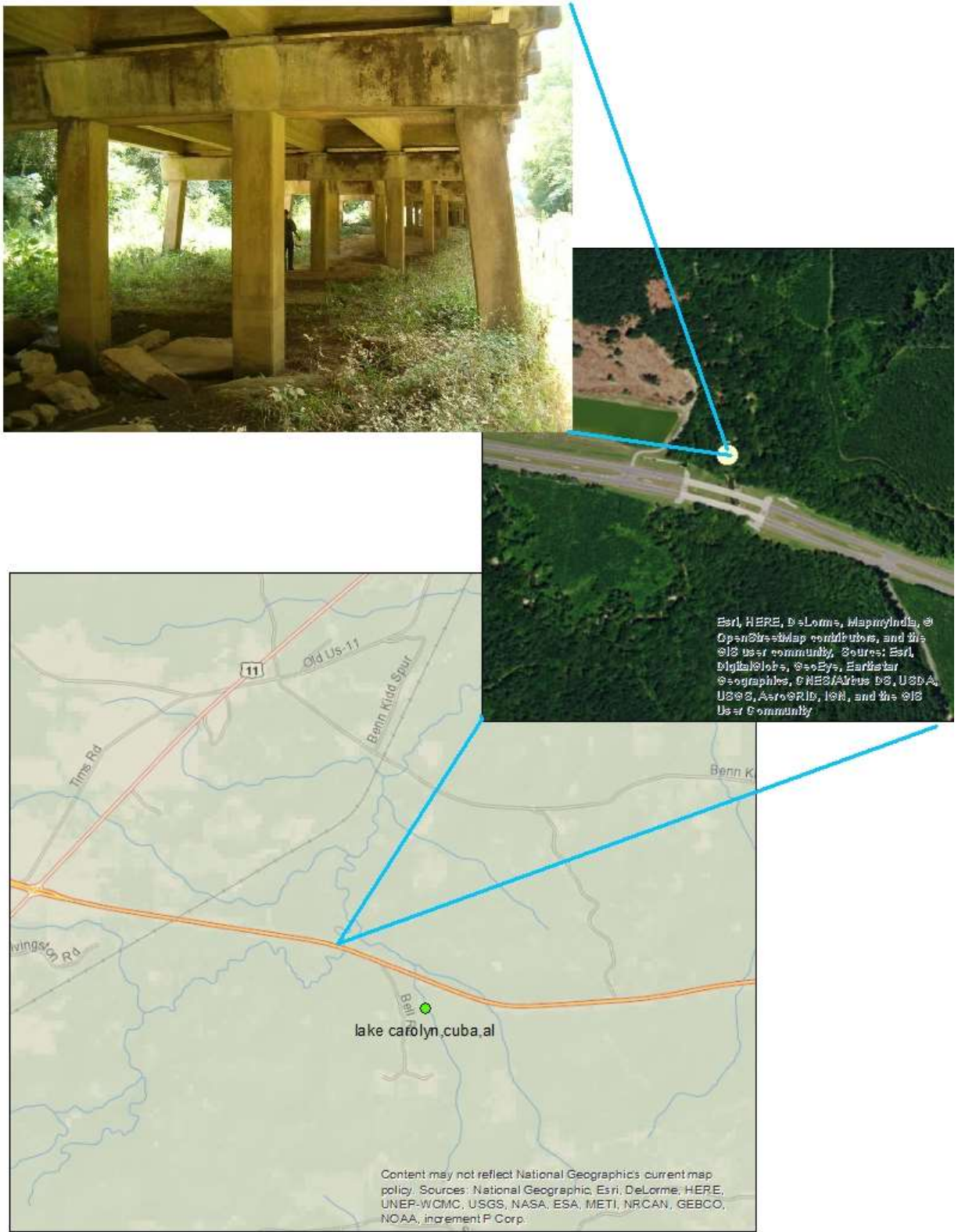


Figure 4.4 Location of Alamuchee Creek and bridge site characteristics.

4.3 SITE AND SOIL INFORMATION OF SPEAR CREEK

As an example, detailed site and soil information provided by ALDOT for the bridge at Spear Creek is summarized below, and similar information for other three bridge sites is also used for the study but not presented here. ALDOT, on September 18, 2008, started a project to replace the existing bridge on SR-10 over Spear Creek. WSPRO was used to compute the water surface profile of Spear Creek by ALDOT. The inputs and outputs data file of the WSPRO model along with the detail of the bridge stationing and boring values at different points around the bridge were used for this study. Figure 4.5 shows the cross section of the Spear Creek bridge: solid line at bottom elevation, the short dashed line shows projected scour depth at 100-year flow; and the long dashed line shows projected scour depth at 500-year flow. Those scour depths were calculated by ALDOT.

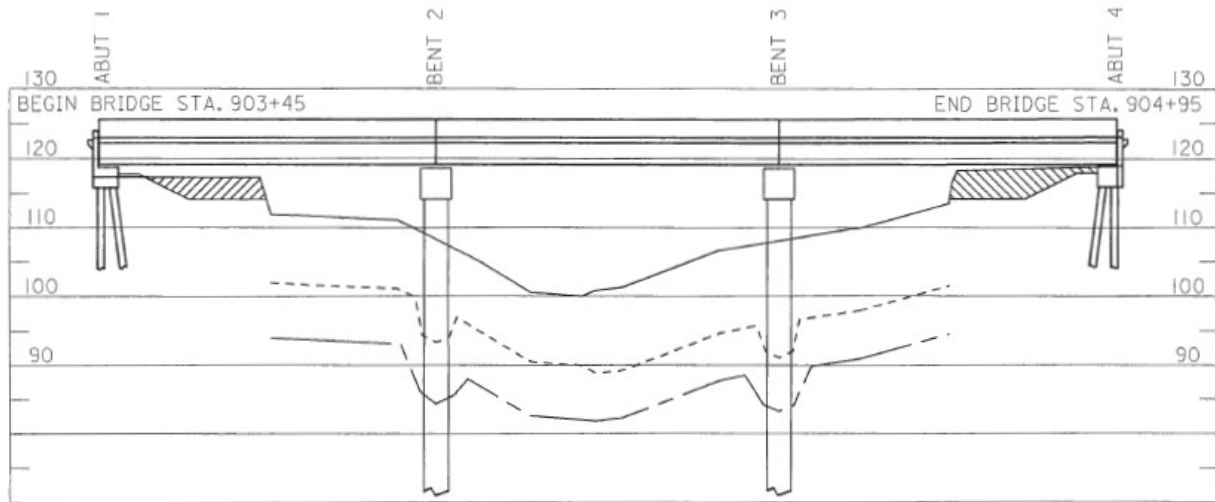


Figure 4.5 Cross-section of the bridge at Spear Creek with station number.

The cross-section of the bridge provides the information about the begin bridge station and end bridge station. Information about the spacing of the piers, abutments, the overbank and main channel was figured out from the station number provided in the cross section (Figure 4.5). The

bridge starts at the station no STA. 903+45 and ends at station STA. 904+95. The total length of the bridge is 150 ft. The distance between the beginning of the bridge and bent 2 (Figure 4.5) is 50 ft. Also, the spacing of bent 3 from bent 2 is 50ft. Bent is a part of a bridge substructure. For example bridge piers or piles.

Different boring locations with station number were provided in the ALDOT bridge report. Seven borings were done around the bridge site. All seven-boring stations around the bridge can be seen in the plan view of the bridge site (Figure 4.6).

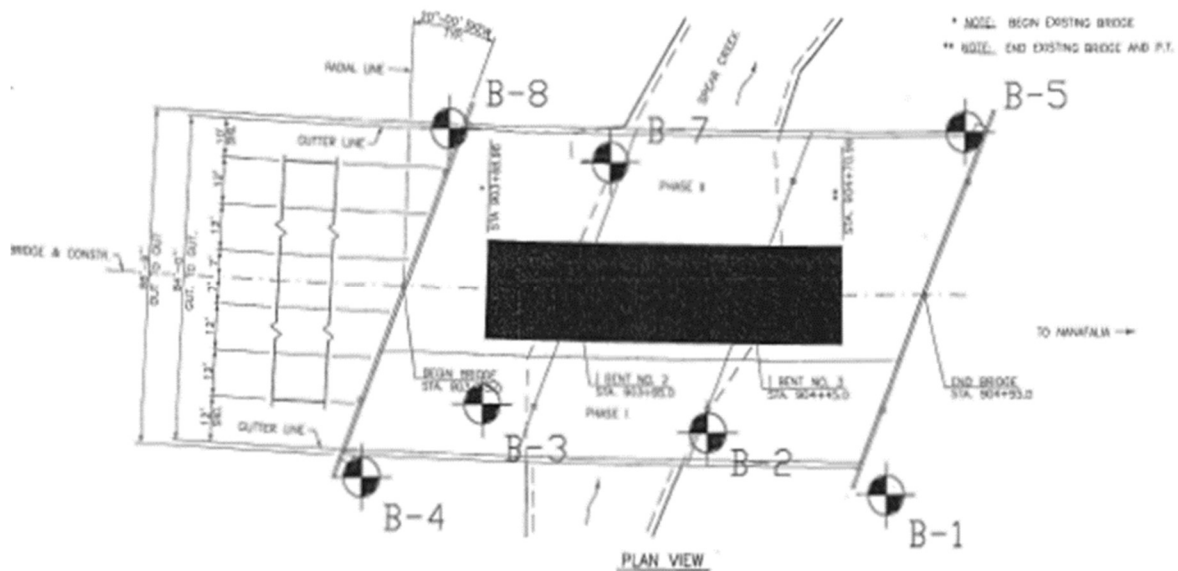


Figure 4.6 Plan view of the bridge side with boring location (Spear Creek).

To figure out the left overbank, main channel, and right overbank, a convention followed by HEC-RAS is applied. HEC-RAS reference manual states (Brunner 1995); from the view looking downstream, if the bank is in right then that is called as right overbank and if the bank is in left then that is called as left overbank. Additionally, the report provides the information about the boring station number with different D_{50} values (Figure 4.7) which helps in determining the location of the borings.

HEC-RAS convention and the station number provided in the report was used to determine the location of the borings as a LOB, CH, and ROB (Table 4.1) where LOB stands for left overbank, CH stands for channel and ROB stands for right over banks.

Table 4.1 Boring location with station number.

Boring NO	Station	Banks
B-01	STA 904+84	ROB
B-02	STA 904+34	CH/ROB
B-03	STA 903+69	LOB
B-04	STA 903+34	LOB
B-05	STA 905+06	ROB
B-07	STA 904+04	CH
B-08	STA 903+56	LOB

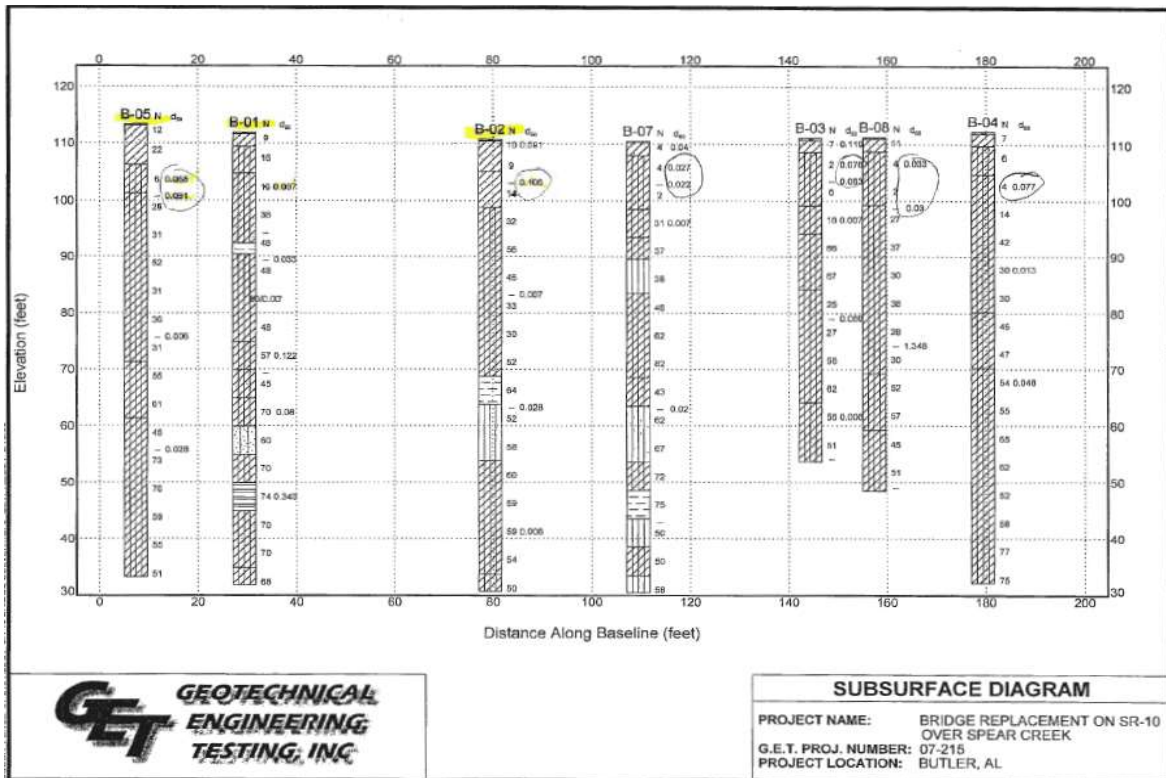


Figure 4.7 D₅₀ values along depth of boring stations (also tabulated in Table 4.2 and Table 4.3)

The peak discharge for 100-year recurrence interval was 3820 ft³/s estimated by ALDOT from USGS regression equation. The borings which are near the bridge were taken for calculation purpose. Boring no B-5 and B-1 are taken for the right overbank calculation. Boring no B-2 D₅₀ value is used for the main channel. Boring no B-3 D₅₀ value is taken for left overbank. From the report provided by the ALDOT, D₅₀ value along depth at four boring sites were extracted and D₅₀ values were tabulated in Table 4.2 and Table 4.3

Table 4.2 D₅₀ value along depth of boring B-1, B-2, B-3, B-5

Depth (ft.)	Boring No	D₅₀ (mm)	Average
0-1.2'	B-2	0.091	0.047
1.2'-8"		0.106	
8'-27.5'		0.007	
27.5'-47.5'		0.028	
47.5'-69.3'		0.006	
0-1'	B-3	0.119	0.055
1'-4.5'		0.076	
4.5'-7.5'		0.063	
7.5'-14.7		0.007	
14.7-32'		0.059	
32'-49'		0.006	

Table 4.3 D₅₀ value along depth of boring B-1, B-2, B-3, B-5 continued

Depth (ft.)	Boring No	D₅₀ (mm)	Average
0-7.5	B-1	0.037	0.123
7.5-21		0.033	
21-29		0.122	
29-39		0.08	
39-54.5		0.343	
0-6.5	B-5	0.065	0.0475
6.5-9.7		0.091	
9.7-34.7		0.006	
34.7-54.2		0.028	

Hydraulic parameters and scour depth for each soil layer were calculated using HEC-RAS developed for each bridge. Detailed information on the development of HEC-RAS model based on the WSPRO input data from ALDOT is presented and summarized in Appendix A. For this part of the study, WSPRO method included in HEC-RAS was used to calculate the water surface profile. The data required for the calculation of scour depth are all automatically updated in the hydraulic design function windows of HEC-RAS after the hydraulic simulation is completed. Contraction scour can be computed in HEC-RAS by either Laursen's clear water (Laursen 1963) or live-bed (Laursen 1962) contraction scour. To compute the contraction scour D_{50} value in mm and water temperature ($^{\circ}\text{F}$) were entered to compute the K_1 factor (Table 1.2). Table 4.4 shows the example data of Spear Creek for the hydraulic design function windows of HEC-RAS.

Table 4.4 Output from HEC-RAS

WSPRO method-(HEC-RAS) with contraction and expansion as 0.0 and 0.5 respectively			
	LOB	CH	ROB
Y_1	4.02	14.67	5.77
V_1	0.65	2.7	0.87
Y_o	3.98	15.54	5.18
Q_2	379.87	2739.17	700.96
W_2	43.18	25.72	47.66
D_{50}	0.03	0.047	0.055
Q_1	1527.66	1255.99	1036.36
W_1	583.98	31.72	205.78
Scour depth	6.54	17.53	6.14

Note: Y_1 = Average depth at the approach section, Q_2 = Discharge in the main channel at the contracted section, Q_1 = Discharge in the main channel at channel section, W_2 = Bottom width of the main channel at section 2, W_1 = Bottom width of the main channel at channel section

Y_2 = Existing flow depth in the main channel at section 2 before scour, D_{50} = Mean particle size diameter in mm, and V_1 = Velocity upstream of the river section.

HEC-RAS has the capabilities to choose the equation as default, i.e., the model will itself calculate the critical velocity and compare with the upstream velocity and choose the governing equations either as live-bed or clear water scour. Also, the user can force the model to calculate the scour on any conditions by changing the default value to either live-bed or clear water scour.

4.4 MULTILAYER METHOD

Based on the knowledge of the multilayer scour, this study proposed/used the multilayer idea to calculate the total scour depth using D_{50} of each soil layer along the depth. As shown in Table 4.2 and Table 4.3 D_{50} values for several soil layers are available. The soil layer thickness Δz_i for the i -th layer can be determined, and the first or surface layer is the layer 1 (Δz_1 for its thickness). Using D_{50} in each layer as HEC-18 input, one can find corresponding scour depth layer by layer. The flood erodes the first layer at first and moves on to the second layer if Δz_1 is less than the scour depth obtained using D_{50} for the first layer, and the same procedure will be repeated for the next layer below until predicted scour depth is less than the layer thickness. A cumulative feasible scour depth is the sum of the scour depth for all layers. To perform this analysis layer by layer a simple IF clause is used in EXCEL and the cumulative feasible scour depth considering D_{50} values at multiple soil layers is then calculated. The clause used is as follows:

If (scour depth $>$ Δz , Δz , scour depth)

where “scour depth” is the scour depth predicted by HEC-RAS using the WSPRO method and the D_{50} value of that layer as HEC-18 input, and Δz is the thickness of the soil layer. The flow chart for the calculation of scour depth is shown in Figure 4.8.

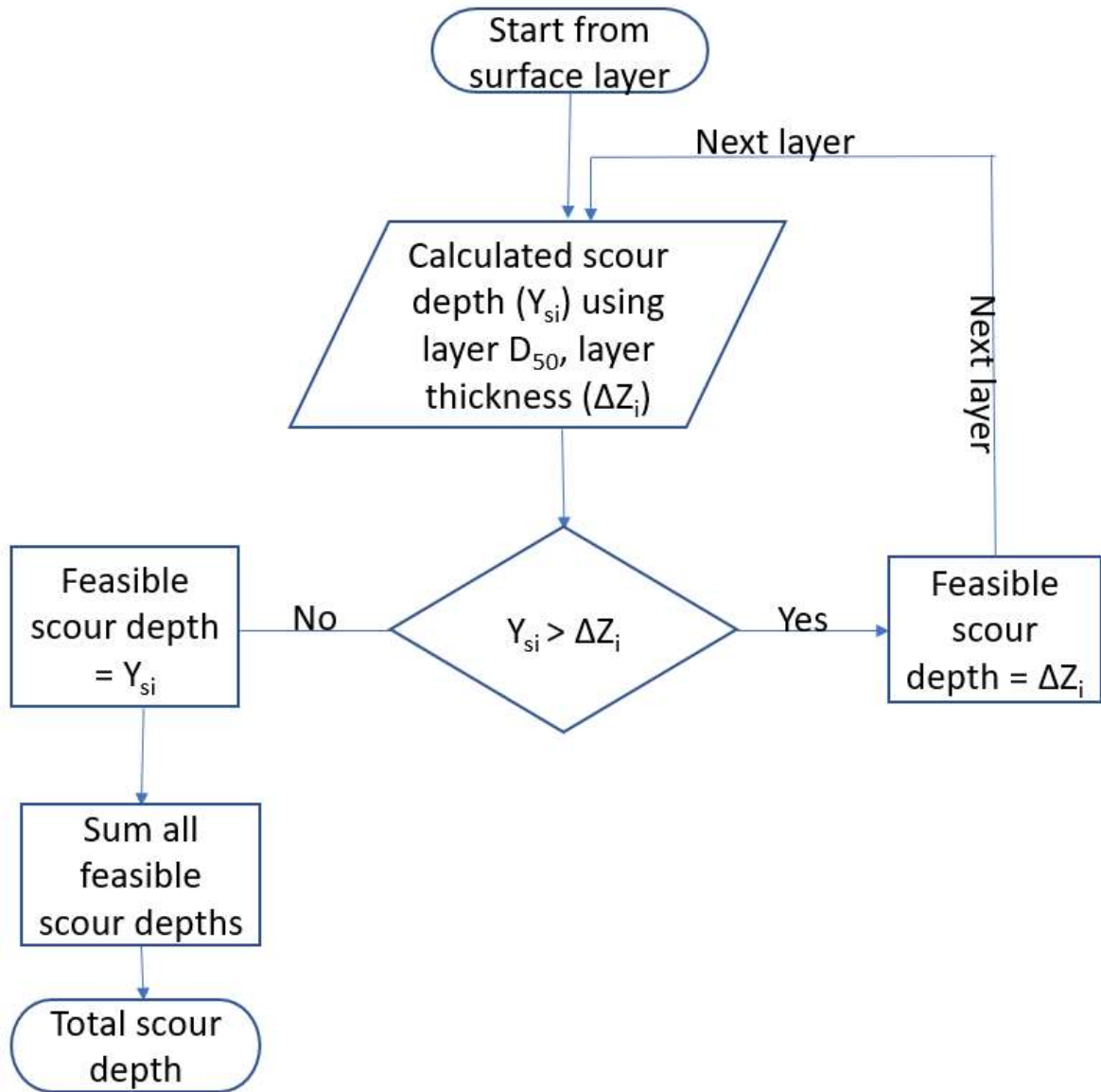


Figure 4.8 Flow chart for multilayer method

4.5 RESULTS FROM MULTILAYER METHOD

Table 4.5 shows the calculation of scour depth using multilayer method for Spear Creek. It includes the layer thickness (Δz), depth range, D_{50} , and computed scour depth from HEC-RAS for each layer in the channel, LOB, and ROB, respectively, in Spear Creek. When the scour depth calculated using the HEC-18 procedure (which is integrated into HEC-RAS) for a layer is less than

the layer thickness (Δz), that layer is eroded. In the main channel of Spear Creek, the erosion stops at the third layer when the layer thickness is 19.5 ft that is greater than predicted scour depth 17.5 ft. Therefore, the cumulative feasible scour depth in the channel is 25.5 ft (Table 4.5) using the multilayer method. The scour depth calculated by HEC-RAS using average D_{50} value (0.0476 mm) in the channel is 17.5 ft. The difference in scour depth calculated by the two methods is 8 ft.

The scour depth calculated by HEC-RAS using average D_{50} value (0.055 mm) in LOB is 4.9 ft whereas the scour depth calculated using the multilayer method is 10.9 ft when the erosion stops at the fourth layer. The difference in the calculated scour depth is 6 ft. Since two borings were done in ROB with layered particle size distribution, above multilayer method was applied to both stations first. At ROB1 station, the erosion (scour) stops in the first later but at ROB2 stops in the fourth layer. The average scour depth was then taken for the calculation for both cases. The average scour depth calculated by HEC-RAS using average D_{50} value in ROB is 7.65 ft whereas the average scour depth calculated using the multilayer method is 10.9 ft. The difference in the calculated scour depth is 3. 25 ft. This means, in Spear Creek, using HEC-18 and average D_{50} underestimates the scour depths in the channel, LOB and ROB (Table 4.5) in comparison to the scour depth determined by the multilayer method. The consequences of this could be the failure of the bridge causing loss of life and property.

Table 4.6 and Figure 4.9 present the differences in scour depths in between two methods in table and bar diagram, respectively. In the main channel, despite having different D_{50} values ranging from 0.007 to 0.028 mm, there is no change in the scour depth calculated from HEC-18 and D_{50} in each layer. Using these D_{50} values predicts the same scour depth of 17.5 ft. D_{50} value is first used to determine critical velocity in HEC-18. If the critical velocity determined is less than the average upstream velocity, then live bed scour equation (1.2) is used to calculate the scour

depth. There is no direct effect of D_{50} value in computing live-bed scour. Only the hydraulic parameters are used for calculating the scour depth in case of the live-bed scour condition. When computed critical velocity is greater than average upstream velocity then clear-water scour occurs. In the clear-water scour equation (1.3) D_{50} is one of the parameters used in calculating the scour depth. Therefore, in case of LOB and ROB where clear-water scour occurs, there is a change in computed scour depth with a change in D_{50} value. Based on the recommendation from an ALDOT engineer, the scour depth in overbank areas is always calculated as the clear-water scour when the overbank areas have much more vegetation and other obstructions that create a larger roughness and slower velocity. For the main channel, depending on the critical velocity and upstream velocity, it could be the live-bed or clear-water scour.

Table 4.5 Calculation of scour depth using multilayer method (Spear Creek)

Main Channel				
Δz (ft)	Depth (ft)	D_{50} (mm) B-2 (pier no3)	Scour depth (ft) (HEC-RAS) (Channel)	Scour depth (ft) (layer by layer) (Channel)
1.2	0–1.2	0.0910	17.5	1.2
6.8	1.2–8	0.1060	17.5	6.8
19.5	8–27.5	0.0070	17.5	17.5
20	27.5–47.5	0.0280	17.5	
	47.5–69.3	0.0060	17.5	
	Average	0.0476	17.5 ft	Total scour = 25.5 ft
Left Overbank (LOB)				
Δz (ft)	Depth (ft)	D_{50} (mm) B-3 (pier no2)	Scour depth (ft) (HEC-RAS) (LOB)	Scour depth (ft) (layer by layer) (LOB)
1	0–1	0.1190	3.1	1.0
3.5	1–4.5	0.0760	4.1	3.5
3.0	4.5–7.5	0.0630	4.5	3.0
7.2	7.5–14.7	0.0070	3.4	3.4
	14.7–32	0.0590	4.7	
	32–49	0.0060	3.4	
	Average	0.0550	4.9 ft	Total scour = 10.9 ft
Right Overbank Station 1 (ROB1)				
Δz (ft)	Depth (ft)	D_{50} (mm) B-1	Scour depth (ft) (HEC-RAS) (ROB1)	Scour depth (ft) (layer by layer) (ROB1)
7.5	0–7.5	0.0370	6.1	6.1
13.5	7.5–21	0.0330	6.1	
8.0	21–29	0.1220	5.8	
10.0	29–39	0.0800	7.2	
15.5	39–54.5	0.3430	3.0	
	Average	0.1230	5.7 ft	Total scour = 6.1 ft
Right Overbank Station 2 (ROB2)				
Δz (ft)	Depth (ft)	D_{50} (mm) B-5	Scour depth (HEC-RAS) (ROB2)	Scour depth(ft)(layer by layer) (ROB2)
6.5	0–6.5	0.0650	7.9	6.5
3.2	6.5–9.7	0.0910	6.7	3.2
25.0	9.7–34.7	0.0060	6.1	6.1
19.5	34.7–54.2	0.0280	6.1	
	Average	0.0475	9.6 ft	Total scour = 15.8 ft
Average over two ROB stations			7.65 ft^a	10.99 ft^b

Note: ^a. Average scour depth at ROB1 and ROB2 (B-1 and B-5) from HEC-RAS = 7.65 ft. ^b Average scour depth at ROB1 and ROB2 (B-1 and B-5) using layer by layer method = 10.99 ft.

Table 4.6 Differences in scour depth using average D₅₀ and the multilayer method (Spear Creek)

Locations	Average D ₅₀ (mm)	Scour depth (ft)				
		Using average D ₅₀	By layers	Difference ¹	% Error ²	% Difference ³
LOB	0.0550	4.9	10.9	-6.0	55.0	76.0
CH	0.0476	17.5	25.5	-7.9	31.2	37.0
ROB1	0.1230	5.7	6.1	-0.4	6.6	6.8
ROB2	0.0475	9.6	15.8	-6.2	39.2	48.8
Average of ROB1 and ROB2(ROB)		7.6	10.9	-3.2	29.8	35.0

Note: ¹ – Difference is the scour depth determined using average D₅₀ value minus the scour depth by the multilayer method, ² - % error is calculated by assuming the scour depth by the multilayer method as “exact or more accurate estimate”, ³ - % difference is calculated as absolute value of the difference dividing by the average scour depth by the two methods and converting that to a percentage value. For example, at LOB, ABS (-6.0)/ ((4.9+10.90)/2) *100% = 76.0 %.

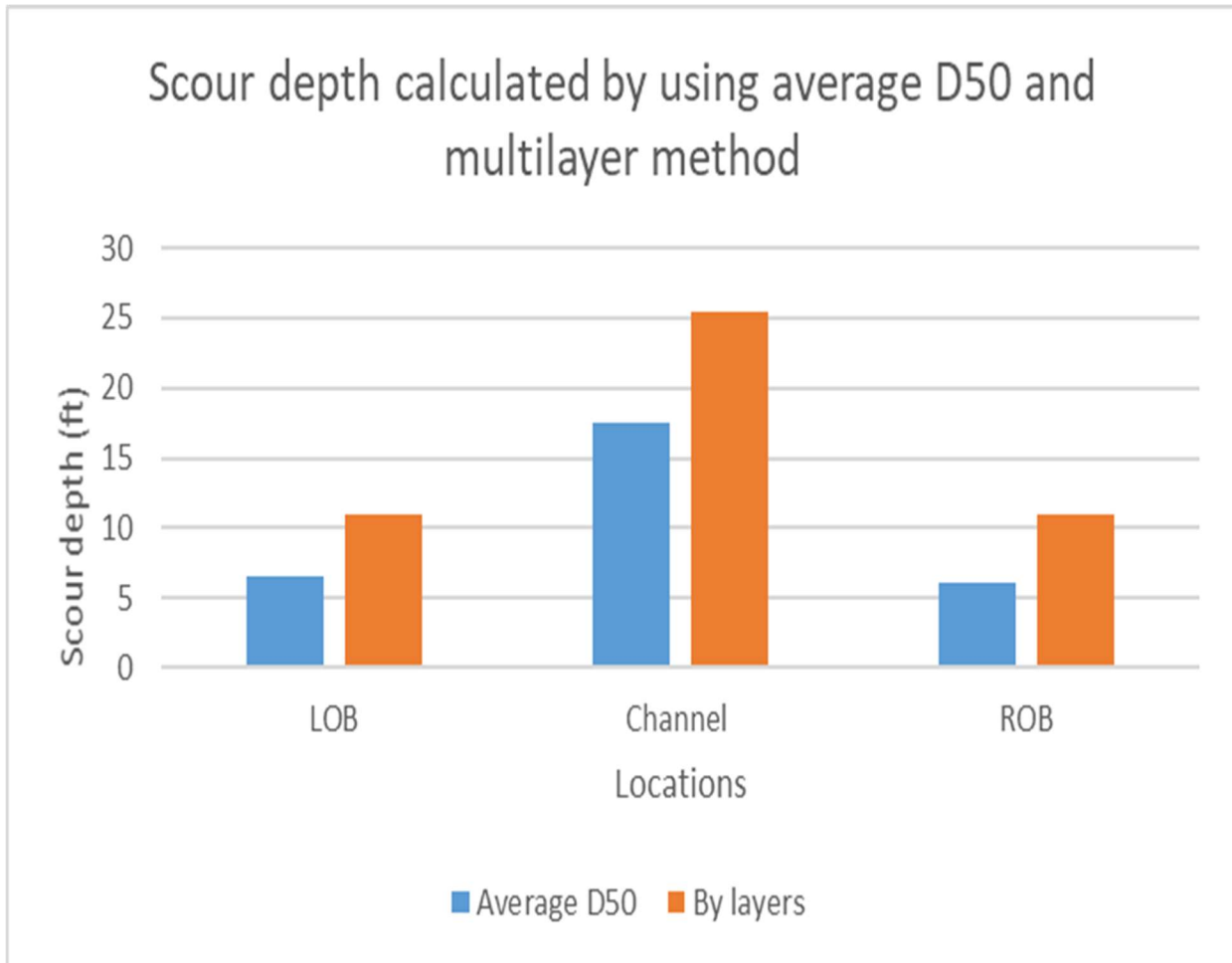


Figure 4.9 Bar diagram showing difference in scour depth using average D₅₀ and the multilayer method

The same procedure and method were also applied for other three bridge cases (Valley Creek, Pintalla Creek, and Alamuchee Creek) to analyze the difference in scour depth using average D₅₀ and the multilayer method (using different D₅₀ layer by layer). For the bridge over Valley Creek, the D₅₀ value of LOB and ROB were on the report provided by ALDOT. Some of the D₅₀ values were in 200-** format, for example, 200-56.9; this means 56.9 % of soil sample pass through the 200-sieve size. The maximum particle size that can pass through 200 sieves is 0.075 mm. According to Unified Soil Classification System percentage passing the No 200 sieve

is considered as fine-grained soil (clay and silt) which is considered as cohesive. For this kind of D_{50} format, the D_{50} value was assumed as 0.0750 mm. In Table 4.8 one depth layer (0–5 ft) at the surface was added and D_{50} value in the layer was assumed as D_{50} in the next layer below. This is because the multilayer method determines whether or not the erosion could be progressed layer by layer starting from the surface layer and requires continuous depth layers. Table 4.7 presents the calculation of scour depth using average D_{50} value and layer-by-layer D_{50} values (multilayer). The scour depth at LOB calculated using average D_{50} is equal to 11.0 ft and less than the scour depth (20.0 ft) calculated using layer-by-layer D_{50} values. The difference in scour depth calculated by the two methods is 9.0 ft (Table 4.7). The scour depth at ROB calculated using average D_{50} (12.0 ft) is also less than the scour depth calculated using layer-by-layer D_{50} values (20.0 ft). The difference in the calculated scour depth is 8.0 ft (Table 4.7). Figure 4.10 presents the differences in scour depth calculated from two methods in a bar diagram. In this case, HEC-18 underestimate the scour depth.

Table 4.7 Calculation of scour depth using multilayer method (Valley Creek)

Left Overbank (LOB)					
Δz (ft)	Depth (ft)	D ₅₀ information	D ₅₀ (mm)	Scour depth (ft) (HEC-RAS) (LOB)	Scour depth (ft) Layer by layer(LOB)
5	0–5		0.150 ¹	9.0	5
5	5–10		0.150	9.0	5
5	10–15	200–56.9	0.075	12.5	5
5	15–20	200–95.5	0.075	12.5	5
	Average		0.100	11.0	Total scour depth = 20.0 ft
Right Overbank (ROB)					
Δz (ft)	Depth (ft)	D ₅₀ information	D ₅₀ (mm)	Scour depth (ft) (HEC-RAS)	Scour depth (ft) Layer by layer
5	0–5		0.075 ¹	12.0	5
5	5–10	200–52.3	0.075	12.0	5
5	10–15		0.075	12.0	5
5	15–20	200–58.0	0.075	12.0	5
	Average		0.075	12.0	Total scour depth = 20.0 ft

Note: ¹ – D₅₀ was assumed as D₅₀ from the layer below

The percent differences of scour depths at LOB and ROB determined using average D₅₀ value and the multilayer method are 58.1 % and 50.0 %, respectively. The error percentage of

scour depth assuming multilayer method as the exact value at LOB and ROB are 45 % and 40 % respectively.

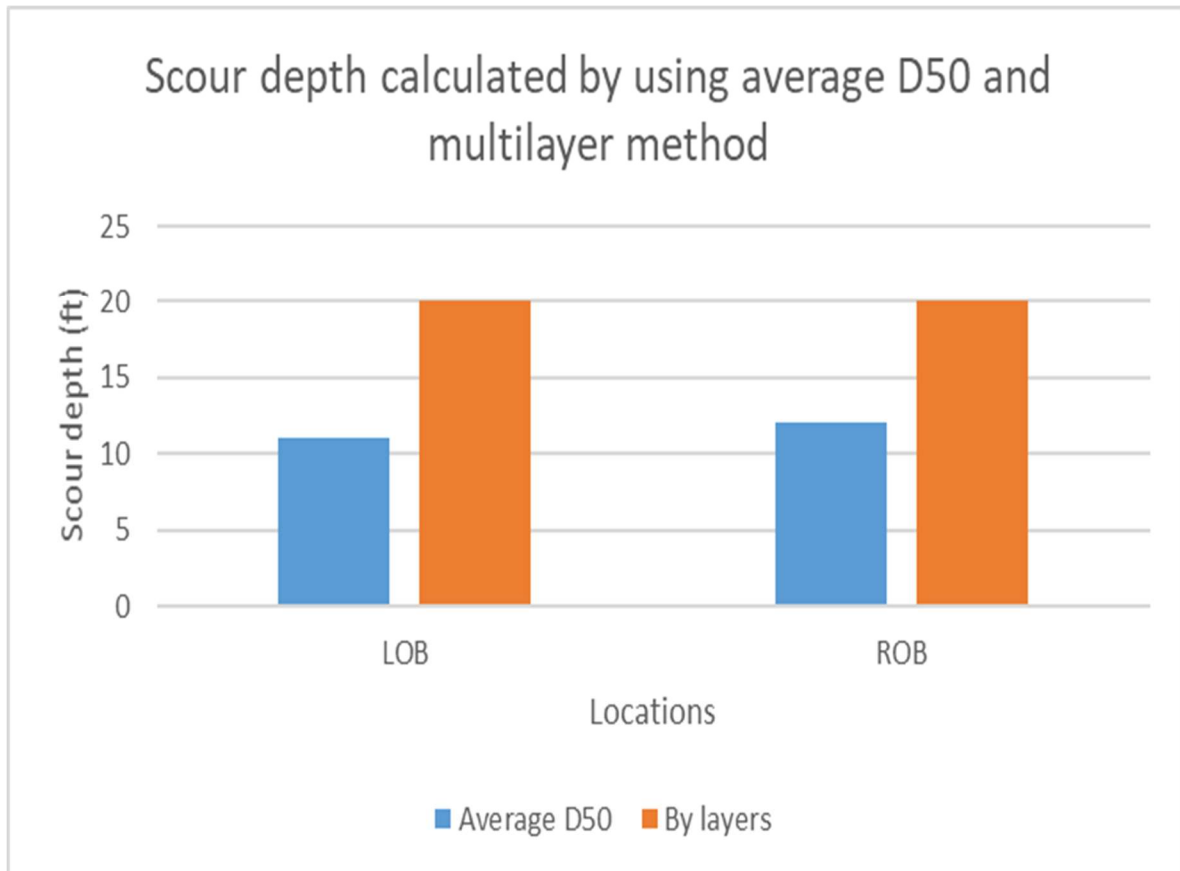


Figure 4.10 Bar diagram showing the difference in scour depth from using average D_{50} and multilayer.

In the report provided by ALDOT for Alamuchee Creek, the D_{50} values were reported only for the LOB at four separate layers. It means depths with D_{50} data are not continuous, and this is different from the bridge site at Spear Creek (Table 4.5). In Table 4.8 three depth layers were added and D_{50} values in these layers were estimated as the average of D_{50} for layers above and below. Table 4.8 presents the calculation of the scour depths using layer-by-layer D_{50} values

(including three layers with estimated D_{50}) and average D_{50} value. The scour depth calculated using layer-by-layer D_{50} values is 15.0 ft and less than the scour depth (24.9 ft) calculated using average D_{50} value. The difference in scour depth calculated using two methods is 9.9 ft.

Table 4.8 Calculation of scour depth using multilayer method (Alamuchee Creek)

Δz (ft)	Depth (ft)	D_{50} (mm)	Scour Depth (ft) HEC-RAS (LOB)	Scour Depth (ft) Layer by layer (LOB)
1.5	0–1.5	0.0826	29.0	1.5
2.0	1.5–3.5	0.0803 ^a	29.3	2.0
1.5	3.5–5.0	0.0781	29.7	1.5
3.5	5.0–8.5	0.1479 ^a	23.4	3.5
1.5	8.5–10.0	0.2178	20.1	1.5
3.5	10.0–13.5	0.1700 ^a	22.2	3.5
1.5	13.5–15.0	0.1223	25.1	1.5
	Average	0.1252	24.9 ft	15.0 ft^b

Note: ^a – D_{50} was estimated as average D_{50} from layers above and below, ^b - % difference of scour depths determined using average D_{50} value and the multilayer method is 49.6 %. The error percentage in scour depth using average D_{50} value and the multilayer method is 66.0%.

In the report provided by ALDOT for Pintalla Creek, the D_{50} value was reported only for the LOB. The D_{50} values were not continuous layer by layer. A continuous layer by layer D_{50} value was created by averaging the D_{50} value above and below the missing layer. At some depths two D_{50} values were reported (for example 3.5-5.0 ft). The average of the two D_{50} values was taken for the calculation.

Table 4.9 presents the calculation of scour depth by using average D_{50} value and layer by layer D_{50} value. The scour depth calculated using average D_{50} value (HEC-18) is less than the scour depth calculated using layer by layer D_{50} values with a difference of 10.2 ft. In this case, HEC-18 underestimate the scour depth.

Table 4.9 Calculation of scour depth at LOB using multilayer method (Pintalla Creek)

Δz (ft)	Depth (ft)	D ₅₀ (mm)	D ₅₀ (mm)	Average D ₅₀ (mm)	Scour Depth (ft) HEC-RAS	Scour Depth (ft) Layer by layer
3.5	0–3.5			0.235 ^a	4.8	3.5
1.5	3.5–5	0.1300	0.3400	0.2350	4.6	1.5
3.5	5–8.5			0.1638 ^b	4.8	3.5
1.5	8.5–10	0.0750	0.1100	0.0925	4.8	1.5
3.5	10–13.5			0.0929 ^b	4.8	3.5
1.5	13.5-15	0.0750, 0.1300	0.0750	0.0934	4.8	1.5
	Average		0.1336		4.8 ft	15 ft^c

Note: ^a – D₅₀ was assumed as D₅₀ from the layer below, ^b – D₅₀ was estimated as average D₅₀ from layers above and below, ^c - % difference of scour depths determined using average D₅₀ value and the multilayer method is 103.0 %. The error percentage from these two methods is 68.0 %.

4.6 SCOUR DEPTHS USING AVERAGE D₅₀ WITH AND WITHOUT OUTLIERS

In the report provided by ALDOT for four bridge cases (except Pintalla Creek), the scour depth is calculated using the average D₅₀ after removing some outliers of D₅₀. The outlier D₅₀ are those D₅₀ which has a large difference from the other D₅₀ values. According to the ALDOT, the outliers are not used while doing the average of the D₅₀. In this section, the scour depths calculated from ALDOT (using average D₅₀ without outliers) and using average D₅₀ using all available D₅₀ data are compared for three bridge cases. ALDOT used the envelope curve to calculate the scour depth for Pintalla Creek. The locations (LOB, CH, ROB) where the D₅₀ information was provided in the report is used for the comparison.

From the cross section (Figure 4.5) and plan (Figure 4.6) view of Spear Creek D₅₀ the borings locations were selected as a LOB, ROB, and Channel (Table 4.1).

Table 4.5 presents the calculation done for the multilayer method and using average D₅₀ from all available D₅₀ data. The scour depths calculated from using average D₅₀ without and with

outliers are presented in Table 4.10. The scour depth calculated from the average D₅₀ removing outliers for Spear Creek in LOB and ROB is greater than the scour depth calculated using all D₅₀ data. In a channel where live-bed scours occur the scour depth calculated using all D₅₀ data is greater than using average D₅₀ removing outliers with a difference of 9.7 ft. The average D₅₀ value for the channel was not found in the report provided by the ALDOT so it was left blank.

Table 4.10 Comparison of scour depths in Spear Creek determined from average D₅₀ without and with outliers

Locations	Average D ₅₀ (mm)		Scour depth (ft)		Difference ¹	% Difference ²
	Removing outliers	Using all data	Removing outliers	Using all data		
LOB	0.030	0.055	10.3	4.9	5.4	71.05
CH	-	0.0476	7.8	17.5	-9.7	76.68
ROB	0.055	0.1230 0.0475	12.1	7.65	4.45	45.06

Note: ¹ - Difference is calculated as scour depth using D₅₀ removing outliers minus the scour depth calculated using all D₅₀ data, ² - % difference is the absolute difference divided by the average of two values. For example, abs (5.4)/average (10.3, 4.9)*100% = 71.05 %

For valley Creek, the D₅₀ value in LOB and ROB was provided in a report by ALDOT. Table 4.7 presents the calculation of scour depth using multilayer D₅₀.

Table 4.11 presents the comparison of the scour depth calculated from using average D₅₀ removing outliers and using all D₅₀ value. The difference in scour depth in LOB and ROB is 7 ft with a percentage difference of 48.28 % and 6 ft with a percentage difference of 40 %.

Table 4.11 Comparison of scour depth in Valley Creek determined from average D₅₀ without and with outliers

Locations	Scour depth (ft)		Difference	% Difference
	Removing outliers (ft)	Using all data ₀ (ft)		
LOB	18	11	7	48.3
ROB	18	12	6	40.0

Table 4.12 presents the comparison of scour depth calculated using average D_{50} removing outliers and using all D_{50} data for Alamuchee Creek. The difference in scour depth is 7.9 ft with a percentage difference of 37.71 %.

Table 4.12 Comparison of scour depth in Alamuchee Creek determined from average D_{50} without and with outliers

Locations	Scour depth (ft)		Difference	% Difference
	Removing outliers (ft)	Using all data (ft)		
LOB	17	24.9	-7.9	37.7

4.7 DISCUSSION

In this study, HEC-RAS model using only WSPRO method was used to calculate the hydraulic parameters required to calculate the scour depth. All the required data to run the HEC-RAS model were taken from the WSPRO input data file. Then the scour depths determined by three methods were discussed and compared. The first method used the average D_{50} from all available D_{50} , the second method considered/used D_{50} for all depth layers to compute the scour depths layer by layer and then determine the feasible cumulative scour depth, and the third method used the average D_{50} after removing outliers of D_{50} . The depths value taken for this study was obtained from the ALDOT report provided. The author of this study has no idea why ALDOT collect soil samples at those depths and determine D_{50} value. The ALDOT experienced engineer used the third method to determine the scour depth. If the calculated scour depth is unusually large (much larger than typical scour in the study region), the USGS envelope method was used by ALDOT to estimate the final scour depth. One could consider that the first method was implemented by a no-experienced engineer who has no engineering judgment to distinguish possible outliers of D_{50} .

D_{50} values along the different depths were used solely to calculate the scour depth in HEC-RAS and then “IF” clause was used to determine the feasible scour depth in each layer. The summation of all the feasible scour depth from each layer gives the total scour depth in the multilayer method. Multilayer methods need all layer D_{50} values to compute the scour depth. Since D_{50} values in all layers are used to calculate the scour depth, the multilayer method predicts the scour depth more accurate than other methods. However, if there is not a complete continuous layer D_{50} value it is required to assume or estimate D_{50} value based on engineering judgment (Table 4.7 and Table 4.8). This could create some uncertainty in the scour depth calculated. Also, if the layer thickness (Δz) with certain D_{50} value is not defined accurately it could affect the cumulative scour depth determined by the multilayer method. For example, if the layer thickness is 3 ft instead of 5 ft with a scour depth of 4 ft calculated from HEC-18, then according to the multilayer method it would erode first 3 ft and moves on to the second layer which would change the scour depth. The maximum cumulative scour depth determined by the multilayer method is the maximum depth of all soil layers with D_{50} when predicted scour depth for each layer using its D_{50} is always larger than the layer thickness.

This study shows the real scenario of how the soil could erode layer by layers. Each soil layers D_{50} have a role in determining the final scour depth. Taking only one average D_{50} value and using that to calculate the scour depth could either overestimate or underestimate the scour depth. If the scour depth is underestimated, it could lead to loss of lives and property. If the scour depth is overestimated, it could cause extra millions of dollars to design the bridge structure (piers). This study leads to the finding that using one average D_{50} value and not considering the nature (cohesive and non-cohesive) of soil could result in different scour depth. Also, this study suggests applying

multilayer methods in calculating the scour depth so that the scour depth calculation could be more accurate.

From the analysis, it can be said that the scour depth calculated from HEC-18 using average D_{50} value could be less than (Spear, Valley, and Pintalla Creek) or greater (Alamuchee Creek) than the scour depth calculated from using the multilayer method (different layer D_{50}). It means that the top layer D_{50} value along with the thickness of the layer plays an important role in scour depth. Scour depth calculated from the average D_{50} value in HEC-18 results in less scour depth as compared to scour depth obtained from using layer by layer D_{50} values in Spear Creek. There is a minimum scour depth difference of 4.36 ft in left overbank (LOB) to a maximum difference of 8.97 ft in the main channel (CH). This means that HEC-18, in this case, is underestimating the scour depth which could result in bridge failure and loss of lives and properties. However, in case of Alamuchee Creek, the scour depth calculated from HEC-18 using average D_{50} value is 24.9 ft, which is greater than the scour depth (15 ft) calculated from using a layer by layer D_{50} . It means that in this case, HEC-18 overestimate the scour depth which results in loss of billions of dollars and mostly the valuable time.

From this study, it is now evident that using only average D_{50} value doesn't accurately predict the scour depth. The D_{50} values of all layers should be considered while calculating the scour depth. Using the layer by layer D_{50} values to calculate the scour depth and summing up all the feasible scour depth could give most accurate scour depth rather than using only average D_{50} value.

In this study, only the average D_{50} value was simply the arithmetic average of D_{50} values in all the layers and the scour depth was calculated. To determine a more accurate or representative D_{50} for a HEC-18 application other techniques or methods could be applied. For example, the

average could be done up to the layer where the scour would stop. In the case of Spear Creek in ROB1 the scour depth obtained using first layer D_{50} value is 6.1 ft which is less than the layer thickness 7.5 ft. This means scour would stop at first layer. The average D_{50} for this part should be only first layer D_{50} value. The first layer D_{50} value could be used to calculate the scour depth from HEC-18 and compare it to the multilayer method for more accurate results. Therefore, it requires an iterative method to compute average D_{50} using D_{50} data up to certain depth, calculate the scour depth, and then update average D_{50} using the scour depth for the next iteration of the calculation. Also, the weighted average D_{50} with layer thickness could be more accurate or representative D_{50} .

For using a multilayer method the D_{50} value should be obtained lower than the scour depth. Also, to figure out the scour depth using average D_{50} value certain layer D_{50} is needed. There arises a question about how deep the boring should be done to obtain D_{50} in different layers for a more accurate prediction of scour depth. Where should the boring be stopped in earth surface? For example, in Alamuchee Creek, D_{50} was available in seven layers up to 15 ft (a few D_{50} between layers were estimated). The total scour depth determined by the multilayer method was 15 ft which is limited by the unavailability of lower layer D_{50} values. Using average D_{50} determined from 15 ft of the soil layers, HEC-18 predicted a scour depth of 24.9 ft (Table 4.8). Without knowing what type of soils below 15 ft, the prediction of 24.9 ft is also not reliable. Therefore, both the scour depth predicted from using average D_{50} and using multilayer D_{50} doesn't accurately represent the scour depth in Alamuchee Creek.

Chapter 5 **COMPARISION OF HYDRAULIC PARAMETERS AND SCOUR DEPTH OBTAINED FROM WSPRO AND HEC-RAS MODEL**

5.1 INTRODUCTION

Current practice to evaluate the scour depth is heavily influenced by FHWA's technical publications HEC-18 and HEC-20 (Arneson et al. 2012; Lagasse et al. 2012). HEC-18 methods need several hydraulic parameters to calculate the scour depth (Equations 1.2 and 1.3). There are different models which could be used to obtain hydraulic parameters of a stream with a bridge crossing. In current practice, WSPRO and HEC-RAS are two computer models which are used to obtain the hydraulic parameters. These two methods solve the energy equation based on standard step methods and/or momentum equation for gradually varied flow. Both models have their own assumptions and procedures to calculate the water surface profiles.

WSPRO is a computer model which was developed 30 years back from now by FHWA. It works on DOS version. All the inputs are in text format. It works on a column based Fortran code which could be daunting if failed to enter the data in a correct format (Arneson and Shearman 1998). HEC-RAS is the newest model which has graphics users interface (GUI) and easy to operate. HEC-RAS integrates the WSPRO method as one of the methods to calculate the energy or momentum losses to determine water surface profile through the bridge. There are four methods included in HEC-RAS to calculate the water surface profiles. The user can select any one or all methods to calculate the losses through the bridge. If the user selects more than one methods,

the program will give the greatest energy loss at section 3 through the bridge as the highest computed upstream energy (Brunner 1995). This function of HEC-RAS was used to compare the hydraulic parameters from several methods. In this study, the hydraulic parameters which are needed in HEC-18 to compute the scour depth are compared in different scenarios. In addition, water surface elevation obtained from both the models are also compared.

Hydraulic parameters are one of the important aspects which can influence the scour depth computation using HEC-18 equations (1.2) and (1.3). The critical velocity in HEC-18, i.e., equation (3.5) is first used to determine whether the live-bed scour or the clear-water scour occurs at the bridge site (Figure 1.5), therefore, the critical velocity plays a critical role in determining the scour depth. The equation (3.5) is used in HEC-18 to compute V_c as a function of y , the average depth of flow upstream of the bridge contraction. The HEC-18 report (Arneson et al. 2012) lacks to provide a clear definition of the average depth y . For an open channel flow, average depth can be interpreted in two ways: flow depth or the hydraulic depth (Chow 1959). The flow depth can be considered as the average value of water depths along the channel cross-section, obtained by the differences between the water surface elevations and the bed elevations. The average depth of a channel can also be computed from average depths of the left and right overbank areas and main channel. Sometimes the flow depth can also be considered the maximum water depth over the cross-section. The hydraulic depth (D) is defined as the ratio of area (A) to the top width (T) of the flow: $D = A/T$.

The hydraulic depth can be computed for left and right overbank areas, main channel, and for the whole channel section. These definitions give different values on y for Equation (3.5). HEC-18 lacks clear instruction in noting down which average depth to be used for the calculation

of the scour depth. The average depth y at the upstream section is an essential hydraulic parameter which is also used in the calculation of contraction scour and pier scour.

HEC-RAS (Brunner 2001) manual indicates that it follows the outline mentioned in HEC-18 for the calculation of the scour depth. HEC-RAS uses the hydraulic depth D in section 4 (Figure 1.4) as the average depth y in Equation (2.6) to perform the scour depth computation. Also, ALDOT is using hydraulic depth as the average depth. This is an essential knowledge that an entry-level engineer should possess which HEC-18 manual lacks to provide.

When HEC-18 is used, typically scour depths are calculated for overbank areas and main channel separately. Equations (1.2) and (1.3) for HEC-18 use average water depths, flows and widths at upstream approaching and bridge-crossing sections for determining the live-bed and clear-water scour depth. Even the same total flow rate over the cross section is given, different hydraulic models may distribute the total flow differently in left and right overbank areas and main channel, which could result in different scour depths in different parts of the channel. This part of the study is to evaluate and illustrate the uncertainty of the scour depth calculation due to hydraulic parameters calculated/simulated by two common hydraulic models (WSPRO and HEC-RAS).

5.2 METHODOLOGY

HEC-RAS was used to obtain the hydraulic parameters needed to calculate the scour depth. For the development of the HEC-RAS model, all the necessary data were taken from one of the report (Spear Creek) provided from ALDOT. Spear Creek data were used to develop the HEC-RAS model (Appendix A). In this part of the study, different sets of model parameters were changed and the differences in the hydraulic parameters and eventually differences in the scour were analyzed. Different sets of model parameters which were changed are as follows:

1. Methods to compute the water surface profile: Energy or WSPRO method
2. Change in expansion and contraction coefficients
3. Changing the expansion and contraction lengths based on HEC-RAS methodology
4. Including the ineffective flow areas in the model

This is not a sensitivity analysis since model coefficients/parameters were not changed or tested based on their natural variations. This part of the study demonstrated and examined the impact of the model configuration based on various technical guidance on the calculation of hydraulic parameters and then the scour depth near a bridge site, which is called uncertainty of hydraulic parameters here. This was not previously studied before by others.

1. Methods to compute the water surface profiles: HEC-RAS or WSPRO method

HEC-RAS has the capabilities to run the model with different methods. As stated earlier there are four methods to calculate the low flow from HEC-RAS. Two methods; HEC-RAS's standard energy method and WSPRO method were used for this study to compare the data. In theory WSPRO method also uses basic flow energy equation with certain special considerations and treatments. Various differences in applying energy equation between HEC-RAS and WSPRO were analyzed and summarized in section Appendix A. Results from WSPRO method presented in Chapter 1 were derived from the text output from running the WSPRO DOS program with text input file. They are not from HEC-RAS using the WSPRO option for bridge simulation method.

2. Change in expansion and contraction coefficients

The default value of expansion and contraction coefficients varies according to the model used. HEC-RAS has its own methodology for the use of contraction and expansion coefficient. As per the HEC-RAS manual (Brunner 2001), the contraction and expansion

coefficient far upstream and downstream the bridge should be 0.1 and 0.3, respectively, when there is no bridge affecting flow contraction and expansion. Whereas near the vicinity of the bridge the contraction and expansion coefficient are 0.3 and 0.5 respectively. WSPRO has its own default value of 0.0 and 0.5 for contraction and expansion coefficient respectively. The contraction and expansion coefficients were changed accordingly and the change in the hydraulic parameter and ultimately the change in scour depth was analyzed.

3. Changing the expansion and contraction length based on HEC-RAS methodology

WSPRO has its own method to select the expansion and contraction length. For the development of the HEC-RAS model, the lengths were first taken from the WSPRO model input data file. HEC-RAS has its own methodology to define expansion and contraction lengths. The change in the hydraulic parameters due to the change in the expansion and contraction length was analyzed.

4. Including the ineffective flow areas in the model

When there is an obstruction to the flow by any inbuilt structure like bridge the flow pattern is affected by the obstruction. The ineffective flow area is the area where there is water but there is no conveyance, i.e., the velocity is zero at that location in the direction of flow. In HEC-RAS, the user can quantitatively configure the ineffective flow areas. For Spear Creek HEC-RAS model, the ineffective flow area is set at stations 510 and 845 with elevation 118 ft. The model was run for the WSPRO method with coefficients of contraction and expansion as 0.0, 0.5. These set of coefficients is used just to mimic the coefficient used in WSPRO program.

In the overbank areas, due to the presence of dense vegetation, it is assumed that these areas have high roughness values. Due to the high roughness of overbank areas the velocity

upstream of the flow is typically less than the critical velocity, which means that there is always a clear-water contraction scour in the overbank areas. In the channel section, the default option was used, which lets the program to determine whether a clear-water or live-bed scour will occur. The equations (1.3) and (1.2) for the clear-water scour and the live-bed scour include some constant values such as C_u and D_m . These parameters are constants for all scenarios so for the comparisons only the discharge at upstream approach section (Q_1) and contraction section (Q_2) and width at approach (W_1) and contraction section (W_2) is taken. Average depth at approach section ($Y_1 = Y_4$ in Figure 1.4) and average depth prior to scour at contraction section ($Y_0 = Y_{BU}$ in Figure 1.4) are found to be different by small percent so those values were not taken for the calculation purpose. For simplicity,

$$\left(\frac{Q_2^2}{W_2^2}\right)^{3/7} - \text{Clear water scour} \quad (5.1)$$

$$\left(\frac{Q_2}{Q_1}\right)^{6/7} * \left(\frac{W_1}{W_2}\right)^{K_1} - \text{Live bed scour} \quad (5.2)$$

In Figure 1.4 used for HEC-RAS, the upstream approach section is the section 4 (*i.e.*, $Q_1 = Q_4$), and the contraction section is the BU section (*i.e.*, $Q_2 = Q_{BU}$). The exponent K_1 has three values 0.59, 0.64, and 0.69 based on Table 1.2, which is affected by the ratio of shear velocity and fall velocity (a function of D_{50}).

5.3 WSPRO INPUTS FOR HEC-RAS MODEL DEVELOPMENT

WSPRO model works in DOS mode (Fortran 77 program). So, all the data inputs are coded in a certain fashion (ASCII character encoding format). Each column has its own meaning. Individual data items must be separated either by a comma; one or more blanks or any combination

of a comma and one or more blanks. The row with * is skipped by the program and the user can provide other notes and information for the model in the * rows. The header of each input line, for example, XS, GR etc. has its own meaning. The users should have a well-known background in surface water hydraulics to understand and write the input code in the required format. As the model runs on DOS version it is very difficult to debug the errors. It could be daunting for the non-experienced users to figure out the errors and resolve it. For more information on the header and the format, readers are encouraged to go through the WSPRO user's manual which is available in FHWA website (Arneson and Shearman 1998). In here, a short description of the header and the content in the header are described so that the reader get some knowledge on how the HEC-RAS model was developed from the input data of the WSPRO model. The following Figure 1.1 shows the input data of WSPRO for Spear Creek which was used to develop the HEC-RAS model.

```

PB10506.WSP
T1 BR-0010(506) SPEAR CK. BUTLER QUAD
T2 1/2 MI W BUTLER NE 1/4 SEC LINE 24/13
T3 CHOCTAW CO. DA=9.41 SQ MI PB10506.WSP
*
* Q100 Q500
* Q 3820 5820
* SK .0021 .0021
*
XS EXIT 0 25 * * .0028
GR 000 120.0 030 114.6
GR 335 112.7 410 112.2 600 113.1 660 112.0 668 100.0
GR 688 100.0 695 111.4 770 108.9 805 109.3 840 112.2
GR 895 113.8 927 117.8 950 118.7 990 130
N .18 .18 .08 .18 .18
SA 610 660 695 748
*
XS FULL 160 25 * * .0028
*
* 3 @ 50' = 150' AASHTO GIRDER BRIDGE
*
BR BRDG 160 117.7 25
GR 610 117.7 620 112.5 658 111.5 665 100.0 685 100 690 111.0
GR 730 110.0 748 117.8 610 117.7
CD 3 82 2 121
N .05 .05 .05
SA 658 690
*
XR ROAD 200 82 1 * 25
GR -700 130.0 -200 121.3 000 121.0 800 121.0 950 128.9
*
AS APRO 400 25 * * .0028
*
HP 1 BRDG 116.4 2 117.8
HP 1 APRO 117.5 2 119.5
*
HP 2 BRDG 116.4 * * 3820
HP 2 APRO 117.5 * * 3820
*
HP 2 BRDG 117.8 * * 5820
HP 2 APRO 119.5 * * 5820
*
EX
ER

```

Figure 5.1 Input data format of WSPRO

T1, T2, T3 is the header which is required to give the title information. The title could be related to the name of the creek, location or/and drainage area. The symbol “*” has its own meaning in WSPRO model. WSPRO model has different default values which are encoded in Fortran code. If the user wants no change in that value, then the users can type an asterisk (*) symbol. The model will take it as a default value and calculate the output accordingly. The row with header “Q” gives the discharge in different return period or event. The users can input discharge(s) for 100 yr. or 500 yr. or both in the model. The row with SK header specifies the energy slope(s) for computing starting water-surface elevation(s). The row with XS header gives the information of the cross section, e.g., EXIT Figure 5.1 for the exit section 4 Figure A.2 and FULL for the unconstructed valley section 3F. Table 5.1 gives the columns, format, and contents of the XS header row.

Table 5.1 Definition of each column of XS header and its content (after WSPRO manual)

Format:		
Columns:	Format:	Contents:
1-2	A2	XS
3	1X	Blank
4	1X	Blank
5	1X	Blank
6-10	A5	SECID
11-80	Free	SRD, [SKEW, EK, CK, VSLOPE]

SECID is the unique cross-section identification code such as “FULL” or “EXIT” in Figure 5.1. SRD is the section reference distance. This is the cumulative distance along the stream measured from an arbitrary zero reference point. In Figure 5.1, at the EXIT section, SRD is 0; at the FULL section, SRD is 160 ft. It means the distance from EXIT to FULL is 160 ft. The SRD

may be negative. This also represents the flow distance between cross sections and is used to compute friction losses for the energy equation balance. SKEW is the acute angle (in degrees) that the section must be rotated to orient the section normal to the flow direction. The default value for SKEW is 0 degree. EK and CK are the coefficients used to compute the expansion and contraction losses, respectively, for the energy equation balance. The default values are either $EK = 0.5$ and $CK = 0.0$ or the current values propagated from downstream data. In the input data provided Figure 5.1, we can see the use of the asterisk (*), which means that the value used for expansion and contraction coefficient is a default value. VSLOPE is the valley (channel bottom) slope used for adjusting cross-section elevations when the geometry data for the section are being propagated from a template.

The GR rows specify the X and Y coordinates to define the cross-sectional geometry. The GR rows immediately follow the XS or BR row to provide geometric data for the section. Table 5.2 defines each column of the GR row.

Table 5.2 Definition of each column of GR header and its content (after WSPRO manual)

Format:		
Columns:	Format:	Contents:
1-2	A2	GR
3	1X	Blank
4	1X	Blank
5	1X	Blank
6-10	A5	Blank
11-80	Free	X(1), Y(1), X(2), Y(2), ... X(NGP), Y(NGP)

X (i) in Table 3.2 is the station number of ground points. Y(i) is the corresponding elevation above elevation datum.

The N row lists the Manning's coefficients in different sub areas. Sub areas are the areas which are divided according to the roughness or geometry of the cross section. In WSPRO, when a cross section is divided for roughness or geometry, the X-coordinates of the subdivision points are coded in SA records.

The SA row (Table 5.3) specifies horizontal break points for subdivision of a cross section for roughness and/or geometry variations. XSA (i) is the X-coordinate of the rightmost limit of the i-th subdivision. XSA values are not required to match with any X-coordinate in the GR data except in the bridge-opening cross-sections. For Spear Creek, the first station starts at 335 ft in GR row, the break points are 610, 660, 695, and 748. Based on N row (Figure 5.1), Manning's coefficient is 0.18 from station 0 to 610, 0.18 from 610 to 660, 0.08 from 660 to 695 (main channel), 0.18 from 695 to 748, and 0.18 for the stations greater than 748.

Table 5.3 Definition of each column of SA header and its content (after WSPRO manual)

Format:		
Columns:	Format:	Contents:
1-2	A2	SA
3	1X	Blank
4	1X	Blank
5	1X	Blank
6-10	A5	Blank
11-80	Free	XSA(1), XSA(2) . . . , XSA(NSA-1)

The bridge opening data begin with the required BR header records Table 5.4 and data to define bridge geometry.

Table 5.4 Definition of each column of BR header and its content (after WSPRO manual)

Format:		
Columns:	Format:	Contents:
1-2	A2	BR
3	1X	Blank
4	1X	Blank
5	1X	Blank
6-10	A5	SECID
11-80	Free	SRD, [PFELEV,SKEW,EK,CK,USERCD]

The SECID, SRD, SKEW, EK, CK are already defined earlier for the XS header row. SECID = BRDG is for the bridge section 2 or 3 (Figure 3.1). PFELEV is the elevation of the low chord of the bridge opening. USERCD is the user-specified coefficient of discharge for the bridge.

The CD row is the mandatory record (Table 5.5) for all bridge openings to specify the parameters used for computing the flow length and the coefficient of discharge for a bridge.

Table 5.5 Definition of each column of CD header and its content (after WSPRO manual)

Format:		
Columns:	Format:	Contents:
1-2	A2	CD
3	1X	Blank
4	1X	Blank
5	1X	Blank
6-10	A5	Blank
11-80	Free	BRTYPE, BRWIDTH, EMBSS, EMBELV, WWANGL, WWWID, ENTRND

BRTYPE defines the type of bridge. There are four different types of the bridge (Table 5.6) which are defined per the slope of the embankment, kind of abutment with or without wing walls (Arneson and Shearman 1998).

Table 5.6 Different bridge types

Bridge Type	Embankment	Abutment	Wing wall
1	Vertical	Vertical	With/without
2	Sloping	Vertical	Without
3	Sloping	Sloping spillway	–
4	Sloping	Vertical	With

BRWIDTH is the total width (ft) of the bridge deck, e.g., 82 ft for Spear Creek bridge (Figure 5.1). EMBSS defines the embankment side slope expressed in the horizontal change in meter per meter change of elevation (m H: 1 V). The default value is zero (i.e., vertical embankment wall). EMBELV represents top of the embankment elevation which must be provided for BRTYPE 2, 3, and 4. WWANGL is the wing wall angle in degree. The default value is zero degree. WWWID represents the wing wall width. ENTRND is the radius of entrance rounding.

The AS row is used to define the approach section. All the content in the AS row is same as ones in the XS row. The cumulative distance is 400 ft from EXIT to APRO for Spear Creek (Figure 3.4).

The HP row (Table 5.7) instructs the model to produce the table of cross-sectional properties and velocity conveyance distribution.

Table 5.7 Definition of each column of HP header and its content (after WSPRO manual)

Format:		
Columns:	Format:	Contents:
1-2	A2	HP
3	1X	Blank
4	1X	IHP
5	1X	Blank
6-10	A5	[SECID]
11-80	Free	[ELMIN, YINC, ELMAX, Q]

IHP = 0 indicates to output table of cross-sectional properties for the entire cross-section. IHP = 1 indicates to output table of cross-sectional properties for each sub area as well as the entire section. IHP = 2 indicates to output tables of velocity and conveyance distribution. ELMIN is the minimum elevation in the cross section for which computations are desired. YINC is the elevation increment between successive elevations for which computations are desired. ELMAX is the maximum elevation for which computations are desired. Q is the discharge required to compute the velocity and conveyance distribution.

Finally, the EX and ER rows represent the execution and termination of the model. The following section describes how the WSPRO input data was used to develop the HEC-RAS model.

5.3.1 CROSS-SECTIONAL GEOMETRY

HEC-RAS needs at least 4 cross sections in a river to compute the hydraulic parameters, which could be used for the scour calculation. One section is at far downstream, one at far upstream and two just above and below the bridge structure (Figure 1.4). WSPRO input data file (Figure 5.1) provides detailed channel geometry (X and Y coordinates) at the downstream EXIT cross section and an energy gradient slope. The EXIT cross section data were used to project the cross-

section geometry upstream from the EXIT section based on the slope. Four cross sections for HEC-RAS were then created. The cross-section just upstream and downstream of the bridge were assumed and created at 10 ft. from the bridge. The cross-section data was adjusted with some adjustments in the elevation points. The reach lengths between two cross sections were set to what they were in the WSPRO model, i.e., 160 ft from the section 1 and 2 for HEC-RAS (Figure 1.4), 102 ft from the section 2 and 3 (82 ft for bridge deck plus 10 ft in each side), and 138 ft from the section 3 to 4 ($400 - 102 - 160 = 138$ ft).

5.3.2 MANNING'S N VALUES

HEC-RAS needs Manning's n value for the left overbank, main channel, and right overbank. WSPRO model provides the n values in the N row according to the sub-areas divided. By knowing the fact that the channel has low roughness than the overbank areas, the Manning's values for HEC-RAS model could be specified as accurately as possible depending on the information in N row of WSPRO model. For Spear Creek, Manning's n was set as 0.18 for the left and right overbank areas and 0.08 for the main channel.

5.3.3 CHANNEL BANK STATIONS AND REACH LENGTHS

The cross section data obtained from WSPRO were plotted and analyzed in Excel. The channel bank stations were decided by examining the cross-section plot. The channel reach lengths for the channel and overbank areas were determined from the input file of the WSPRO, which was discussed in section 3.6.2 for Spear Creek. It is necessary to mimic the same input reach length used in WSPRO when it is possible. Without additional information, the reach length is set to be the same for the overbank areas and the main channel.

5.3.4 EFFECTIVE FLOW AREA

The ineffective flow area is the area where the flow velocity remains zero. Any kind of obstruction (bridge in this case) to the flow of water will change the flow pattern. Due to the smaller opening of the bridge compared to the width of the full flow over the floodplain (including overbank areas), the flow must contract towards the bridge opening. Thus, floodplain areas immediately upstream of the bridge on either side of the bridge opening (Figure A.2) do not convey flow and do not move, so these areas are called ineffective areas. The dotted line in (Figure A.2) separates the ineffective and effective flow area in HEC-RAS. For the WSPRO model, its input data do not consider the ineffective flow area when the flow passes through a bridge. At first, we tried to mimic the WSPRO's no-ineffective-flow-area condition in HEC-RAS. At the next step, because of the less information about how to choose the ineffective flow area exactly, the ineffective flow areas were assumed at the left and right overbank areas, and the results for different cases were analyzed and compared.

5.3.5 BRIDGE CROSSING GEOMETRY

Bridge data from the WSPRO input file were used to create a bridge geometry. Detailed information about the bridge (road embankment, bridge deck, and abutments) was well documented in each input file (Figure 5.1) provided. Due to the insufficient data for the bridge pier, some engineering judgment with some assumptions were made in the length, width, and angle of attack of the pier. Figure 5.2 shows the bridge geometry of spear creek in HEC-RAS.

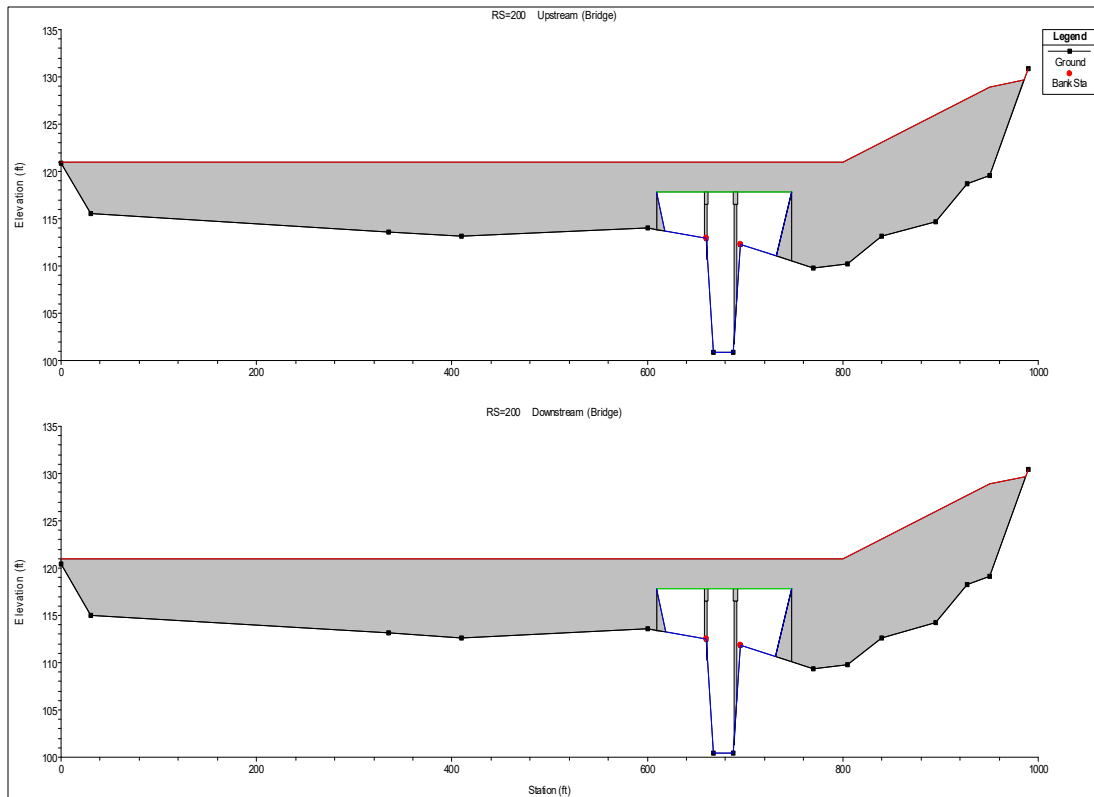


Figure 5.2 Bridge geometry of Spear Creek in HEC-RAS

5.3.6 CONTRACTION AND EXPANSION COEFFICIENTS

From the WSPRO input data (Figure 5.1), contraction and expansion coefficients were set to 0.0 and 0.5, respectively. Near the bridge, the coefficients, per HEC-RAS methodology, should be 0.3 and 0.5 for contraction and expansion coefficient (Section 2 and 3 in (Figure A.2)). So, the coefficients were changed accordingly at the bridge site with different discreet settings (Table 5.8). In general, the changing of the contraction and expansion coefficients did not influence the results to any significant degree because the velocity head was low even at the bridge site.

Table 5.8 Expansion and contraction coefficients in WSPRO and HEC-RAS

Coefficients	WSPRO	HEC-RAS	HEC-RAS
	(Default value)	(Near Bridge)	(Far from bridge)
Expansion	0.5	0.5	0.3
Contraction	0.0	0.3	0.1

5.3.7 FINAL MODEL DEVELOPMENT

All the data required were obtained from the input of the WSPRO model. Next, the flow data and the boundary conditions were set up. The flow data used was the 100-yr. return flow as in WSPRO model. For the calculation of subcritical water surface profile, the downstream boundary was set to normal depth by inputting a friction or river-bottom slope. The model was run for the steady-state condition.

5.4 OUTPUT OF WSPRO

WSPRO model generates detailed output describing the processing of the input data and the result of all profile computations. The model offers no option to suppress any output but users can edit out unwanted segments of the file before printing (Arneson and Shearman 1998). As stated in Table 5.7 HP records are used to generate tables of cross-sectional properties and (or) velocity and conveyance distribution for any section(s). Cross-sectional properties can be obtained for the total cross-section, with or without a sub-area breakdown. Velocity and conveyance distribution can be obtained for one or more discharge(s) at one or more elevation(s) (HP row in Figure 5.1). For more information about the output of the WSPRO model readers are referred to read User's Manual for WSPRO (Arneson and Shearman 1998).

This section explains the determination of the required parameters in HEC-18 for scour depth calculation from the output of WSPRO. The required parameters needed for scour depth calculation in HEC-18 are mentioned in section 1.2. These parameters needed are calculated using the data in the cross-sectional properties of WSPRO output as shown in Figure 5.3

1
 WSPRO FEDERAL HIGHWAY ADMINISTRATION - U. S. GEOLOGICAL SURVEY
 V082195 MODEL FOR WATER-SURFACE PROFILE COMPUTATIONS

BR-0010(506) SPEAR CK. BUTLER QUAD
 1/2 MI W BUTLER NE 1/4 SEC LINE 24/13
 CHOCTAW CO. DA=9.41 SQ MI PB10506.WSP

*** RUN DATE & TIME: 04-05-16 14:17
 CROSS-SECTION PROPERTIES: ISEQ = 3; SECID = BRDG ; SRD = 160.

WSEL	SA#	AREA	K	TOPW	WETP	ALPH	LEW	REW	QCR
	1	165	12160	41	42				1869
	2	414	55751	29	43				8883
	3	257	22440	50	51				3313
116.40		836	90351	120	137	1.18	613	745	11520
	1	221	12096	0	88				0
	2	453	45986	0	72				0
	3	327	20549	0	107				0
117.80		1001	78632	0	267	1.22	610	748	0

1
 HP 1 APRO 117.5 2 119.5

1
 WSPRO FEDERAL HIGHWAY ADMINISTRATION - U. S. GEOLOGICAL SURVEY
 V082195 MODEL FOR WATER-SURFACE PROFILE COMPUTATIONS

BR-0010(506) SPEAR CK. BUTLER QUAD
 1/2 MI W BUTLER NE 1/4 SEC LINE 24/13
 CHOCTAW CO. DA=9.41 SQ MI PB10506.WSP

*** RUN DATE & TIME: 04-05-16 14:17
 CROSS-SECTION PROPERTIES: ISEQ = 5; SECID = APRO ; SRD = 400.

WSEL	SA#	AREA	K	TOPW	WETP	ALPH	LEW	REW	QCR
	1	1703	30500	535	535				17242
	2	178	3658	45	45				1997
	3	440	37354	32	45				9297
	4	282	7577	48	48				3870
	5	744	17731	152	152				9342
117.50		3346	96821	812	826	3.65	20	916	20167
	1	2782	68263	545	545				35676
	2	268	7270	45	45				3705
	3	503	46758	32	45				11378

Figure 5.3 Cross-sectional properties output from WSPRO (Spear Creek)

The required data to get the parameters needed for scour depth calculation in HEC-18 are, SA (subarea), Area (A), K (conveyance), TOPW (top width), hydraulic depth (y) at the approach section and the bridge section. Discharges in each subsection (lob, ch, and rob) of a compound channel section were calculated using Manning's equation introduced in 1891 by Flamant (Henderson 1996).

$$Q = \frac{K_n}{n} AR^{2/3} S_f^{1/2} \quad (5.3)$$

Equation (5.3) can be rewritten as,

$$Q = KS_f^{1/2} \quad (5.4)$$

where K = conveyance, defined as

$$K = \frac{K_n}{n} AR^{2/3} \quad (5.5)$$

The conveyance of each subsection can be defined as,

$$K = \frac{K_n}{n_i} A_i R_i^{2/3} \quad (5.6)$$

where i = index referring to the i -th subsection. The total discharge Q_T in the compound section is equal to the sum of the subsection discharges, Q_i . Assuming the energy head doesn't vary cross the compound section, i.e., S_f is the same for all subsections we can calculate the discharge of each subsection.

$$Q_T = K_T S_f^{1/2} \quad (5.7)$$

$$Q_i = K_i S_f^{1/2} \quad (5.8)$$

$$Q_i = \frac{K_i}{K_T} Q_T \quad (5.9)$$

where Q_T = total discharge, K_T = total conveyance, Q_i = discharge at subsections, K_i = conveyance at subsections. After calculation of each subsection discharge, velocity (V) for each subsection is calculated by the ratio of discharge (Q) to the area (A). Hydraulic depth (y) is calculated from the ratio of total area to top width.

5.5 RESULTS OF HYDRAULIC PARAMETERS AND SCOUR DEPTHS

The hydraulic parameters obtained from the HEC-RAS model (using different methods) is compared with the hydraulic parameters obtained from the WSPRO model. The outputs from the WSPRO model using the default value for contraction and expansion coefficient (0.0 and 0.5) were compared with the outputs from the HEC-RAS methods selecting the energy method with default contraction and expansion coefficient, i.e., 0.1 and 0.3 respectively far upstream and downstream and 0.3 and 0.5 near the bridge. The WSPRO model doesn't output the hydraulic parameter in sequence as HEC-RAS model. It outputs the velocity distribution and cross-sectional properties in a text format. Some calculation is needed to obtain the hydraulic parameter needed for scour depth calculation using HEC-18 (which is integrated into HEC-RAS). The data reduction process of the WSPRO method to get hydraulic parameter is described in section 5.4. All the hydraulic parameters obtained from both the models were similar but different, the discharge at upstream approach section Q_1 , discharge at the contraction section Q_2 , width at upstream approach section W_1 were different by a relatively large percent (Table 5.9).

Discharge at upstream section Q_1 , width at upstream section W_1 , discharge at contraction section Q_2 , and width at contraction section W_2 are selected hydraulic parameters for the ratio comparison using Equations (5.1) and (5.2). Table 5.9 clearly shows the flow contraction from the section 1 to 2, for example, from WSPRO output, LOB contracts from 290 ft to 41 ft, and discharge changes from 1347.6 to 514.1 cfs at LOB and from 1473.9 to 2357.1 cfs at the main channel. In the main channel, discharge at the contraction section (bridge crossing) from WSPRO is 1.6 times larger than the discharge at the approach section, but it is 2.4 times larger from HEC-RAS (from 1332.12 to 3195.65 cfs). It means HEC-RAS lets much more flow in the main channel due to the contraction. At the contraction section, discharge at the main channel from HEC-RAS is 838.52 cfs more than the channel discharge from WSPRO.

Table 5.9 Comparison of the hydraulic parameters from WSPRO's and HEC-RAS's energy methods.

Hydraulic Parameters	WSPRO Output			HEC-RAS (Energy Method)		
	LOB	CH	ROB	LOB	CH	ROB
Y_1 (ft)	3.56	13.75	5.38	3.81	14.46	5.61
V_1 (ft/s)	0.72	3.35	0.97	0.67	2.90	0.87
Y_o (ft)	4.02	14.28	5.14	3.24	14.67	4.50
Q_2 (cfs)	514.12	2357.13	948.75	206.19	3195.65	418.16
W_2 (ft)	41.00	29.00	50.00	41.66	25.72	45.84
D_{50} (mm)	0.03	0.047	0.055	0.03	0.047	0.055
Scour Eqn.	Clear-water	Default	Clear-water	Clear-water	Default	Clear-water
Q_1 (cfs)	1347.64	1473.89	998.48	1494.37	1332.12	993.51
W_1 (ft)	290.00	32.00	100.00	582.91	31.72	204.25
Scour (ft)	10.25	7.74	11.97	3.19	20.70	4.63

Note: subscript 1 for the upstream approach section, 2 for the contraction section at the bridge crossing. Y_o is the average depth prior to scour at contraction section, i.e., Y_{BU} in Equations (1.2) and (1.3).

The comparison of the hydraulic parameters and then the scour depth from both the models is shown in Table 5.10. The clear-water scour was selected for computing the scour depths in the overbank areas. The hydraulic design function windows in HEC-RAS used for the calculation of the scour need the value of D_{50} entered in millimeter (mm). For the main channel, HEC-18 determines that the live-bed scour could occur and D_{50} could affect the exponent K_I . The exponent K_I is related to the ratio of shear velocity (V^*) to fall velocity (w). The fall velocity depends on the D_{50} value of the bed material. For Spear Creek study, the value of exponent K_I was 0.69, when $V^*/w > 2.0$. Since K_I becomes a constant, the calculated depth for the live-bed scour does not

depend on D_{50} . Based on Equation (1.2), the ratio in Equation (5.2) times Y_l (water depth at upstream approach section) minus Y_o or Y_{BU} (average depth prior to scour at the bridge) will be the scour depth; therefore, three factors: the ratio, Y_l , and Y_o possibly affect the live-bed scour depth calculation.

For the overbank areas, the clear-water equation (5.1) was used to obtain the ratio of hydraulic parameters. Based on Equation (1.3), the ratio in Equation (5.1) times the ratio $[1/(C_u D_m^{2/3})]^{3/7}$ minus Y_o will be the scour depth; therefore, three factors: two ratios and Y_o possibly affect the clear-water scour depth calculation. Even though C_u is a constant depending on units, $D_m = 1.25 D_{50}$ is a function the particle size D_{50} and directly affect the scour depth. The discharges in LOB and ROB at the contraction section (Q_2) calculated from WSPRO are 307.93 cfs and 530.59 cfs larger than corresponding discharges from HEC-RAS model, respectively. The absolute differences in the width of the contraction section (W_2) are 0.7 ft and 4.16 ft, respectively, at LOB and ROB (Table 5.9). For both the methods the D_{50} value used is the same.

The ratio of selected hydraulic parameters (5.1) from both the methods for LOB and ROB is 2.22 and 1.87, respectively. Although the ratio of average depth prior to scour is close to 1 for both case, it could affect the scour depth ratio if the selected parameters are changed. For example, the average depth prior to scour at contraction section for WSPRO and HEC-RAS is 4.02 and 4.5 ft, respectively. The ratio of hydraulic parameters (Equation (5.1)) is 8.74 for WSPRO and 3.94 for HEC-RAS at LOB. The ratio $[1/(C_u D_m^{2/3})]^{3/7}$ is 1.62 at LOB but 1.33 at ROB since D_{50} at LOB is 0.03 mm, half of 0.06 mm at ROB, but there is no change in the ratio for both the methods because of the same D_{50} . Based on Equation (1.3), calculated water depth after scour (Y_{AS} in Table 5.2) is the product of the ratio of hydraulic parameters (Equation 5.1) and $[1/(C_u D_m^{2/3})]^{3/7}$. The ratio of Y_{AS} values is the same as the ratio of hydraulic parameters between two methods (Table

5.2). The ratios of scour depths at LOB and ROB using hydraulic parameters from WSPRO and HEC-RAS are 3.21 and 2.59, respectively. Since the final scour depth is the difference of Y_{AS} and Y_o , the ratio and the percent difference of scour depths between the two methods are always different from the ratio and the percent difference of Y_{AS} and hydraulic parameters in Equation 5.1. When Y_o is close to Y_{AS} , above differences in the ratio and the percent difference become larger.

Based on Equation (1.3), the water depth after scour (Y_{AS}) is proportion to $[1/D_{50}]^{2/7}$. If D_{50} is 50% or 100% larger than the true D_{50} , it makes Y_{AS} 89% and 82% of the true Y_{AS} for the clear-water scour. For hydraulic parameters, the water depth after scour (Y_{AS}) is proportion to $[Q_2/W_2]^{6/7}$, since the exponent 6/7 is close to 1, the change in hydraulic parameters will have a similar impact on Y_{AS} , which means hydraulic parameters could have relatively large impacts on calculating the scour depth. Table 5.10 shows the ratio of hydraulic parameters (Equation 5.1) from WSPRO is 61% and 76% larger than the ratio from HEC-RAS at ROB and LOB, respectively. Figure 5.4 graphically presents the difference in scour depth predicted by the two methods.

Table 5.10 Comparison of ratios of the hydraulic parameters and scour depths from WSPRO and HEC-RAS's energy method at overbank areas (LOB and ROB)

Hydraulic parameters	WSPRO		HEC-RAS (0.3,0.5)		Ratio ¹		%Difference ²	
	LOB	ROB	LOB	ROB	LOB	ROB	LOB	ROB
$\left(\frac{Q_2^2}{W_2^2}\right)^{3/7}$	8.74	12.46	3.94	6.66	2.22	1.87	76	61
$\left(\frac{1}{C_u D_m^{2/3}}\right)^{3/7}$	1.62	1.33	1.62	1.33	1	1	0	0
Y_{AS}^3	14.16	16.57	6.43	9.13	2.20	1.81	75	58
Y_0	4.02	5.14	3.24	4.5	1.24	1.14	21	13
Scour depth (Y_s) ft	10.25	11.97	3.19	4.63	3.21	2.59	105	88

Note: ¹ - Ratio is calculated from WSPRO method divided by the HEC-RAS method. For example, 10.25/3.19=3.21, ² - % Difference is calculated as the difference divided by the average of WSPRO and HEC-RAS method. For example, (10.25 – 3.19)/(average (10.25,3.19)* 100 % = 105/ %, and ³ – water depth at the contraction section (bridge crossing) after scour.

For the main channel, Equation (5.2) is used to calculate the ratio of hydraulic parameters for the live-bed scour. The exponent K_I used for the live-bed scour has three values (Table 1.2). There is a small change in calculated scour depth when K_I is changed. This is because W_1/W_2 in

the main channel is close to 1 (1.10 from WSPRO and 1.23 from HEC-RAS). The scour depth could be 7.73, 7.62, and 7.51 ft when K_I used was 0.69, 0.64 and 0.59, respectively, when hydraulic parameters from WSPRO were used. The K_I value remains same (analyzed for Table 5.9 Channel case) for large range of D_{50} values keeping hydraulic parameter Y_I constant (used to calculate the shear velocity), the K_I value remains as 0.69 for D_{50} changing from 0.005 mm to 0.74 mm and changes to 0.64 when D_{50} is from 0.75 to 7 mm. The K_I value changes to 0.59 when $D_{50} > 7.1$ mm. When D_{50} changes but K_I does not change, the difference in scour depth is due to the difference in the hydraulic parameters obtained from two methods.

The ratio of the hydraulic parameters between WSPRO and HEC-RAS method at the channel is 0.66 but the ratio of the scour depth ratio is 0.37. This means the scour depth predicted from WSPRO model at the channel is 37% of the scour depth predicted from HEC-RAS. The major cause for large scour depth from HEC-RAS is a large flow contraction: $Q_2/Q_1 = 2.3$ or $(Q_2/Q_1)^{6/7} = 2.1$ but $Q_2/Q_1 = 1.6$ from WSPRO. The water depth Y_I at the approach section is about 12% more from HEC-RAS, and calculated depth after scour (Y_{AS}) is 60.7 % from HEC-RAS, which is 13.37 ft more than Y_{AS} from WSPRO.

Table 5.11 Comparison of ratios of the hydraulic parameters and scour depths from WSPRO's and HEC-RAS's energy method at channel

Hydraulic Parameters	WSPRO	HEC-RAS	Ratio	% Difference
	CH	CH	CH	CH
$\left(\frac{Q_2}{Q_1}\right)^{6/7} * \left(\frac{W_1}{W_2}\right)^{0.69}$	1.60	2.44	0.66	41.6
Y_l	13.75	14.46	0.95	5.0
Y_{AS}	22.0	35.37	0.62	46.6
Y_0	14.28	14.67	0.97	2.7
Scour depth (Y_s), ft	7.74	20.7	0.37	91.1

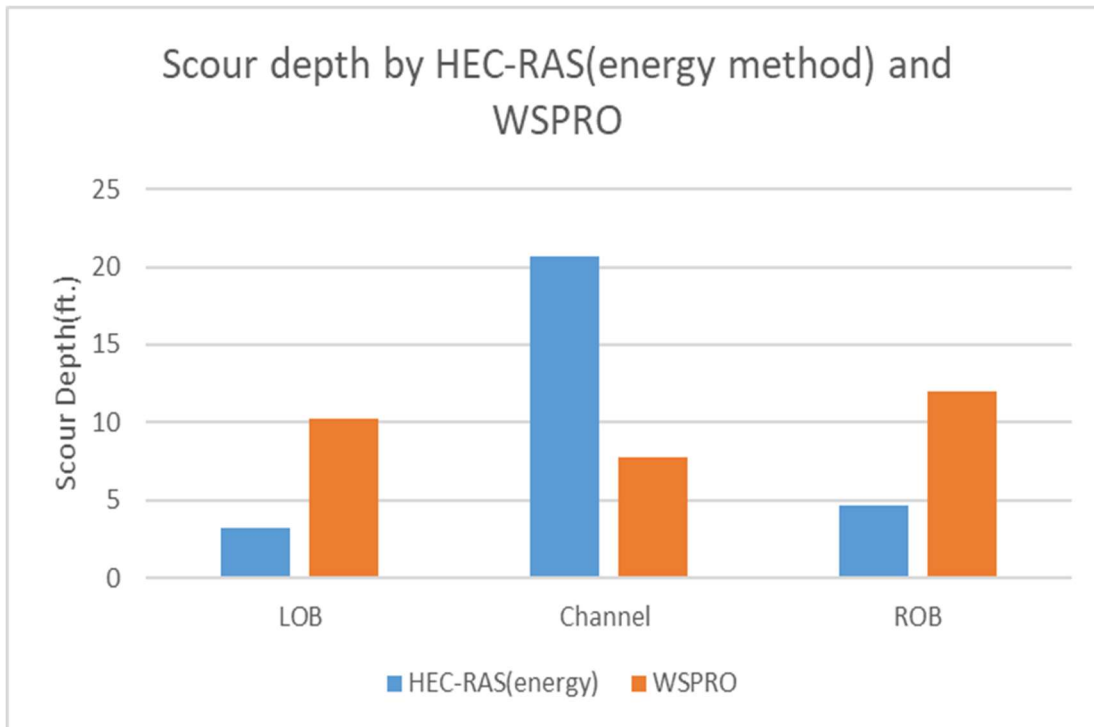


Figure 5.4 Comparison of scour depth from WSPRO and HEC-RAS (energy method)

For all other comparisons below, only the ratio of selected parameters, Equations (5.1) and (5.2), are shown in Tables 5.4 to 5.7. However, the scour depth is calculated using all the hydraulic parameters as in Equations (1.2) and (1.3).

Also, to mimic the similar scenario the WSPRO method in HEC-RAS was used to compare to the output from the Energy method in HEC-RAS model by keeping the expansion and contraction coefficient same. These coefficients were set as the HEC-RAS methodology (0.3 and 0.5) and comparison results are summarized in Table 5.12. Then WSPRO method in HEC-RAS model was compared by changing the expansion and contraction ratio from 0.3, 0.5 to 0.0, 0.5 respectively (Table 5.13). The HEC-RAS results for the scour depth for the first case is same to the results (Table 5.10 and Table 5.11) when only energy method was used. There is not much change in hydraulic parameters eventually giving very close scour depth value (Table 5.12). The ratio of selected hydraulic parameters (5.1) for the clear-water scour from both the methods for LOB and ROB are 1.0. The ratio of scour depth obtained from the two methods at LOB and ROB are 1.0 (Table 5.12). The ratio of selected parameters (Equation (5.2)) from both the methods at the channel is 1.02 with a scour depth ratio of 1.02 (Table 5.12). That means scour depth predicted from energy method from HEC-RAS model at the channel is 1.02 times less than the scour depth predicted from the HEC-RAS using WSPRO method.

For the second case, using WSPRO method in HEC-RAS with contraction and expansion coefficients as 0.0, 0.5; and 0.3, 0.5; there was a small change in the HEC-RAS results as obtained in the first case, i.e., using different contraction and expansion coefficient (Table 5.13). The discharge at contraction section differs (absolute) by 66.1, 63.76 and 2.35 cfs in LOB, CH and ROB, respectively. This difference in the discharge affects the scour depth mainly in the channel with a difference of 2.01 ft. The scour depth at the main channel is 1.10 times the scour depth

obtained using WSPRO method using expansion and contraction coefficients as 0.0 and 0.5 ft, respectively. In this case there is a small difference, however, there could be a large difference in cases where the difference in the velocity head between the sections is large.

Table 5.12 Comparison of the hydraulic parameters and scour depth from Energy method and WSPRO method of HEC-RAS model using same contraction and expansion coefficient as HEC-RAS methodology

Ratio	Energy method (HEC-RAS) (0.3, 0.5)			WSPRO method (HEC-RAS) (0.3, 0.5)			Ratio ¹		
	LOB	CH	ROB	LOB	CH	ROB	LOB	CH	ROB
$\left(\frac{Q_2^2}{W_2^2}\right)^{3/7}$	3.94	–	6.65	3.94	–	6.65	1.0	–	1.0
$\left(\frac{Q_2}{Q_1}\right)^{6/7}$ * $\left(\frac{W_1}{W_2}\right)^{0.69}$	–	2.44	–	–	2.49	–	–	1.02	–
Scour depth (Y_s) ft	3.19	20.7	4.63	3.18	21.4	4.63	1.0	1.03	1.0

Note: ¹ - Ratio is calculated as WSPRO method divided by the energy method in HEC-RAS. For example, 3.94/3.94=1.

Table 5.13 Comparison of the hydraulic parameters and scour depth from HEC-RAS WSPRO method using different contraction and expansion coefficient

Ratio	WSPRO (HEC-RAS) method (0.3, 0.5)			WSPRO (HEC-RAS) method (0.0, 0.5)			Ratio ¹		
	LOB	CH	ROB	LOB	CH	ROB	LOB	CH	ROB
$\left(\frac{Q_2^2}{W_2^2}\right)^{3/7}$	3.94	–	6.65	3.87	–	6.6	1.02	–	1.01
$\left(\frac{Q_2}{Q_1}\right)^{6/7} * \left(\frac{W_1}{W_2}\right)^{0.69}$	–	2.44	–	–	2.40	–	–	1.02	–
Scour depth(Y_s)	3.18	21.4	4.63	3.14	19.39	4.61	1.01	1.10	1.0

The effect of using a different contraction and expansion lengths on scour depth calculation was also analyzed by changing the contraction and expansion length based on HEC-RAS methodology. The model was run for three times with different expansion and contraction length. The expansion and contraction length was taken based on one of the HEC-RAS methodology. US Army Corps of engineers (Brunner 1995) provides a table of ranges of expansion ratios which can be used as a guide to determine the expansion length. The average of distances A to B and C to D (Figure 1.4), i.e., an average of bridge embankment lengths into the floodplain) is multiplied by the expansion ratio obtain from (Table 5.14) to get the expansion length.

Table 5.14 Ranges of expansion ratio

		$n_{ob} / n_c = 1$	$n_{ob} / n_c = 2$	$n_{ob} / n_c = 4$
$b/B = 0.10$	$S = 1$ ft/mile	1.4 – 3.6	1.3 – 3.0	1.2 – 2.1
	5 ft/mile	1.0 – 2.5	0.8 – 2.0	0.8 – 2.0
	10 ft/mile	1.0 – 2.2	0.8 – 2.0	0.8 – 2.0
$b/B = 0.25$	$S = 1$ ft/mile	1.6 – 3.0	1.4 – 2.5	1.2 – 2.0
	5 ft/mile	1.5 – 2.5	1.3 – 2.0	1.3 – 2.0
	10 ft/mile	1.5 – 2.0	1.3 – 2.0	1.3 – 2.0
$b/B = 0.50$	$S = 1$ ft/mile	1.4 – 2.6	1.3 – 1.9	1.2 – 1.4
	5 ft/mile	1.3 – 2.1	1.2 – 1.6	1.0 – 1.4
	10 ft/mile	1.3 – 2.0	1.2 – 1.5	1.0 – 1.4

Note: b/B is the ratio of bridge opening width to the total floodplain width, S is a longitudinal slope, and n_{ob}/n_c is the ratio of Manning’s roughness coefficients in the overbank area and main channel.

In case of Spear Creek, the bridge opening (b) is 138 ft and the total floodplain width (B) is 990 ft. The ratio of b/B is 0.13, which is near to 0.10. The Manning’s coefficient for the overbank area is 0.18 and for the channel is 0.08. The ratio n_{ob}/n_c is 2.2, which is close to $n_{ob}/n_c = 2$. The longitudinal slope is ~5 ft/mile in Spear Creek. Based on above calculation, the expansion ratio is taken as 0.8 (minimum) and 2 (maximum), which lies in the range of 0.8 and 2.0. The contraction length is usually shorter than the expansion length. Therefore, the minimum expansion ratio of 1.0 is used and multiplied to 426 ft (the average of distances from A to B and C to D) to get the expansion length as 426 ft and the maximum ratio 2 is multiplied to 426 ft (the average of distances from A to B and C to D) to get the expansion length as 852 ft. HEC-RAS (Brunner 1995) recommends the contraction length in between 1 and 1.5 times the average of distance A to B and C to D in Figure 1.4. From this range, 1 is chosen and multiplied to 426 to get 426 ft as the minimum contraction length and 1.5 is chosen and multiplied to 426 to get 639 as the maximum contraction length. WSPRO method in HEC-RAS was used for gathering the hydraulic parameters. There was

a change in discharge value both upstream and at the contraction section with a change in the scour depth value when minimum expansion length as recommended by HEC-RAS is used. The absolute difference in discharge upstream (Q_1) at LOB, CH, and ROB were 314.1 cfs, 321.9 cfs and 7.8 cfs, respectively, whereas the absolute difference in discharge at the contraction section (Q_2) were 43.06 cfs, 95.53 cfs and 52.47 cfs respectively. The scour depth obtained using expansion and contraction length at 160 ft and 138 ft is 1.5, 1.5, and 1.4 times larger than the scour depth obtained using expansion and contraction length 426 ft and 426 ft at LOB, Channel and ROB respectively.

Table 5.15 Change in scour depth with the change in minimum expansion and contraction length using HEC-RAS model.

Hydraulic parameters	Expansion length = 160 ft, contraction length = 138 ft			Expansion length = 426 ft, contraction length = 426 ft			Ratio ¹		
	LOB	CH	ROB	LOB	CH	ROB	LOB	CH	ROB
Y_1 (ft)	3.53	14.16	5.37	2.52	13.13	4.52	1.4	1.1	1.2
V_1 (ft/s)	0.69	3.04	0.96	0.69	3.67	1.06	1.0	0.8	0.9
Y_0 (ft/s)	3.19	14.61	4.45	2.68	13.87	4.02	1.19	1.0	1.1
Q_2 (cfs)	202.13	3204.69	413.18	159.07	3300.22	360.71	1.3	1.0	1.1
W_2 (ft)	41.56	25.72	47.72	46.07	29	50.46	0.9	0.9	0.9
D_{50} (mm)	0.03	0.047	0.055	0.03	0.047	0.055	–	–	–
Q_1 (cfs)	1414.20	1365.17	1040.63	1100.14	1687.06	1032.81	1.3	0.8	1
W_1 (ft)	581.42	31.72	202.11	635.76	35	214.69	0.9	0.9	0.9
Scour (y _s) ft	3.14	19.39	4.61	2.04	12.70	3.39	1.5	1.5	1.4

Note: ¹ - Ratio is calculated as 3.53/2.52=1.4

When the expansion and contraction length was changed from 426 and 426 ft to 639 and 426 ft there was a change in discharge at contraction section (Q_2) (Table 5.15 and Table 5.16). The absolute difference in Q_2 is 31.3 cfs, 69.8 cfs in LOB and Channel, respectively. Due to the decrease in Q_2 value at the channel, the scour depth decreases from 12.7 to 10.69 ft. This indicates that scour depth is affected by the change in the expansion and contraction length in the same model. Also, when the expansion and contraction length is changed to 852 and 639 ft from 639 and 426 ft, there is an increase in the discharge at contraction section in overbank areas and a decrease in the main channel which makes the scour depth at overbank areas to increase and

decrease in the main channel. The scour depth obtained from using WSPRO expansion and contraction length (160 and 138 ft) is 1.19, 2.28, and 1.25 times larger than the scour depth obtained from using maximum expansion and contraction length (852 and 639 ft) recommended by HEC-RAS. This indicates that using different expansion and contraction length could change the hydraulic parameter which eventually changes the scour depth.

Table 5.16 Change in scour depth with the change in maximum expansion and contraction length using HEC-RAS model.

Hydraulic parameters	Expansion length = 639 ft, contraction length = 426 ft			Expansion length = 852 ft, contraction length = 639 ft			Ratio		
	LOB	CH	ROB	LOB	CH	ROB	LOB	CH	ROB
Y_1 (ft)	2.36	12.96	4.38	2.17	12.77	4.22	1.1	1.0	1.0
V_1 (ft/s)	0.70	3.85	1.10	0.71	4.02	1.15	1	1	1
Y_0 (ft/s)	3.08	14.32	4.39	3.50	14.81	4.78	0.9	1.0	0.9
Q_2 (cfs)	190.35	3230.41	399.24	224.17	3155.81	440.02	0.8	1.0	0.9
W_2 (ft)	46.94	29	51.49	47.88	29	52.63	1	1	1
D_{50} (mm)	0.03	0.047	0.055	0.03	0.047	0.055	–	–	–
Q_1 (cfs)	1042.67	1745.29	1032.05	972.12	1817.42	1030.46	1.1	1.0	1.0
W_1 (ft)	634.85	35	213.38	633.78	35	211.85	1.0	1.0	1.0
Scour (y_s) ft	2.34	10.69	3.35	2.63	8.52	3.69	0.9	1.3	0.9

The HEC-RAS model for all above cases was configured without including the ineffective flow area. The HEC-RAS model was run using the ineffective flow areas as discussed in section 5.2 using WSPRO method with contraction and expansion coefficient as 0.0 and 0.5 (Table

5.17). The ratio of the selected hydraulic parameter (Equation (5.1)) for LOB and ROB were close to 1 for both. The scour depth ratio for a LOB and ROB were also close to 1. The scour depth ratio at channel was 0.95 (Table 5.17). That means the scour depth obtained without ineffective flow area is 0.95 times smaller than scour depth obtained with ineffective flow area at channel section.

When scour depths at LOB, CH, and ROB from HEC-RAS with ineffective areas are compared corresponding scour depths from WSPRO, one can see that the differences become larger at LOB and ROB but smaller in the main channel. It means ineffective areas reduce effective flow velocity in the overbank areas and channel that result in smaller scour depths. The ineffective flow areas were set for the sections immediately upstream and downstream of the bridge crossing in HEC-RAS.

Table 5.17 Change in scour depth with and without including ineffective flow area using HEC-RAS model with WSPRO method.

Ratio	WSPRO (without ineffective flow)			WSPRO (with ineffective flow)			Ratio ¹		
	LOB	CH	ROB	LOB	CH	ROB	LOB	CH	ROB
$\left(\frac{Q_2^2}{W_2^2}\right)^{3/7}$	3.87	–	6.6	3.98	–	6.69	0.97	–	0.99
$\left(\frac{Q_2}{Q_1}\right)^{6/7} * \left(\frac{W_1}{W_2}\right)^{0.69}$	–	2.4	–	–	2.44	–	–	1.0	–
Scour depth(<i>Y_s</i>) ft	3.14	19.39	4.61	3.21	20.32	4.65	0.98	0.95	0.99

Note:¹- Ratio is calculated as WSPRO without ineffective flow divided by WSPRO with the ineffective flow.

The water surface elevation from both the models was also compared and tabulated in Table 5.18. Both models compute the water surface profiles within the tolerance. There was not much difference in the values obtained from both the models. The variation of the water surface elevations (WSE) at any cross section for four bridge cases was in the order of 0.02 to 1.15 feet. Alamuchee Creek has the variation of the WSE in the range of 0.34 to 0.37 ft . The average absolute error for Alamuchee Creek is 0.36 ft. In case of Spear Creek at the approach section, the WSE computed by HEC-RAS and WSPRO differ by 1.28 ft which is the largest difference in WSE for all the bridge cases. The error ranges from 0.34 to 1.15 with an average of 0.65 ft for the Pinatall Creek. The WSE computed for Spear Creek by WSPRO and HEC-RAS varies within a range of 0.21 to 1.2 ft with a average of 0.41 ft. For the case of Valley Creek, the WSE computed by WSPRO and HEC-RAS varies within a range of 0.02 to 0.08 ft with an average of 0.054. Due to the unavailability of the observed WSE for all the bridge cases, these study could not accurately point out the best method to compute the water surface elevation. In the report published by US Army Corps of Engineers (Brunner and Hunt 1995) seventeen flood events were analyzed at 13 different bridge sites and the observed WSE was compared to the calculated WSE from HEC-RAS and WSPRO. There was a variation of 0.1 to 0.3 ft. In this case, the variation is large at approach section of Pintalla Creek and Spear Creek. Other WSE vary within a range of 0.02 to 0.46 ft which is somewhat close to the variation in the different bridge site provided in the report. Therefore, it is believed that any of the models could be used to compute the water surface profiles at bridge location if given variance in the results.

Table 5.18 Comparison of simulated water surface elevations between WSPRO and HEC-RAS models

	Cross Sections	HEC-RAS WSE (ft)	WSPRO WSE (ft)	Absolute error (ft)
Alamuchee Creek	Exit	181.42	181.79	0.37
	Full Valley	181.56	181.95	0.39
	Approach	183.66	183.32	0.34
	Average			0.36
Pintalla Creek	Exit	163.97	163.63	0.34
	Full Valley	164.19	163.73	0.46
	Approach	165.58	164.43	1.15
	Average			0.65
Spear Creek	Exit	115.92	115.90	0.02
	Full Valley	116.26	116.25	0.01
	Approach	118.09	116.81	1.28
	Average			0.44
Valley Creek	Exit	101.67	101.69	0.02
	Full Valley	101.85	101.91	0.06
	Approach	102.52	102.44	0.08
	Average			0.05

Chapter 6 SUMMARY AND CONCLUSIONS

6.1 SUMMARY

Scour is crucial in bridge designing. Bridge designing should be done with accuracy to minimize the future disasters. The ability to determine the hydraulic parameters and eventually scour depth is imperative to designing safe, economic, and efficient bridge foundations. Different types of soils either cohesive or non-cohesive soil are present in the earth surface. Scour behavior for the non-cohesive soil is well understood. However, much research has been performed in an effort to understand scour behavior in cohesive soils. The cohesive soils act differently than the non-cohesive soils, which erode particle by particle. In the USA, currently, scour depths are calculated by HEC-18, which is used by many DOT's to calculate the scour depth in an around the bridge. HEC-18 provides different sets of equations to calculate the different types of scour depth, which are contraction scour, pier scour or abutment scour. The HEC-18 equations are derived based on the lab experiment on non-cohesive soils. These equations are also used to calculate the scour depth in cohesive soils. Different sets of hydraulic parameters like discharge, width, and depth at different sections are needed by HEC-18 equations to calculate the different-type scour depths. The hydraulic parameters can be obtained from either WSPRO or HEC-RAS or other flow simulation programs. The HEC-RAS is the newest software package from HEC. This study was done to figure out and illustrate some uncertainties in HEC-18 equations that are being used for calculating the scour depth in cohesive soils.

Different models which are used to obtain the hydraulic parameters were compared and the effect of the change in the hydraulic parameters to the scour depth were discussed.

Four bridge cases in which the scour depths were calculated using HEC-18 equations were provided by the ALDOT. These bridge cases were used to evaluate, understand, and illustrate the uncertainty in bridge scour calculation. The critical velocities and shear stresses of the six cohesive soils that were obtained from the EFA from the published report “Evaluation of cohesive soils-phase 2” were used to analyze the uncertainties of the HEC-18 equations. The uncertainties in the hydraulic parameters used in the HEC-18 equations were also discussed.

The HEC-18 equations for contraction scour (clear-water and live-bed) use several hydraulic parameters for the scour depth calculations. These hydraulic parameters were calculated in this study from two methods: WSPRO and HEC-RAS. Both models were setup and different simulations were done using the same channel geometrical and flow data to obtain the hydraulic parameters. The differences in the hydraulic parameters obtained from WSPRO and HEC-RAS were analyzed and discussed. Also, the scour depths resulting from respective hydraulic parameters were compared and analyzed.

There are possible different types of soil in different layers (depths) with different D_{50} values. Current DOTs typically use HEC-18 and the average D_{50} removing outliers to calculate the scour depth. The effect of using average D_{50} value and using layer by layer D_{50} value was analyzed and discussed. Also, the effect of averaging D_{50} removing the outliers and without removing the outliers on scour depth was evaluated and discussed.

There were various difficulties in past to obtain the soil samples to test the erosion rate in Alabama. The soil samples obtained were unusable for performing the soil erosion test due to cracks and fractures. A part of the initial plan for this study was to develop soil samples with

different percentage of sand, clay, and silt in pugger mixer and do the erosion testing on the EFA. However, due to the problem in the motor of the EFA, which is used to push the soil sample out of the Shelby tube, the EFA test could not be performed for more than two soil samples. The procedure of running the pugger mixer was figured out. Two soil samples with different soil percentage were developed and tested in EFA using old methods (not using the ultrasonic sensor). The critical shear stress and the critical velocity from EFA and HEC-18 were compared and analyzed for two soil samples with different percentage of sand, clay, and silt.

6.2 CONCLUSION

It was concluded that there exist certain uncertainties in HEC-18 equations and it is best and more suitable to be used to calculate the scour depth of non-cohesive soil as the equations were derived based on lab experiment on non-cohesive soils. The uncertainty of predicting and estimating the scour depth comes from various sources such as soil properties (D_{50} , critical velocity and scour rate) and hydraulic parameters. HEC-18 use only D_{50} value to calculate the critical velocity. Although, having same D_{50} value the percentage of cohesiveness could be different which would affect scour depth. For cohesive soils (e.g., clay) with small particle sizes (i.e., D_{50}), the HEC-18 method calculates smaller critical velocities and then make the scour occur earlier than it is supposed to occur. Calculated critical velocities and modeled velocity at the upstream approach section decides the equation to be used either as live-bed or clear-water scour. The critical shear stress obtained from EFA (τ_{c1}) was compared to the critical shear stress obtained from the HEC-18 (τ_{c2}) using D_{50} as input. The ratio of τ_{c1}/τ_{c2} ranges from 3.2 to 115 with an average of 31.8 and standard deviation of 37.9; therefore, it means for these clay soils ($D_{50} < 0.09$ mm) the critical

shear stress from HEC-18 is significantly smaller than the critical shear stress determined using EFA tests.

The critical velocity calculated from HEC-18 (V_{c1}) and the critical velocity using τ_{c-EFA} and D_{50} (V_{c2}) were compared when the upstream water depth (y) is taken as 1.5 or 4 m for calculations. The ratio of V_{c2}/V_{c1} ranges from 1.7 to 10.4 with an average of 4.8 and standard deviation of 2.7. That means the HCE-18 predicts the scour earlier than it happens which would overestimate the scour depth. For the main channel, V_C obtained from HEC-18 Equation 2.5 (Table 3.3) is less than V_I (Table 3.4) which would make it a live-bed scour. Table 3.4 shows the scour depth of 7.74 ft calculated using default method from HEC-18, which allows HEC-18 to determine whether or not the clear-water or live-bed scour would occur. HEC-18 results show the live-bed scour would occur. However, V_C obtained from Equation 2.6 is greater than V_I for same channel section which would make it as a clear-water scour. The particle size D_{50} has a direct impact on calculating the clear-water scour depth after the scour (Equation 1.3), i.e., proportion to $1/D_{50}^{2/7}$. The scour depth calculated using the clear-water scour would result in 47.76 ft of scour in the main channel. This is a huge difference in calculated scour depth that explains the uncertainty in the HEC-18 equation. So, it was concluded that using HEC-18 with average D_{50} for cohesive soil has certain uncertainties and could overestimate the scour depth. Therefore, the USGS envelope curves developed for ALDOT are used at the bridge sites where the scour depth predicted using HEC-18 is not reasonable. Two main variables influencing the clear-water scour were velocity index and channel contraction ratio. These two variables were used as independent variables to develop two envelope curves. The envelope curves developed for ALDOT can only be used to bridge sites that fall on the Black Prairie Belt (Figure A.5). If the scour depth calculated from HEC-18 of any bridge site that falls on the Black Prairie Belt seems not reasonable then engineers are suggested to use those

envelope curves to calculate the scour depth. Many DOTs do not have the envelope curves developed from observed scour depths as USGS did for ALDOT. DOTs may not have other additional tools to help designers estimate/predict the scour depth more accurately.

From the study of multilayer method, it was concluded that using only average D_{50} value doesn't accurately predict the scour depth. The D_{50} value of all layers should be considered while calculating the scour depth. Using the layer by layer D_{50} values to calculate the scour depth from HEC-18 and summing up all the feasible scour depths in each layer could give more accurate scour depth rather than using only average D_{50} value. When recommending the multilayer method for predicting the scour depth, it is desired to have D_{50} for many layers up to deep depths, otherwise, limited data may affect the accuracy of the multilayer method. For more accuracy in multilayer method, one can use the weighted average D_{50} with layer thickness or just take an average of D_{50} up to the layer where the soil is eroded.

There is uncertainty to accurately determine representative D_{50} in the field in different depth layers and specify D_{50} for some depth layers where D_{50} was not determined. The variations of D_{50} could affect the scour depth calculation, for example, for the bridge site in Valley Creek, D_{50} is 0.15 mm in the first 10 ft and 0.075 mm in the next 10 ft, and using hydraulic parameters from HEC-RAS, HEC-18 predicts 9.0 ft and 12.5 ft of clear-water scour in the left overbank area. In above case, the particle size in deeper depth is half of D_{50} in the surface layers but the scour depth is about 39% more. For Spear Creek, D_{50} in the main channel ranged from 0.006 to 0.106 mm but it has no effect on the scour depth of the live-bed, and only hydraulic parameters dominantly control the scour depth calculation. The scour depth from all the D_{50} value of the layers was 17.5 ft. Since the water depth after live-bed scour is linked with D_{50} through an exponent K_I in Equation (1.2), K_I has three values (0.59, 0.64, and 0.69) as the ratio of shear velocity and fall

velocity (depends on the D_{50} value of the bed material) falls into three ranges (<0.5 , ≥ 0.5 but ≤ 2.0 , and >2.0).

WSPRO and HEC-RAS models using the same geometry and flow input data outputs/simulates similar but not exactly same magnitude of hydraulic parameters (e.g., discharges, width, and depths at the approach and contraction sections), although both use the standard step method to solve the one-dimensional energy equation. WSPRO model distributes more flow in the overbank areas than HEC-RAS does but HEC-RAS distributes more flow in the main channel for this case study. Therefore, HEC-RAS predicts much more scour in the main channel than WSPRO does, for example, HEC-RAS predicts 17.9 ft and WSPRO predicts 7.7 ft of live-bed scour in the main channel of Spear Creek under 100-year flood (the percent difference is 79.3%), but HEC-RAS predicts 6.6 and 8.6 ft and WSPRO predicts 10.3 and 12.0 ft of clear-water scour in overbank areas (the percent differences of 43.3% and 32.8%). Hydraulic parameters in Equations (1.2) and (1.3) play an important role in calculating the scour depth. Scour depths are typically calculated for overbank areas and the main channel separately, and the clear-water scour is determined for heavily vegetated overbank areas. The effects of these hydraulic parameters on the scour depth were studied in Spear Creek as a case study (Table 5.10). It is evident that predicted scour depth could be different according to the 1-D hydraulic model used for obtaining the hydraulic parameters. Results show there is not much change in the hydraulic parameters by changing the expansion and contraction lengths and the contraction and expansion coefficients for energy losses; therefore, they have not much impact on the scour depth also. However, in other studies (Brunner and Hunt 1995) these lengths and coefficients could play a much greater role in predicting the energy losses and water surface elevations near the bridge. This study also suggests considering the ineffective flow area while doing the simulation using HEC-RAS. Using

ineffective flow areas could change the hydraulic parameters which will eventually change the scour depth. Given that a limited number of data sets were used in this study and due to the unavailability of observed data of hydraulic parameters this study could not accurately point out which model to be the best one to calculate the hydraulic parameters for calculating scour depth.

The soil samples collected from the field which could be unusable for EFA tests could be made usable by using the pugger mixer. Different soil component which could be in or near the bridge site and is difficult to obtain can be engineered in the lab using pugger mixture. The EFA test can be run with the soil samples developed by using pugger mixer. It would be easier and most reliable to use pugger mixer when the soil sample obtained from the site is not usable in EFA.

6.3 FUTURE STUDIES

The hydraulic parameters could be calculated from different models and using those hydraulic parameters to calculate scour depth could give different scour depth. A study can be carried out to figure out the best model for obtaining the hydraulic parameters by comparing them to the observed data, and this will lead to a more accurate scour depth prediction. Some of the hydraulic parameters are also difficult to measure in the field, especially during the flood event; therefore, two- or three-dimensional computational fluid dynamics models and laboratory experiments could be used/performed to determine how much flow should go to the main channel and overbank areas and which one-dimensional model is more accurate. Through the study, it was still difficult to figure out the percentage effect of a change in the hydraulic parameters to scour depth. The more in-depth study could be carried out to create a relationship/trend of change in hydraulic parameters to scour depth.

EFA test is used to determine the critical velocity and the scour rate for both cohesive and noncohesive soil. EFA test results should be used in the calculation and specifying the critical

velocity and the erosion rate of cohesive soils for determining the scour depth. The soil samples with different percentage of soil components developed from the pugger mixer should be used in EFA to see the difference in critical velocity and scour rate. The percentage of sand for the soil sample 1 and 2 were higher which makes the D_{50} of the whole sample to 0.20 and 0.27 mm. For the future, soil samples with a high percentage of clay and silt than sand should be prepared to make it more cohesive. Soil samples with different moisture content can be made from the pugger mixer. The critical velocity and the scour rate for same soil samples with different soil moisture content could be performed and analyzed in future so that the effect of moisture content in scour could be known. Another method called Scour rate in cohesive soil (SRICOS-EFA)(Briaud et al. 2005) could be used to calculate the scour depth of a fine-grained soil more accurately. SRICOS-EFA use the data obtained from the EFA. The program needs the shear stress and scour rate in different layers for the calculation of the scour. SRICOS-EFA performs a site-specific scour calculation using soil properties (Briaud et al. 2005) and long-term discharge time-series data because it uses site-specific soil samples which are not only coarse and EFA to determine critical velocity and scour rate. Also, it includes the time effect using a long-term hydrograph unlike using peak flow rate of 100 or 500 years return flow rate as in HEC-18. In addition to that, the SRICOS-EFA method can handle layered soil system which could be much more beneficial in a site where there a different soil types or properties in different layers.

References:

- Akan, A. O. (2011). *Open channel hydraulics*, Butterworth-Heinemann.
- Anderson, J. B., Fang, P. X., Walker, P. M. E., Wright, W. H., and Chen, G. (2015). "Evaluation of Scour Potential of Cohesive Soils–Phase 2." *Project report to Alabama Department of Transportation*, Highway Research Center, Auburn University, AL 36849.
- Angel, J. R., and Huff, F. A. (1997). "Changes in heavy rainfall in midwestern united states." *Journal of Water Resources Planning and Management*, 123(4), 246-249.
- Arneson, L., and Shearman, J. (1998). "USER'S MANUAL FOR WSPRO--A COMPUTER MODEL FOR WATER SURFACE PROFILE COMPUTATIONS." *Technical document*, FHWA, Lakewood, Colorado.
- Arneson, L., Zevenbergen, L., Lagasse, P., and Clopper, P. (2012). "Evaluating scour at bridges." *Technical Report*, FHWA, Fort Collins, Colorado 80525.
- Benedict, S. T. "Development of regional envelope curves for assessing limits and trends in scour." *Proc., World Environmental and Water Resources Congress 2007: Restoring Our Natural Habitat*, 1-11.
- Benedict, S. T., and Caldwell, A. W. (2006). *Development and evaluation of clear-water pier and contraction scour envelope curves in the Coastal Plain and Piedmont provinces of South Carolina*, US Department of the Interior, US Geological Survey.
- Benedict, S. T., Deshpande, N., Aziz, N. M., and Conrads, P. A. (2006). "Trends of abutment-scour prediction equations applied to 144 field sites in South Carolina." Geological Survey (US).

- Breusers, H., Nicollet, G., and Shen, H. (1977). "Local scour around cylindrical piers." *Journal of Hydraulic Research*, 15(3), 211-252.
- Briaud, J.-L., Chen, H.-C., Li, Y., Nurtjahyo, P., and Wang, J. (2005). "SRICOS-EFA method for contraction scour in fine-grained soils." *Journal of geotechnical and geoenvironmental engineering*, 131(10), 1283-1294.
- Briaud, J.-L., Govindasamy, A. V., Kim, D., Gardoni, P., Olivera, F., Chen, H.-C., Mathewson, C., and Elsbury, K. (2009). "Simplified method for estimating scour at bridges." *Report 0*, 5505-5501.
- Briaud, J.-L., Ting, F., Chen, H., Cao, Y., Han, S. W., and Kwak, K. (2001a). "Erosion function apparatus for scour rate predictions." *Journal of geotechnical and geoenvironmental engineering*, 127(2), 105-113.
- Briaud, J.-L., Ting, F. C., Chen, H., Gudavalli, R., Perugu, S., and Wei, G. (1999b). "SRICOS: Prediction of scour rate in cohesive soils at bridge piers." *Journal of Geotechnical and Geoenvironmental Engineering*, 125(4), 237-246.
- Briaud, J., Chen, H., Kwak, K., Han, S., and Ting, F. (2001). "Multiflood and multilayer method for scour rate prediction at bridge piers." *Journal of Geotechnical and Geoenvironmental Engineering*, 127(2), 114-125.
- Briaud, J., Chen, H., Nurtjahyo, P., Kwak, K., and Han, S. (1999a). "Bridge scour in cohesive materials." *Interim Rep. on NCHRP Project 24*, 15.
- Brunner, G. W. (1995). "HEC-RAS River Analysis System. Hydraulic Reference Manual. Version 1.0." DTIC Document, Fort Belvoir, VA 22060-6218.

- Brunner, G. W. (2001). *HEC-RAS River Analysis System: User's Manual*, US Army Corps of Engineers, Institute for Water Resources, Hydrologic Engineering Center.
- Brunner, G. W., and Hunt, J. H. (1995). "A Comparison of the One-Dimensional Bridge Hydraulic Routines from HEC-RAS, HEC-2 and WSPRO." DTIC Document.
- Chang, F., and Davis, S. "Maryland SHA Procedure for Estimating Scour at Bridge Abutments Part 2-Clear Water Scour." *Proc., Proceeding Paper*, Water Resources Engineering (Hydraulics) Division of the American Society of Civil Engineers (ASCE).
- Chow, V. (1959). *Open channel hydraulics*, McGraw-Hill Book Company, Inc; New York.
- Crim, S. H. (2003). "Erosion functions of cohesive soils." Master degree thesis, Auburn University, Auburn,AL, 36489.
- Gates, T. K., Watson, C. C., and Wittler, R. J. "How spacing of cross-section surveys affects understanding of variability in channel hydraulic geometry." *Proc., Water Resources Engineering'98*, ASCE, 1703-1708.
- Gjunsburgs, B., Govša, J., and Jaudzems, G. "Influence of the River Bed Stratification on Scour at Foundations." *Proc., publication. editionName*, Riga Technical University 1-9.
- Gjunsburgs, B., Govsha, J., and Lauva, O. "Scour at layered river bed: reason of the structures failure." *Proc., Environmental Engineering. Proceedings of the International Conference on Environmental Engineering. ICEE*, Vilnius Gediminas Technical University, Department of Construction Economics & Property, 1.
- Henderson, F. M. (1996). *Open channel flow*, Macmillan.

- Johnson, P., Clopper, P., Zevenbergen, L., and Lagasse, P. (2015). "Quantifying uncertainty and reliability in bridge scour estimations." *Journal of Hydraulic Engineering*, 141(7), 04015013.
- Lagasse, P. F. (2007). *Countermeasures to protect bridge piers from scour*, Transportation Research Board.
- Lagasse, P. F., Zevenbergen, L., Spitz, W., and Arneson, L. (2012). "Stream stability at highway structures." *Technical report document*, FHWA.
- Laursen, E. M. (1962). "Scour at bridge crossings." *Transactions of the American Society of Civil Engineers*, 127(1), 166-179.
- Laursen, E. M. (1963). "An analysis of relief bridge scour." *Journal of the Hydraulics Division*, 89(3), 93-118.
- Lee, K., and Hedgecock, T. (2008). "Clear-Water Contraction Scour at Selected Bridge Sites in the Black Prairie Belt of the Coastal Plain in Alabama, 2006." Geological Survey (US).
- Matthai, H. F. (1967). *Measurement of peak discharge at width contractions by indirect methods*, US Government Printing Office.
- Melville, B. W., and Coleman, S. E. (2000). *Bridge scour*, Water Resources Publication.
- Mobley, T. (2009). "Erodibility testing of cohesive soils." Master Thesis, Auburn University, Auburn.
- Mueller, D. S., and Wagner, C. R. (2005). "Field observations and evaluations of streambed scour at bridges." *Technical report document*, FHWA,USGS.

- Richardson, E., and Davis, S. (2001). "HEC-18: Evaluating Scour at Bridges." *FHWA Hydraulic Engineering Circulars (HEC)*.
- Schneider, V., Board, J., Colson, B., Lee, F., and Druffel, L. (1977). "Computation of backwater and discharge at width constrictions of heavily vegetated flood plains." US Geological Survey, Gulf Coast Hydrosience Center, National Space Technology Laboratories.
- Shan, H., and Kerenyi, K. (2014). "Scour in Cohesive Soils." *Technical report document FHWA*, Hampton, VA 23669.
- Shearman, J., Kirby, W., Schneider, V., and Flippo, H. (1986). "Bridge waterways analysis model-research report: US Department of Transportation Publication No." FHWA/RD-86/108, Turner Fairbank Highway Research Center, 6300 Georgetown Pike McLean, Virginia 22101-2296.
- shearman, j., Kirby, W., Schneider, V. R., and Flippo, H. (1986). "Bridge Waterways Analysis Model- research report: US Department of Transportation Publication No." FHWA/RD-86/108, Turner Fairbank Highway research Center, 6300 Georgetown PIke McLean, Virginia 22101-2296.
- Shields, A. (1936). "Anwendung der Aehnlichkeitsmechanik und der Turbulenzforschung auf die Geschiebebewegung." *PhD Thesis Technical University Berlin*.
- Shirole, A., and Holt, R. (1991). "Planning for a comprehensive bridge safety assurance program." *Transportation Research Record*(1290).
- Sturm, T. W., Ettema, R., and Melville, B. W. (2011). *Evaluation of bridge-scour research: Abutment and contraction scour processes and prediction*, National Cooperative

Highway Research Program, Transportation Research Board of the National Academies
Washington, DC, USA.

Walker, M. (2013). "Scour potential of cohesive soils." Auburn University, Auburn, AL 36849.

Wright, W. (2014). "Laboratory Scour Testing of Hard Cohesive Soils in Alabama." Master
Thesis, Auburn University, Auburn, AL, 36849.

Yao, C., Briaud, J.-L., and Gardoni, P. (February 23-26, 2014). "LRFD Calibration of Bridge
Foundations Subjected to Scour." *Proc., Geo-Congress 2014*, Atlanta, Georgia.

Zhang, G., Hsu, S. A., Guo, T., Zhao, X., Augustine, A. D., and Zhang, L. (2013). "Evaluation of
Design Methods to Determine Scour Depths for Bridge Structures." *Technical Report*,
FHWA, Baton Rouge, LA 70804-9245.

APPENDIX A HEC-RAS AND WSPRO MODEL PROCEDURE AND DEVELOPMENT OF HEC-RAS MODEL FOR THE STUDY

A.1 INTRODUCTION

Bridge hydraulics is an important aspect of designing a safe bridge structure. Flow through bridges is an important aspect of computing water surface profiles. The accurate computation of water surface profiles through bridges is necessary for flood damage studies, channel design and analysis, and stream stability and scour evaluations (Brunner and Hunt 1995). In the early 70's bridge design was done by hand. Bridge analysis was conducted using one surveyed cross-section. In the late 1970's and early 1980's hydraulic engineers began to use computers to assist in their design work. The Corps of Engineers and the Federal Highways Administration both introduced programs for computing flood profiles through bridges. Some widely used programs are HEC-2 and WSPRO (Brunner and Hunt 1995). The Hydrologic Engineering Center introduced HEC-RAS (HEC, 1995) in 1995, which is the modernized (with windows graphical user interface) and enhanced version of HEC-2, for computing one-dimensional water surface profiles. In this study, the computational process of two models (WSPRO and HEC-RAS) is highlighted. Some significant differences in determining hydraulic parameters, which affect the calculation of scour depth, are mention.

Generally, both models use the standard step method in calculating the water surface profiles in natural rivers. However, both models compute the water surface profile through a bridge differently.

A.2 WSPRO

The WSPRO program was designed to provide a water surface profile for six major types of open channel flow situations: (i) unconstructed flow, (ii) single-opening bridge, (iii) bridge opening(s) with spur dikes, (iv) single opening embankment overflow, and (v) multiple alternatives for a single site and multiple openings. WSPRO computes the water surface profile through a bridge by solving the energy equation. The model uses/requires several cross sections, which are defined by a series of ground points with horizontal coordinate (station from a reference point on the left overbank area) and elevation, for the profile computation. The cross sections used in WSPRO are shown in the Figure A.1 in reference to the bridge opening.

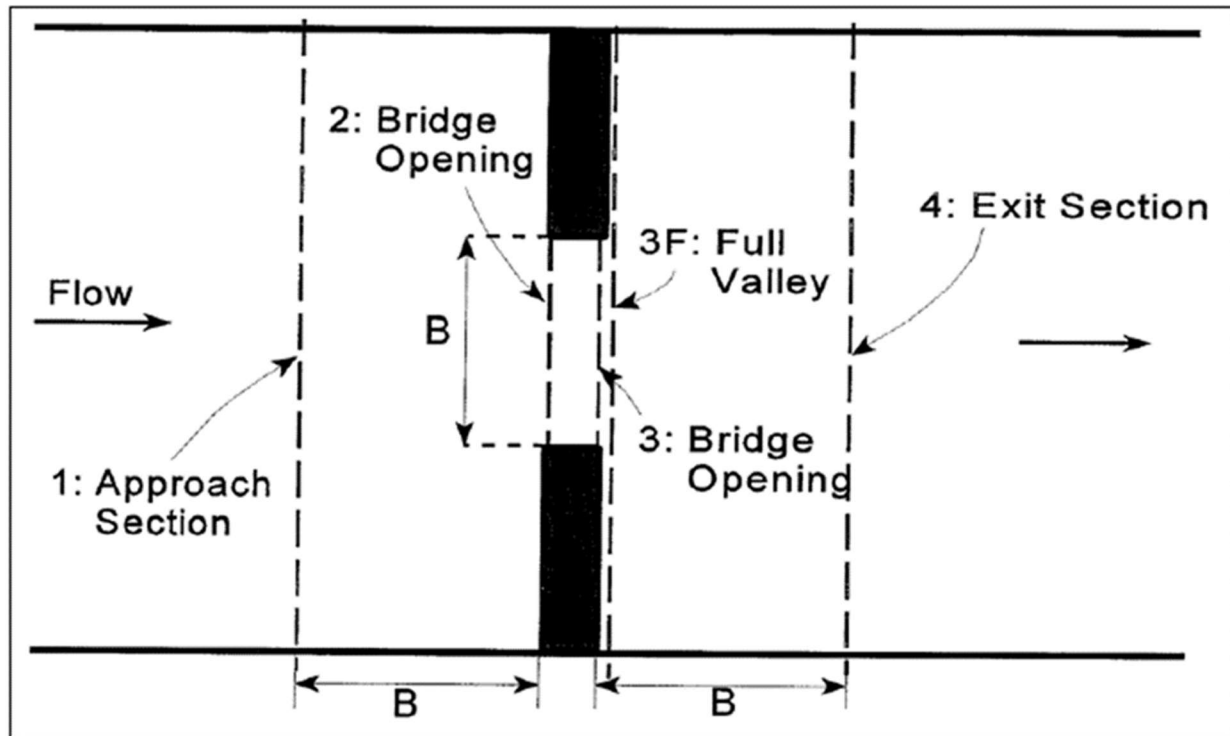


Figure A.1 Definition sketch of cross-section locations used in WSPRO for a single opening bridge

For WSPRO model, there should be at least four cross sections to compute the water surface profiles. As shown in Figure A.1, the cross sections 4, 3F, 3 and 1 are the required cross sections. The cross sections 4, 3F and 1 are unconstructed full valley sections (or natural river cross sections without the bridge), while the cross section 3 is the downstream bridge opening section. The cross section 2 is the upstream bridge opening section as like the cross section 3 which is an additional control point. It depends on the users to input data for the cross section 2. The approach section 1 is similar to the cross section 4 for HEC-RAS (Figure 1.4) when the flow is not affected by the bridge and starts the contraction afterward.

The model starts the single-opening bridge hydraulic analysis with the computation of the natural profile (no bridge structure) from the exit section 4 to the full valley section 3 and then to

approach section 1. These data permit determination of the amount of backwater caused by the constriction and are used as the initial trial elevation in the iterative solution for the water surface profile through the bridge. The program then computes the profile with the bridge in place. The energy balance is performed from the cross section 4 (exit section, Figure A.1) to the section 3 (bridge opening); then from the section 3 to 2; and finally, from the section 2 to 1.

The energy equation from the exit section to approach section can be written as,

$$h_1 + \frac{V_1^2}{2g} = h_4 + \frac{V_4^2}{2g} + h_{L(1-4)} \quad (\text{A.1})$$

where h_1 = water surface elevation at section 1, V_1 = average velocity at section 1, h_4 = water surface elevation at section 4, V_4 = average velocity at section 4, $h_{L(1-4)}$ = head (energy) losses from section 1 to 4.

Energy losses from section 1 to 4 are equal to friction losses from 1 to 4 and an expansion loss from 3 to 4. The energy losses between the different sections are calculated by using different equations. So, a heading is created which defines the head loss in that section.

Section 3-4

Since head loss is the sum of the frictional loss and the expansion loss, there are two separate equations to calculate the losses. Frictional losses are calculated using the geometric mean friction slope (discharge divided by the conveyance) times the straight-line distance between section 3 and 4, i.e., the distance “B” in Figure A.1.

$$h_{f(3-4)} = \frac{BQ^2}{K_3K_4} \quad (\text{A.2})$$

where K_3 and K_4 are the total conveyance at section 3 and 4, respectively. Q is the total discharge.

The expansion loss is calculated from 3 to 4 by the following equation,

$$h_e = \frac{Q^2}{2gA_4^2} \left[2\beta_4 - \alpha_4 - 2\beta_3 \left(\frac{A_4}{A_3} \right) + \alpha_3 \left(\frac{A_4}{A_3} \right)^2 \right] \quad (\text{A.3})$$

Where α and β are energy and momentum correction factors for non-uniform flow. A_4 and A_3 are the respective cross section area at 4 and 3. α_4 and β_4 are computed as follows

$$\alpha_4 = \frac{\sum \left(\frac{K_i^3}{A_i^2} \right)}{\frac{K_T^3}{A_T}} \quad (\text{A.4})$$

$$\beta_4 = \frac{\sum \left(\frac{K_i^2}{A_i^2} \right)}{\frac{K_T^2}{A_T}} \quad (\text{A.5})$$

where k_i and A_i are the conveyance and area at the i th-subsection and K_T and A_T are the total conveyance and area respectively.

The coefficients α_3 and β_3 are related to the bridge geometry and are calculated as follows;

$$\alpha_3 = \frac{1}{C^2} \quad (\text{A.6})$$

$$\beta_3 = \frac{1}{C} \quad (\text{A.7})$$

where C is the coefficient of discharge.

The coefficient of discharge is a function of bridge geometry and flow characteristics. The first step to finding out the coefficient of discharge is to find out the base coefficient which depends on the channel contraction ratio and a ratio of flow length to the bridge opening width. Once this base coefficient is figured out, the final coefficient for discharge is computed by multiplying the

base coefficient by a series of the adjustment factor. The adjustment factor depends on the type of bridge opening. Matthai outlined the procedure to calculate the coefficient of discharge for the bridge. For a full explanation, the readers are referenced to read the paper by Matthai (1967).

Section 2-3

The energy loss from section 2 to 3 is based on frictional losses only. The frictional loss is calculated using following equation:

$$h_{f(2-3)} = L_{(2-3)} \left(\frac{Q}{K_3} \right)^2 \quad (\text{A.8})$$

where $L_{(2-3)}$ the distance between the bridge sections and K_3 is the conveyance at section 3 inside the bridge.

Section 1-2

Energy losses from section 1 to 2 are based on friction losses only. The friction loss is calculated by the following equation:

$$h_{f(1-2)} = \frac{L_{av} Q^2}{K_1 K_c} \quad (\text{A.9})$$

where L_{av} is the effective flow length in the approach reach and K_c is the minimum of the conveyance inside the bridge. The effective flow length is the average length of the 20 equal conveyance stream tubes (Angel and Huff 1997; Shearman et al. 1986). Since frictional losses are directly proportional to the flow length, it is imperative to obtain the best possible estimate of the flow length (Shearman et al. 1986). Usually, before the introduction of the effective flow length concept, the friction loss on the approach reach was calculate on the basis of the straight-line

distance between sections. This was accurate enough for the minor degree of constriction. However, for more significant degree of constriction the straight line distance is only representative of portion of flow that is in direct line with the opening. Flow not always flows downstream after the opening. It could flow across the valley to get to the opening. This means the flow is travelling farther than the straight line distance. Schneider et.al (1977) tabulated average streamlines length for various approach section for symmetric constriction in channels having uniform ,homogeneous flow conveyance characteristics. For further details about the effective flow length and the simplified computational technique readers are refer to the report “Bridge Waterways Analysis Model (shearman et al. 1986).

A.3 HEC-RAS

HEC-RAS is the newest model in bridge hydraulics. HEC-RAS is widely used for calculating water surface profiles for steady, gradually varied flow in a natural or constructed channel. Both subcritical and supercritical flow profiles can be calculated. The effects of bridges, culverts, weirs, and structures in the floodplain may be also considered in the computations. These programs are also designed for application in floodplain management and flood insurance studies.

HEC-RAS needs at least four users defined cross-section in the computation of the energy losses for the bridge water surface profiles. Figure A.2 is the sketch showing the cross sections needed in HEC-RAS.

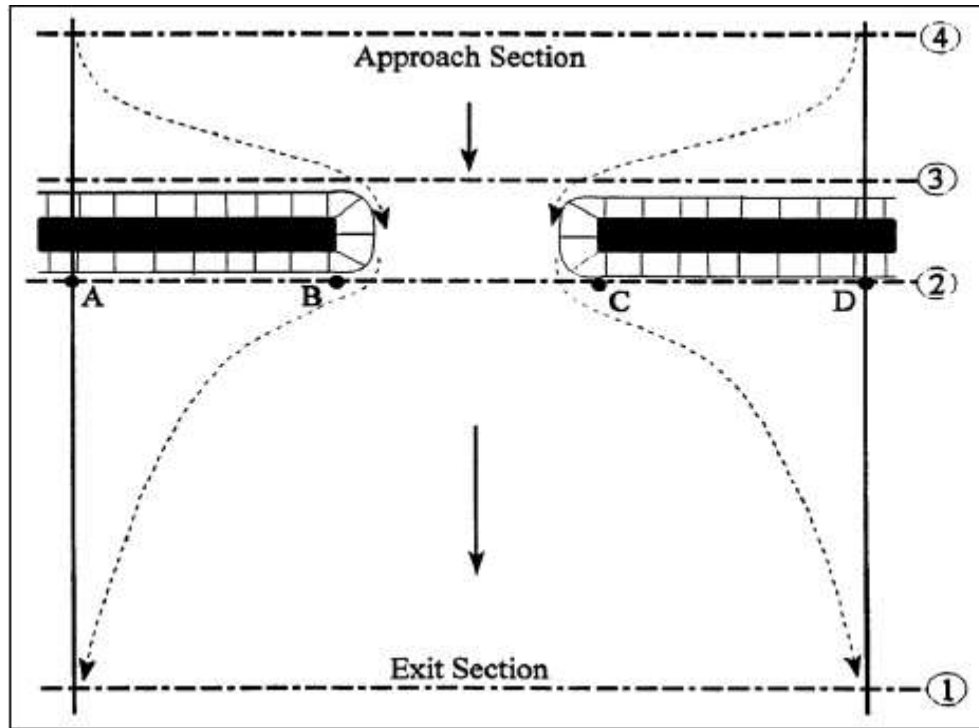


Figure A.2 Cross-section location at bridge (HEC-RAS)

In HEC-RAS, channel cross sections used for the water surface profile computations are named by real numbers decreasing from upstream to downstream along the flow direction, therefore, it is convenient to add more cross sections between two existing sections. The cross section 1, generally called the exit section (Figure A.2) which is located sufficiently downstream from the structures (bridge or culvert) that the flow is not affected by the structure. It means that a sufficient distance is taken to that section where flow gets fully expanded. The cross section 2 (Figure A.2) is located immediately downstream from the bridge (typically at the downstream toe of the embankment). The cross section 3 (Figure A.2) should be located just upstream from the bridge (typically at the upstream toe of the embankment). The distance between cross section 3 and the bridge should be relatively short. The cross section 4 (Figure A.2) is an upstream cross section where the flow lines are approximately parallel and the cross section is fully effective. Basically, the distance between 3 and 4 should be roughly one times the average width of the

opening (e.g., distance BC in Figure 3.2). During the hydraulic computation, the program automatically formulates two additional cross sections inside of the bridge structure. The cross-section geometry developed inside the bridge structure is the combination of the boundary cross section, i.e., section 2 and 3.

Water surface profiles are computed from one cross section to the next by solving the energy equation with an iterative procedure called the standard step method. The energy equation used in HEC-RAS is written as follows:

$$Z_2 + Y_2 + \frac{\alpha_2 V_2^2}{2g} = Z_1 + Y_1 + \frac{\alpha_1 V_1^2}{2g} + h_e \quad (\text{A.10})$$

where Z_1, Z_2 = elevation of the main channel inverts (bottom elevation), Y_1, Y_2 =depth of water at cross sections, V_1, V_2 =average velocities (total discharge /total flow area), α_1, α_2 =kinetic energy correction coefficients, g =gravitational acceleration, h_e =energy head loss (Brunner 1995)

Figure A.3 graphically shows the terms of the energy equation between two cross sections.

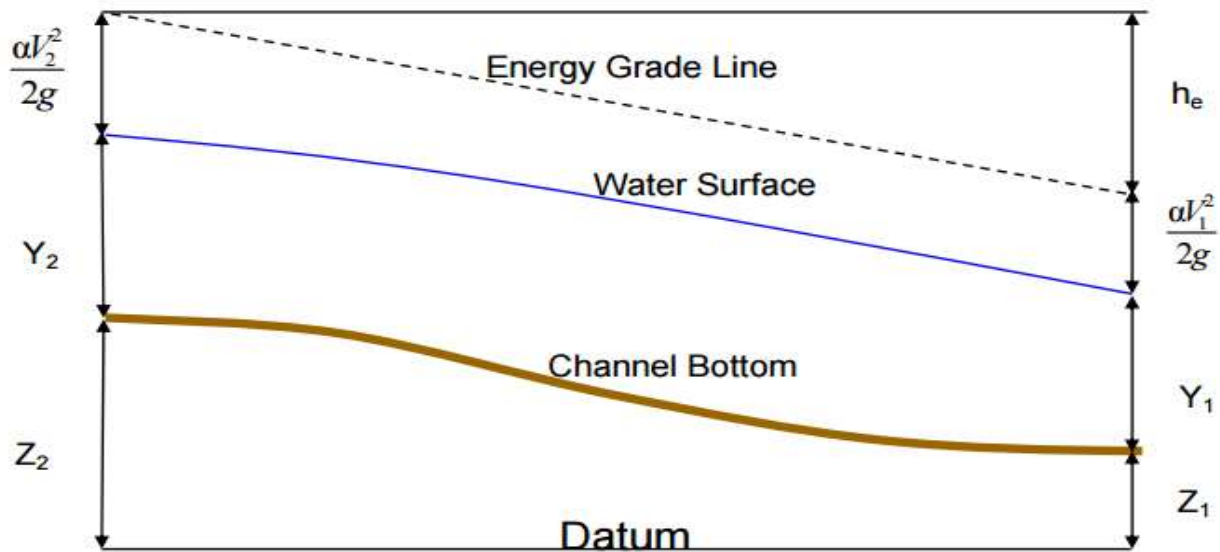


Figure A.3 Representation of terms of energy equation

The head loss is the combination of the friction loss and contraction or expansion losses.

The equation for the energy head loss is as follows:

$$h_e = L\bar{S}_f + C \left| \frac{\alpha_2 V_2^2}{2g} - \frac{\alpha_1 V_1^2}{2g} \right| \quad (\text{A.11})$$

where L = discharge-weighted reach length, \bar{S}_f = representative friction slope between two sections, C =expansion and contraction loss coefficient

The discharge-weighted reach length, L , is calculated as:

$$L = \frac{L_{lob}\bar{Q}_{lob} + L_{ch}\bar{Q}_{ch} + L_{rob}\bar{Q}_{rob}}{\bar{Q}_{lob} + \bar{Q}_{ch} + \bar{Q}_{rob}} \quad (\text{A.12})$$

where, L_{lob} , L_{ch} , L_{rob} = cross-sectional reach lengths specified for flow in the left overbank (lob), main channel (ch), and right over bank (rob), respectively, \bar{Q}_{lob} , \bar{Q}_{ch} , \bar{Q}_{rob} = arithmetic average of the flows between sections for the left overbank, main channel, and right over bank, respectively

Also, the frictional slope is calculated as:

$$S_f = \left(\frac{Q}{\sum K_i} \right)^2 \quad (\text{A.13})$$

Where i = index referring to the i th subsection of the compound channel section and K_i is the conveyance calculated as:

$$K_i = \frac{K_n}{n_i} A_i R_i^{2/3} \quad (\text{A.14})$$

where K_i = Conveyance of the i -th section, K_n =Constant value, 1.49 in English unit and 1 in SI unit, n =Manning's roughness coefficient for subdivision, A_i =Flow area for subdivision, R_i = Hydraulic radius for subdivision (area/wetted perimeter)

Although, both the models use standard step methods to solve the energy equation there is a significant difference in the way of solving them. The way of solving the energy equation could change the value of the hydraulic parameters which are essential in calculating the scour depth from HEC-18. On the verse of study, some significant differences between HEC-RAS and WSPRO were figured out from literature review as well as from the calculation of hydraulic parameter from WSPRO and HEC-RAS. The differences between them are as follows:

1. HEC-RAS is based upon obstruction length while WSPRO is based upon bridge opening length (B in Figure 3.1). Obstruction length is a direct measurement of the channel length of flow contraction and expansion required. It is directly related to the length required for flow contraction and expansion. Obstruction length is also dependent upon both bridge length and flood plain width. Bridge length has no definite relationship to floodplain width and is not directly related to expansion and contraction width.

The exit section 4 in WSPRO is not exactly similar to the cross section 1 for HEC-RAS (Figure 1.4) where the flow has been fully expanded to the whole cross-section.

2. While the WSPRO program doesn't restrict the user about the chosen expansion reach length to be used in determining frictional losses, the user's manual seems to

recommend a reach length equal to one bridge opening width, as opposed to HEC's recommendation of relating the expansion distance to the obstruction width.

3. WSPRO uses the effective flow length concept, whereas HEC-RAS uses discharge-weighted reach length
4. Streamlines are not always parallel. They are transitioning. HEC-RAS can use this by providing users the right to give the main channel and overbank reach length. But in WSPRO there's no function to provide the reach length.
5. HEC-RAS computes expansion losses as the product of a coefficient and the absolute change in velocity head from the section just downstream of the bridge to the exit. WSPRO uses an expansion loss equation that was derived from the approximation solution of the momentum, energy, and continuity equations.
6. The WSPRO uses text only and is deficient in the graphical viewing of results. Debugging those can be daunting when faced with pages of only numbers crammed with text. HEC-RAS has GUI which helps or provides great assistance in detecting bugs and errors in data input.
7. WSPRO uses the coefficient of discharge for the calculation of the expansion length.

A.4 USGS ENVELOPE CURVE FOR ALDOT

As discussed earlier in Chapter 1 bridge scour equation can have substantial uncertainty. The HEC-18 equations are an empirical equation which is derived from the laboratory testing and has simplifying assumptions that do not reflect the complex real conditions typically found in the field. The result that is obtained from using those equations must be scrutinized to assure that

predicted scour is reasonable. The uncertainty of current bridge scours equation has been highlighted by various field investigations of bridge scour.

The uncertainty of the scour prediction equations noted in both laboratory and field investigations indicates a need for caution and judgment when using them to assess potential scour at bridges (Benedict 2007). Richardson and Davis (2001) note that engineer must, “Evaluate whether the computed scour depths are reasonable and consistent with the design engineer’s previous experience and engineering judgment. If the scour predicted is unreasonable, then the HEC-18 procedure provides latitude for engineers to modify the computed values noting that “this modification must reflect sound engineering judgment (Benedict 2007).” Historic scour data which are obtained from high flows could be used in evaluating the reasonableness of predicted scour. However, it is rare that such field data is available at or near the site of interest. To solve this issue, one way is to collect the historic scour depth within a region having similar geology and hydrology (also called physiographic regions). The data collected can then be organized into envelope curves that display the range and limitation of scour within that region. Envelope curves are the curves that define the upper limit of scour throughout the range of collected data.

USGS in cooperation with the ALDOT, made field measurements of clear-water contraction scour at 25 bridge sites in the Black Prairie Belt of the Coastal Plain of Alabama. This comparison showed theoretical scour depth using D_{50} as input, in general, exceeded the observed scour depths about 475 percent (Lee and Hedgecock 2008). Different variables that could influence the scour were investigated and analyzed in the report. It was found that the strongest influencing variables for clear-water contraction scour were the channel-contraction ratio and the velocity index. Envelope curves were developed relating both of these variables to observe scour.

The velocity index is defined as the ratio of average bridge overbank velocity to the average approach overbank velocity within the q subsection (Figure A.6), which is from the main channel bank station to a station projected upstream from the bridge embankment. The q subsection is only a portion of the overbank area. If HEC-RAS is used, the program does not output the information of the q subsection, but manually computation of the average velocity using HEC-RAS data is still feasible. The velocity index is computed for both q subsections in the left and right overbank areas, and the maximum velocity index is finally used to project the scour depth. The velocity index envelope curve is valid for velocity indexes between 1 and 11. The minimum and maximum scour depth that could be obtained from velocity index envelope curve is roughly 4 and 11 ft.

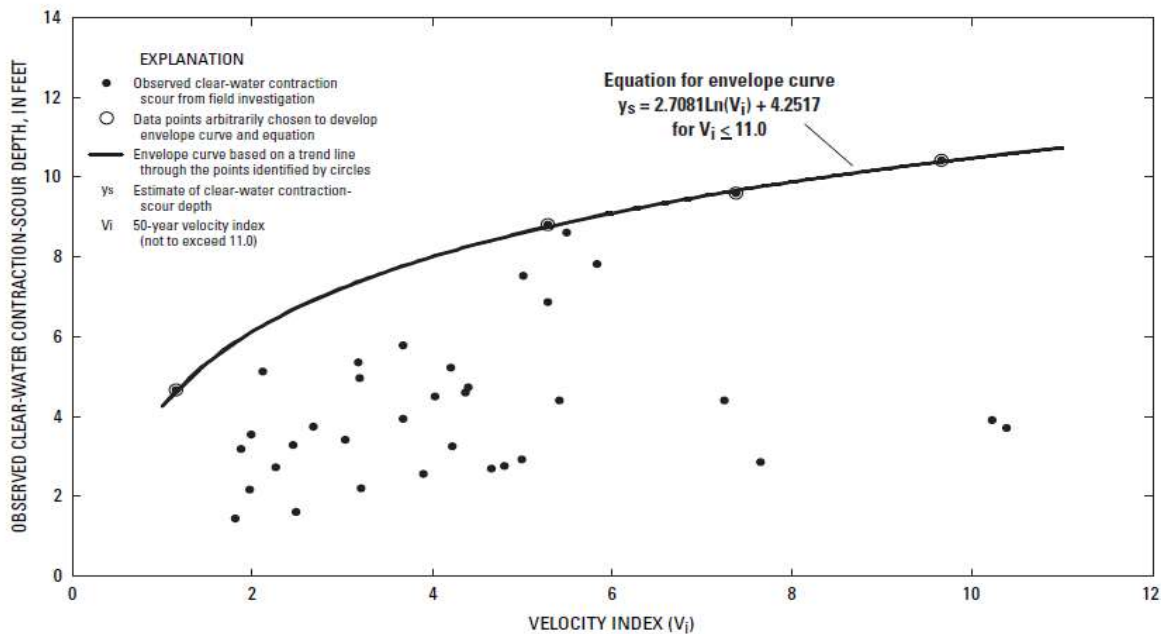


Figure A.4 Envelope curve of observed clear-water contraction-scour depths based on the velocity index at selected sites in the Black Prairie Belt of the Coastal Plain of Alabama (Lee and Hedgecock 2008)

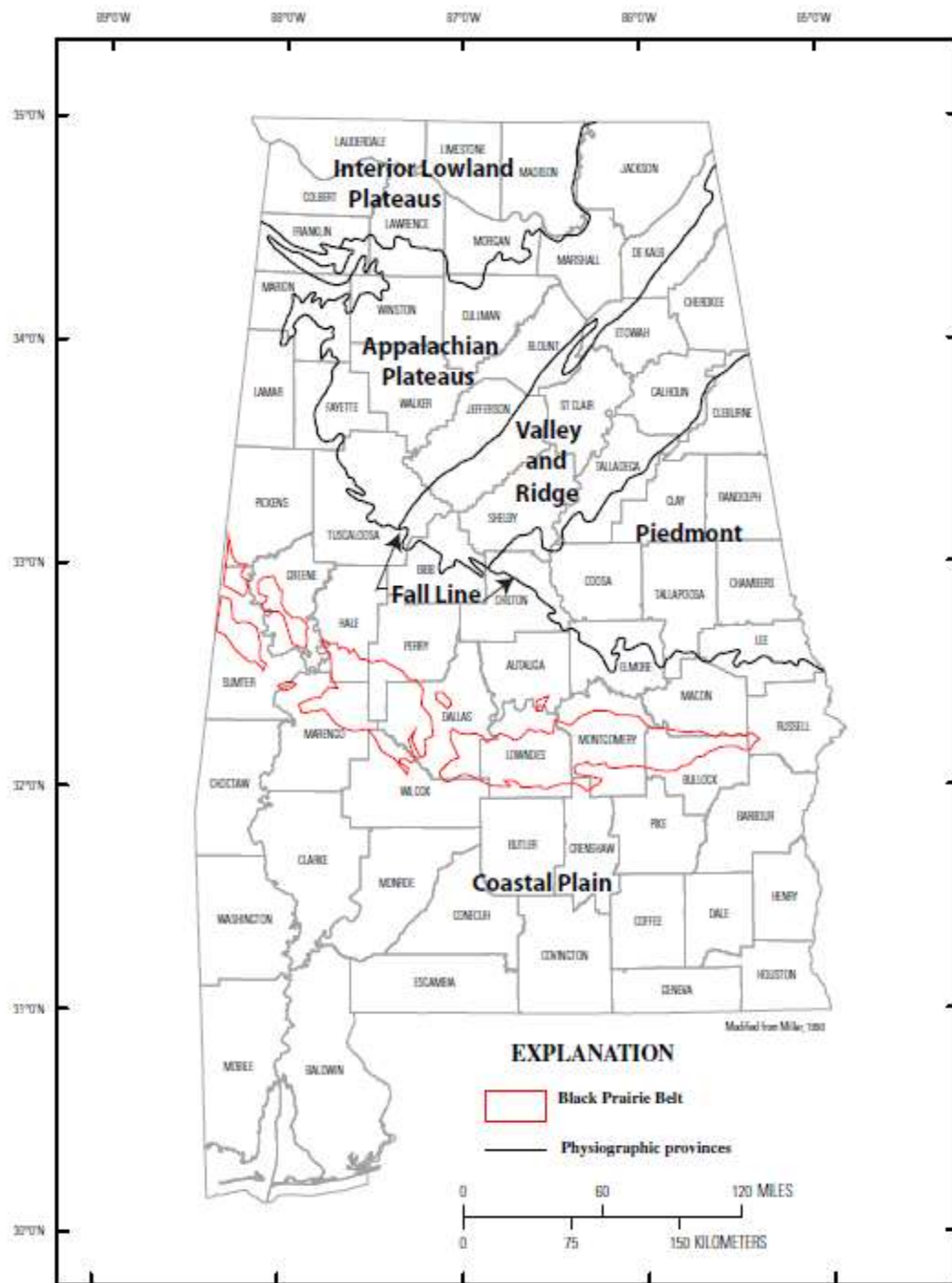


Figure A.5 Location of physiographic provinces in Alabama (Lee and Hedgecock 2008)

where

$$V_i = \frac{\overline{V_{bo}}}{\overline{V_{qo}}} \quad (\text{A.15})$$

V_i = velocity index

$\overline{V_{bo}}$ = respective average bridge overbank velocity in feet per second (Figure A.6)

$\overline{V_{qo}}$ = respective average approach overbank velocity between the top of bank and the projected bridge abutment in feet per second (Figure A.6)

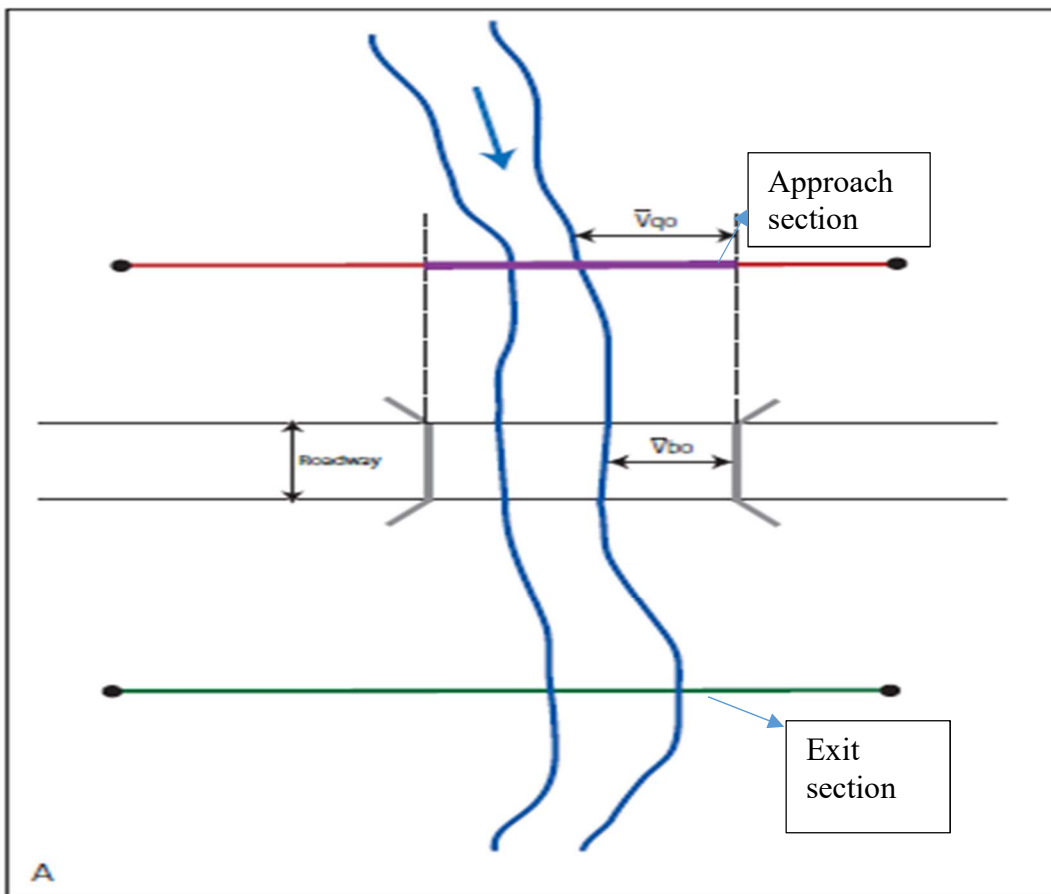


Figure A.6 Definition sketch of variable used (Velocity Index)

WSPRO model was used by USGS to estimate the hydraulic data for all the bridge sites. The model was constructed with series of cross sections. The exit section is defined downstream from the bridge. This cross section represents the section of the minimum area and controls the water surface elevation at the bridge. For the sites that have the uniform reaches, the exit section was propagated upstream from the bridge to represent the approach section. For the sites, which has non-uniform reaches additional cross sections were surveyed. The inspection area was limited to the bridge abutments projected onto the approach section to eliminate any significant changes in geometry on the outer boundaries of the floodplain.

The channel-contraction ratio (m) describes the degree of contraction imposed by a bridge opening on the normal (unconstructed) stream channel and floodplain. The envelope curve using channel contraction ratio is shown in (Figure A.7). The channel contraction ratio envelope curve is valid for channel contraction ratios between 0.25 and 1.0. The minimum and maximum scour depth obtained from channel contraction ration envelope curve is between 2 and 13ft.

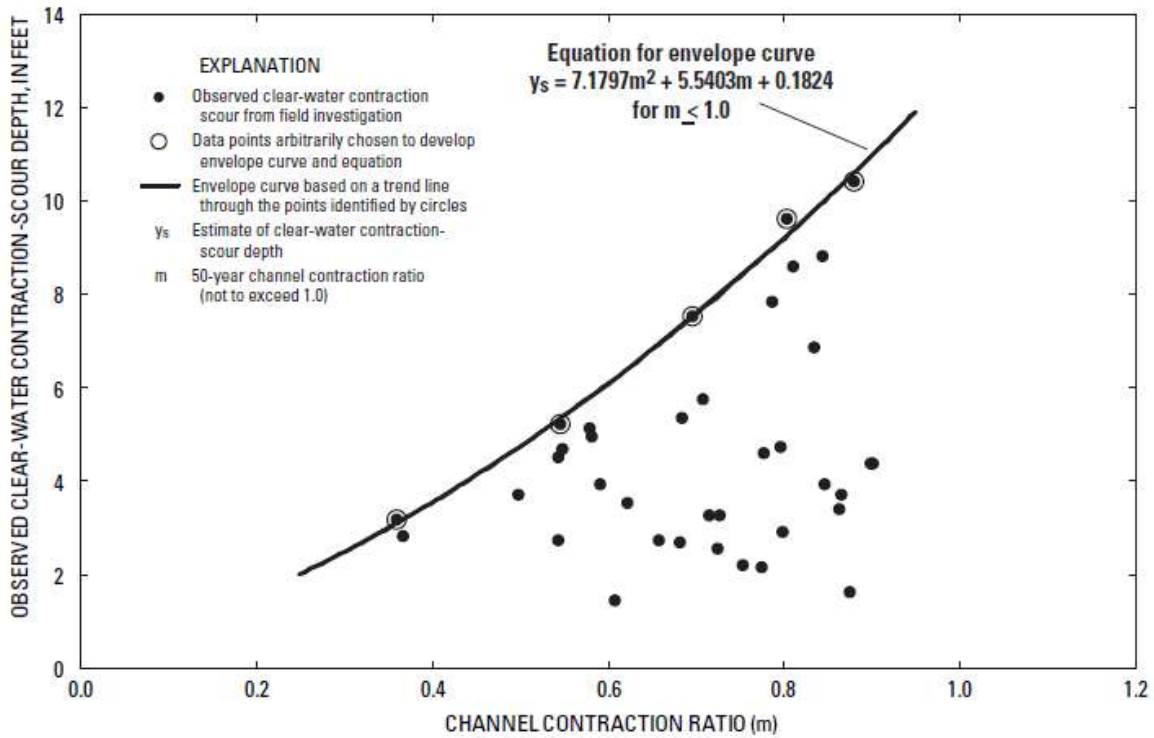


Figure A.7 Envelope curve of observed clear-water contraction-scour depths based on the channel-contraction ratio at selected sites in the Black Prairie Belt of the Coastal Plain of Alabama (Lee and Hedgecock 2008)

where

$$m = \left(1 - \frac{K_q}{K_t}\right) \quad (\text{A.16})$$

m = channel contraction ratio

K_q = the approach conveyance within the projected bridge opening in cubic feet per second

K_t = the total approach conveyance, in cubic feet per second.

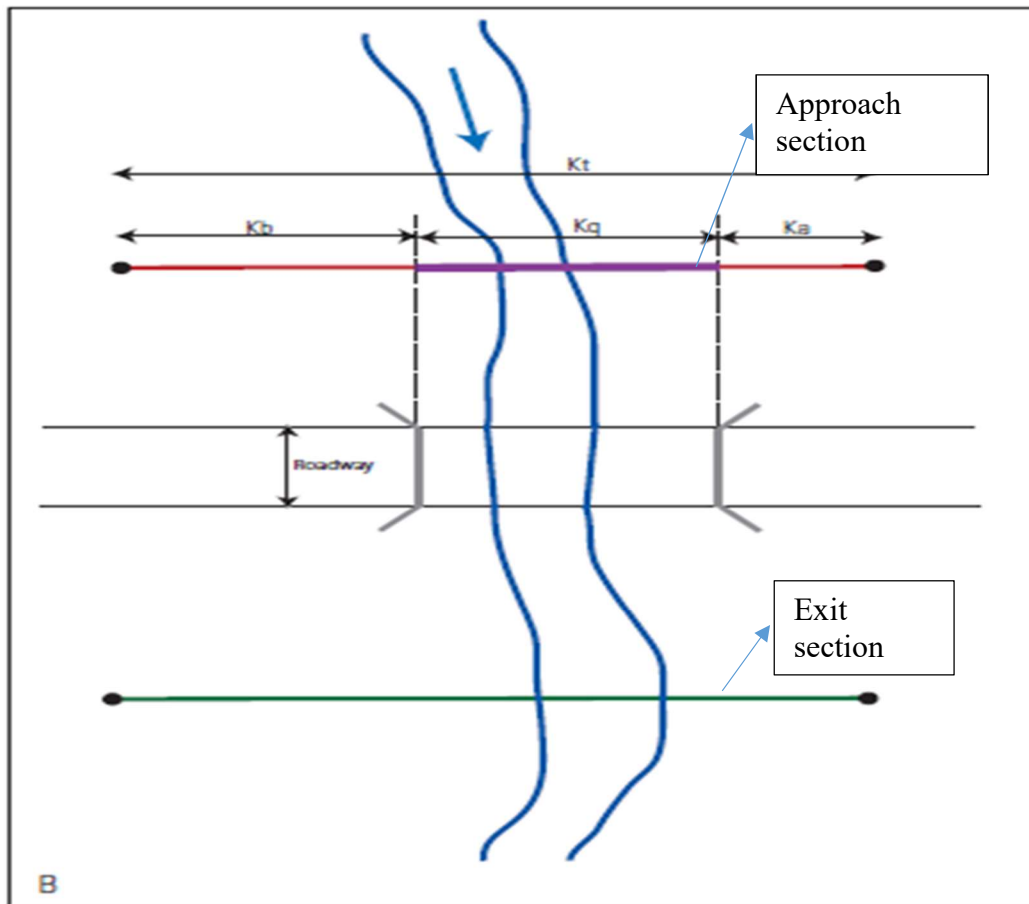


Figure A.8 Definition sketch of variable used (Channel-contraction ratio)

Both the velocity index and the channel contraction ratio envelope curve should be applied to the site of interest when assessing the clear-water contraction scour. These two curves will give two different values. After comparing the values of two envelope curves, the one with the largest value is used to estimate scour depth. These envelope curves were developed using the hydraulic data estimated with hypothetical 50-year flood flow (Lee and Hedgecock 2008). The envelope curve is not suggested to be used in more than 100-year flood flow. The report suggests engineers use a factor of safety (by engineering judgment and experience) if the envelope curve is used for more than 50-year flood flow. For more information on envelope curve, readers are suggested to go

through the report by USGS “Clear-Water Contraction Scour at Selected Bridge Sites in the Black Prairie Belt of the Coastal Plain in Alabama, 2006 (Lee and Hedgecock 2008).

The envelopes curves were used to figure out the scour depth at one of the bridge site (Pintalla Creek) provided by ALDOT. The scour depth calculated using HEC-18 and hydraulic parameters from WSPRO done by ALDOT was 23.07 ft in overbank areas. The scour depth calculated using hydraulic parameters obtained from HEC-RAS in this study was 17.3 ft. The scour depth from calculated using hydraulic parameters from both methods is larger and unreasonable than the maximum scour depth that could occur in that region. Pintalla Creek falls on the black prairie belt of the coastal plain in Alabama. So the USGS report 2007-5260 (Lee and Hedgecock 2008) was used to estimate the scour depth. Figure A.6 taken from the USGS report only presents the variables to calculate velocity index at the right side of the bank up to the abutment projection. This does not mean that left side part of the q subsection is not included in the calculation of the velocity index. Velocity index should be calculated for both sides of the q subsection using $\overline{V_{bo}}$ and $\overline{V_{qo}}$ of each part individually. Greater velocity index from this two is taken as the final velocity index. Calculation of velocity index and channel contraction ratio is shown below:

Table A.1 Velocity indexes (Pintalla Creek)

Velocity Index (left)			
\overline{V}_{bo} (ft/s)	\overline{V}_{qo} (ft/s)	$\frac{\overline{V}_{bo}}{\overline{V}_{qo}}$	Y_s (ft)
4.47	1.82	2.46	6.69
Velocity Index (Right)			
\overline{V}_{bo} (ft/s)	\overline{V}_{qo} (ft/s)	$\frac{\overline{V}_{bo}}{\overline{V}_{qo}}$	Y_s (ft)
4.37	1.79	2.44	6.67

Table A.2 Channel contraction ratio (Pintalla Creek)

Channel contraction ratio			
K_q	K_t	m	Y_s (ft)
1077146	1642752	0.34	2.90

The scour depth calculated from velocity index left is greater than the velocity index at right part of the q subsection. So, velocity index left is taken as the final velocity index. The scour depth calculated from final velocity index (left) is greater than the channel contraction ratio. So, 6.69 ft is taken as the scour depth. The discharge return period was 100 years so a safety factor should be used. Engineers should be aware that deeper scour in this region is possible so a factor of safety should be used with the engineering judgment. The safety factor is taken as 1.2 as taken by ALDOT for this site which makes the final scour depth at Pintalla Creek as 8.02 ft.

APPENDIX B USING PUGGER MIXER TO DEVELOP SOIL SAMPLES FOR EFA TESTING

B.1 INTRODUCTION

Cohesive Soil means clay (fine-grained soil) or soil with high clay content, which has cohesive strength. These soils generally include fine-grained silt and clay mineral particle passing the No. 200 sieve (less than 0.003 inches or 0.075 mm). Cohesive soil does not crumble. These are hard to break up when dry, and exhibits significant cohesion when submerged. There are several devices (Shan and Kerenyi 2014) currently available to study the scour in cohesive soil by more accurately determining the critical shear stress. Some of the devices are as follows:

- Sediment erosion at depth flume (SEDflume).
- Jet erosion test (JET).
- Erosion function apparatus (EFA)
- Adjustable shear stress erosion and transport flume (ASSET)
- Hole erosion test (HET)
- Sediment erosion rate flume (SERF)

EFA was used at Auburn University to determine the critical shear stress for various soil samples collected at or near bridge sites at Alabama (Crim 2003; Mobley 2009; Walker 2013; Wright 2014). In May 2015 FHWA published a report named “ Scour in Cohesive Soils” (Shan and Kerenyi 2014) which has two main objectives. The first was to introduce and demonstrate a new ex-situ erosion testing device (ESTD) that can mimic the near-bed flow of open channels to

erode cohesive soils within a specified range of shear stresses. The second objective was to develop a method for estimating a critical shear stress and erosion rates for a limited range of cohesive soils in the context of the HEC-18 scour framework. For making the soil samples for testing, special consideration was taken to avoid slaking. The soil samples created using compaction method slake and is not useful to do a testing. So pugger mixture was used to make a soil sample to test in ESTD. The report only mentions about the use of pugger mixer but did not provide any information about how to use and procedure of Pugger mixer. So that one of the objectives of this study was to figure out the use and procedure of the Pugger mixer. The critical shear stress of soil samples created and tested in ESTD could be compared with the critical shear stress from EFA in future studies.

In this project, a Peter Pugger, VPM-7 vacuum power Wedger, which is the vacuum deairing pugger-mixer, was purchased for current and future study. This part of the study is primarily to document the procedure using the Pugger mixer to create soil samples for EFA testing. The soil samples prepared by Peter pugger don't slake. Slaking is the breakdown of large, air-dry soil aggregates into smaller sized micro aggregates when they are suddenly immersed in water. Slaking occurs when aggregates are not strong enough to withstand stresses caused by rapid water uptake. The aim of the chapter was to figure out and document how to use the pugger mixer to mix soil components (clay, silt, and sand) of certain percentages into a sample soil of certain soil moisture content and test it using EFA for determining the scour rate. The two soil samples were tested using visual observations on critical velocity and time of eroding 1 mm of the soil sample. Ultrasonic sensors were not used to collect the data and determine the scour rate for these two soil samples but will be used for future EFA tests. There were serious issues from the electronic motor that supposes to push/advance the soil sample into EFA, therefore, the information for two soil

samples and corresponding EFA testing were to demonstrate that soil samples prepared using the pugger mixer can be successfully tested using EFA.

B.2 SOIL PREPARATION AND PROPERTIES

B.2.1 PETER PUGGER

Peter pugger is an instrument which is used to mix the different proportion of dry soil samples with the fastest mixing times in the industry. A Peter pugger does the job of two machines. Unlike other pug mills that require a separate mixer to prepare the clay, the unique design of Peter pugger combines the best of both the machine into a clay mixing machine with pug mill output. Peter pugger machine is different from all another studio pug mill because it has the ability to start with powder and/or dry scrap and finish by pugging a uniform batch of moist clays sets. Pugger mixer mix the soil sample in batch size without continuously force feeding for hours. In another word, the pugger mixer is rated by the size of the batch they can mix. The Peter pugger mixer can mix up to 14 lb. per batch size. Each batch mixing is similar to a washing machine because you can throw the whole batch at once. The large size of the hopper allows for easy loading in pugger mixture. The pugger can pug itself in the form of 3-inch diameter logs. Due to the presence of vacuum pump each batch can be de-aired by starting the vacuum pump during the last stage of mixing, leaving an air-free product when pugged out.

The pugger mixer purchased for the study can pug out a 3-inch (76.2mm) diameter cohesive soil specimen after sufficient mixing. The pugger mixer is capable of mixing sands with a maximum particle size of 0.20 inches (5 mm). Clay, commercial silt, and non-uniform sands in varied percentage can be mixed into cohesive soils with a range of characteristics.

B.2.2 FEATURES

A Peter pugger (mixer) used to create the soil sample for EFA tests has the following features:

Stainless steel: Peter pugger has got the shaft, augers, and paddles made of stainless steel, along with aluminum mixing/pugging chamber which ensures rust-free clay processing.

Large hoppers: The oversized hopper door allows for easy loading of up to 14 lbs. of soil per batch.

Batch mixing capability: Peter pugger has got full batch mixing and blending capability which allows for moisture adjustment before pugging.

Pug mills output: The Peter pugger has the capabilities of pugging out the soil sample itself in 3-inch diameter soil log.

Vacuum de-aired: Each batch can be de-aired by starting the vacuum pump during the last stage of mixing, leaving an air-free product when pugged out.

Sealed chamber: Each Pug mill casting has precision CNC machined O-ring grooves incorporated into them which allow pug mill to effectively store moist clay indefinitely.

Intellectual mixing technology: The pugger mixture can automatically speed up or slow down based on the hardness of the clay being processed.

Patented vacuum chamber: The patented vacuum chamber serves as a separation chamber between the processing chamber (where clay is mixed and pugged) and the gear drive system. If in the event, the pug mill is overfilled, the excess soil is collected in the vacuum chamber where it can be easily accessed and redirected back into the processing chamber in time for the next batch.

Stainless work surface: The stainless-steel work surface creates a durable work surface for convenience of the operator while loading.

Corrosion resistant: Peter pugger is corrosion resistant.

Figure B.1 and Figure B.2 show the Peter pugger mixer used for soil preparation.



Figure B.1 Peter pugger mixer

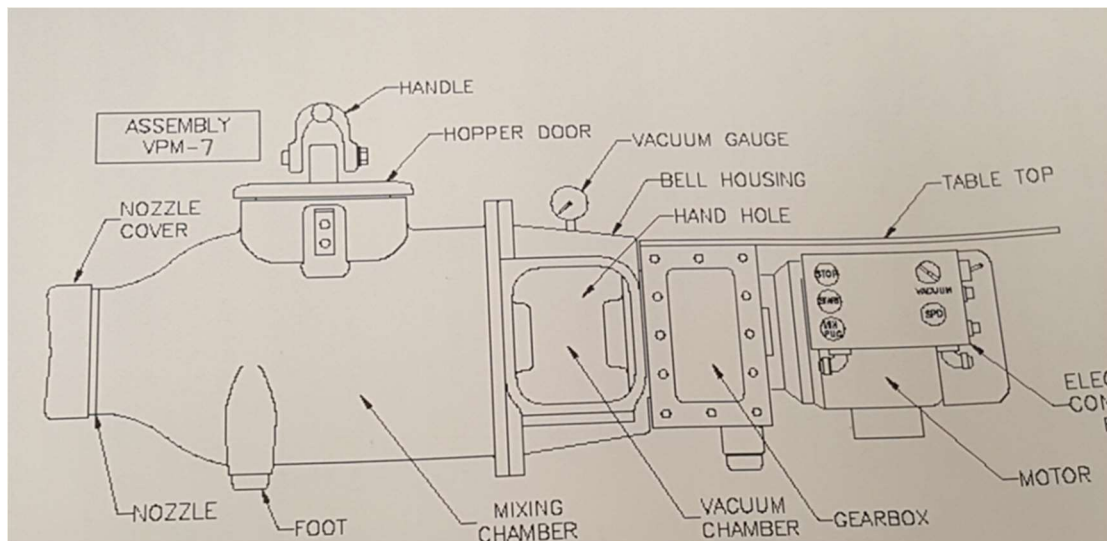


Figure B.2 Assembly of Peter pugger

B.2.3 PROCEDURE TO RUN PETER PUGGER

The step by step procedure to run Peter pugger is as follows:

1. Check all the connections, mixing chamber, and vacuum chamber first to get started.
Remove any unwanted material from the mixing chamber and the vacuum chamber.
2. The large hopper door allows to load up to 14 lb of soil mixture (mixed before loading to pugger mixer either by a machine or by hand) per batch size. To load the pug mill simply open the hopper door and begin loading the various form of the soil sample. If the sample could not be loaded at once, one can try to load it and then mix and again load it to the mixing chamber effectively.
3. Add water to make desired consistency. Place the water to the nozzle end of pug mill. These allow water adequate time to work its way through the sample as the entire batch is mixed.
4. Once the pug mill has been loaded securely the hopper door in position by using the latch provided.
5. Set the control in mix position and press start.
6. The speed control can be used to increase or decrease the speed of the mixing steel inside the mixing chamber.
7. Mix up to 5-10 minutes depending on the soil sample being processed.
8. Once the clay has been mixed, open the hopper door and check the consistency, make any final adjustment to the sample at this time.
9. Once the sample has been mixed to the desired consistency, shut the hopper door, confirm the vacuum check valve in the closed position, and turn on the vacuum for 15 to 30 sec to vacuum to stabilize.

10. With the vacuum still running in a stabilized position, press stop. Switch the control switch from mix to pug and begin pugging.

11. Allow warm de-aired log to be extruded from the pug mill.

Now you can collect the log as desired

B.2.4 CAPABILITIES

Peter pugger is the most versatile studio clay processing machine on the market today. It can perform various functions efficiently. Some of the capabilities are listed below:

- Mix moist clay from powder and water
- Reclaim Scrap-wet or dry
- Blend two or different soil components.
- Add materials (wet or dry) to an already moist body
- Adjust moisture of an already wet body

B.2.5 VACUUM PUMP TROUBLESHOOTING

Peter Pugger mixer is well equipped with a vacuum pump which is used to de-air the soil sample mixed in the mixing chamber. The vacuum pump is used when the final mixing is done and ready to pug out. As mentioned in the procedure, the vacuum pump should be in stabilize position (27 mm of Hg) before pugging out the soil sample. Sometimes, the vacuum pump does not work and remains in 0 mm of Hg, which means the vacuum pump is not de-airing the air from the soil sample. This problem could be due to the air leakage from the hopper door or the vacuum chamber. To trouble shoot this problem, clean the hopper door properly. Make sure the hopper door is free from any dry or wet soil. The lid of the hopper door should be locked tightly. Pressing the lid of the hopper door and making it tight would help in solving the air leakage problem. The

vacuum chamber door should also be clean and held tight to control the air leakage. Once the hopper door and the vacuum chamber door is cleaned and held tight the vacuum pump will start working.

B.2.6 SOIL COMPOSITION

Two soil composition was made in the pugger mixture by changing the percentage of Ottawa sand, red art clay, and commercial silt (SILCOSIL-52). The specific gravity of the Ottawa sand, red art clay, and commercial silt are 2.65, 2.84, and 2.65, respectively. Ottawa sand D_{50} was figured out as 0.37 mm (Figure B.3). Two types of soil samples were prepared for the EFA test with different proportion (% by weight) of the red art clay, silt, and Ottawa sand (Table B.1). The particle size distribution of these soil samples is presented in Figure B.4.

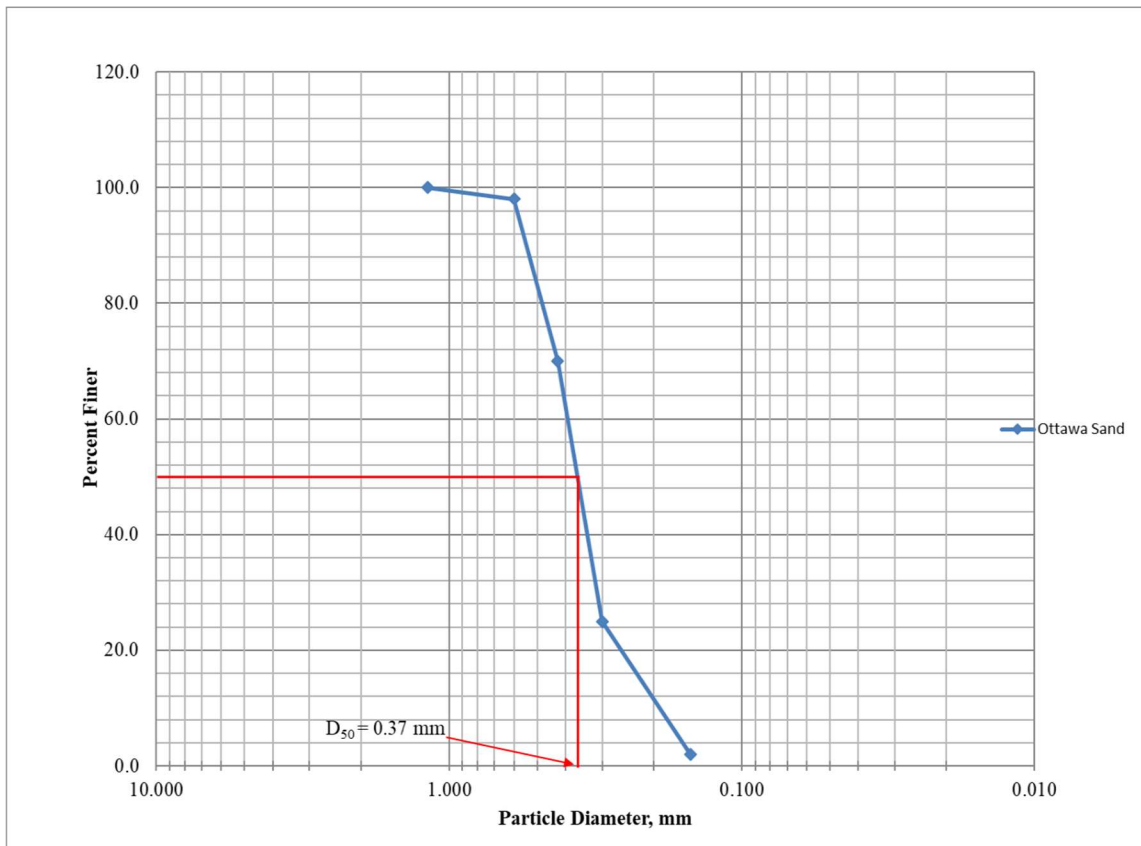


Figure B.3 Particle size distribution of Ottawa sand

Table B.1 Percentage mixture of two soil samples

Soil Index	Source mix (%)		
	Red art clay	Silt	Sand
1	20	40	40
2	30	20	50

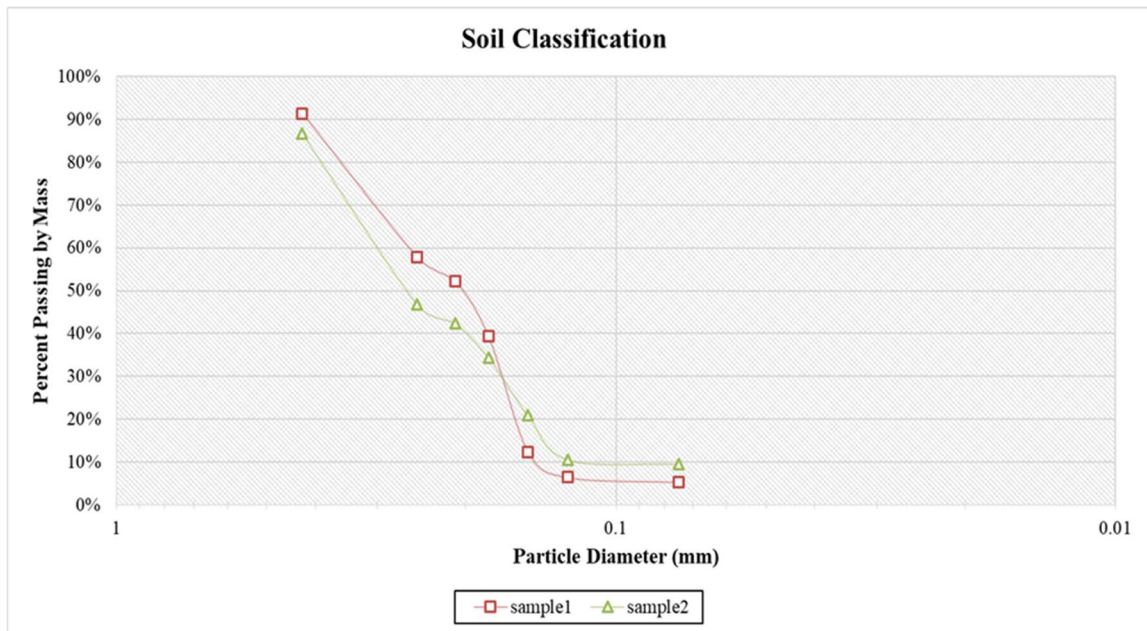


Figure B.4 Particle size distribution of two soil samples

The moisture content, density, void ratio and degree of saturation was calculated for each soil samples (Table B.2)

Table B.2 Properties of soil samples prepared by the pugger mixer

Soil Index	Measured water content (w) %	Wet density (kg/m ³)	Dry density (kg/m ³)	Void ratio (e) %	Degree of saturation (S) %
1	13.56	2058.54	1779.47	51.33	83.43
2	15.00	2017.45	1705.32	58.00	86.00

B.2.7 SAMPLE PREPARATION

The soil samples to test in EFA were prepared from the pugger mixer. The soil samples from the pugger mixer was transferred to a standard Shelby tube of outside diameter 76.2 mm by holding the Shelby tube at the mouth of the pugger mixer (Figure B.5). It needs more force to hold the Shelby tube at the mouth of the pugger as the soil pugging out from the pugger pushes the tube outside from the mouth of the pugger. FHWA's Turner-Fairbank Highway Research Center (Hydraulics Laboratory) and Genex System have proposed and fabricated a flange (pugger adapter) at the mouth of the pugger to hold the Shelby tube. A Shelby tube of 16-inch length was used in the EFA so that the piston in the EFA could push the soil sample through the Shelby tube into the EFA.



Figure B.5 Holding Shelby tube to transfer soil from pugger

B.3 EFA TEST PREPARATION

The EFA at the Auburn University (Figure B.6) is essentially same as the EFA described by Briaud et al (2001a). At first, the EFA tank was cleaned of dirt and debris and filled with a clean regular tap water. The drainage valve and sump pump help in draining the water out of the EFA tank. Clean water was continuously added to the tank to regulate the clean water and maintain the temperature of the water in the tank. Once the EFA tank has been filled with water a test can be started.



Figure B.6 Auburn University EFA

The sample prepared from the pugger mixer is installed into the EFA. A lubricant (vaseline) is applied to the piston and the Shelby tube to make inserting the sample easier over the piston. The Shelby tube is held by the clamp and is held vertically over the piston and is slowly pushed down over the piston. Once the Shelby tube is over the piston properly, it is tightened by the clamp. After the Shelby tube is placed over the piston the sample is raised by using the crank

wheel. When the sample is below the conduit opening of the EFA the soil sample is pushed upward by using the piston control on the EFA. The soil sample is pushed upward to trim it evenly. The trimming can be done with a wire or small shaw. The trimming of the soil sample should be done carefully to minimize the soil sample disturbance.

Once all this is done the sample is then raised into the opening. The sampling tube should be aligned flush with the bottom of the conduit. The screws of the crank wheel should be tightened so that the platform cannot move. After doing this, the EFA is ready to run a test. The detailed procedure to run a EFA can be found in the report “Evaluation of scour potential of cohesive soils-Phase2” (Anderson et al. 2015).

B.4 RUNNING AN EFA

At first, the desired velocity is set by using the valve to regulate the water velocity. After the velocity is set up the sample is placed in the opening and the pump is turned on. Then the soil sample was raised into the flow by 1 mm in 0.5 mm increment by the computer connected with the EFA. The test is run until 1 mm of soil is completely scoured away or up to one hour. The scour sometimes won't be homogeneous (Figure B.7) always and becomes uneven through the duration of the test. When this happens, the operator decides when the scour is complete.



Figure B.7 Uneven scour of the soil sample

The test is run with a different set of velocities. The scour rate (mm/hr) is found from the time it takes to scour 1 mm of soil. By doing the test at several velocities the scour rate vs velocity data is obtained. This data is then used to get a scour rate vs shear stress relationship, which is defined as the erosion function of the soil.

B.5 RESULTS

The computer connected with the EFA records time, average velocity, temperature, soil pushed, and elapsed time (Figure B.12). Also, the operator records the time taken for 1 mm of soil to scour by looking visually through an observation window. The data reduction was done using an excel spreadsheet. Shear stress and scour rate were calculated at different velocities and time obtained from a computer and visual observation (Table B.3)

The time recorded by the computer and the operator is used separately in the calculation of the scour rate. Soil sample 1 doesn't scour at 0.3 m/s velocity. Another velocity 0.4 m/s was set

and the test was run. There was a scour in the soil sample which means that the critical velocity lies in between 0.3 and 0.4 m/s. Several tests were performed in between 0.3 and 0.4 m/s velocity. From that, it was figured out that the erosion starts at 0.32 m/s. So, the critical velocity of soil sample 1 is 0.32 m/s. After finding the threshold velocity, two tests were done at each velocity higher than the threshold velocity. The critical shear stress for sample 1 is 0.33 Pa. The velocity and calculated shear stress were used to draw the velocity based erosion function (Figure B.8) and the shear based erosion function (Figure B.9). The average velocity and time from two set tests were taken for the calculation. There was a difference in scour rate calculated from using recorded time by computer and by the operator with the smallest difference of 0.04 mm/hr to the largest difference of 10 mm/hr.

Table B.3 Calculation of shear stress and scour rate for sample 1

Velocity (m/s)	Reynold number	friction factor (f)	Shear stress (pa)	elapsed time (computer) min	elapsed time (visual) min	Scour rate (mm/hr) (computer)	scour rate (mm/hr) (visual)
0.4	30306	0.024	0.48	38	37	1.6	1.6
0.62	46974	0.021	1.03	12	12.19	5.0	4.9
1.15	87129	0.018	3.04	4	4.12	15.0	14.6
1.5	113646	0.018	5.04	2	2	30.0	30.0
2.02	153044	0.017	8.62	1	1.2	60.0	50.0

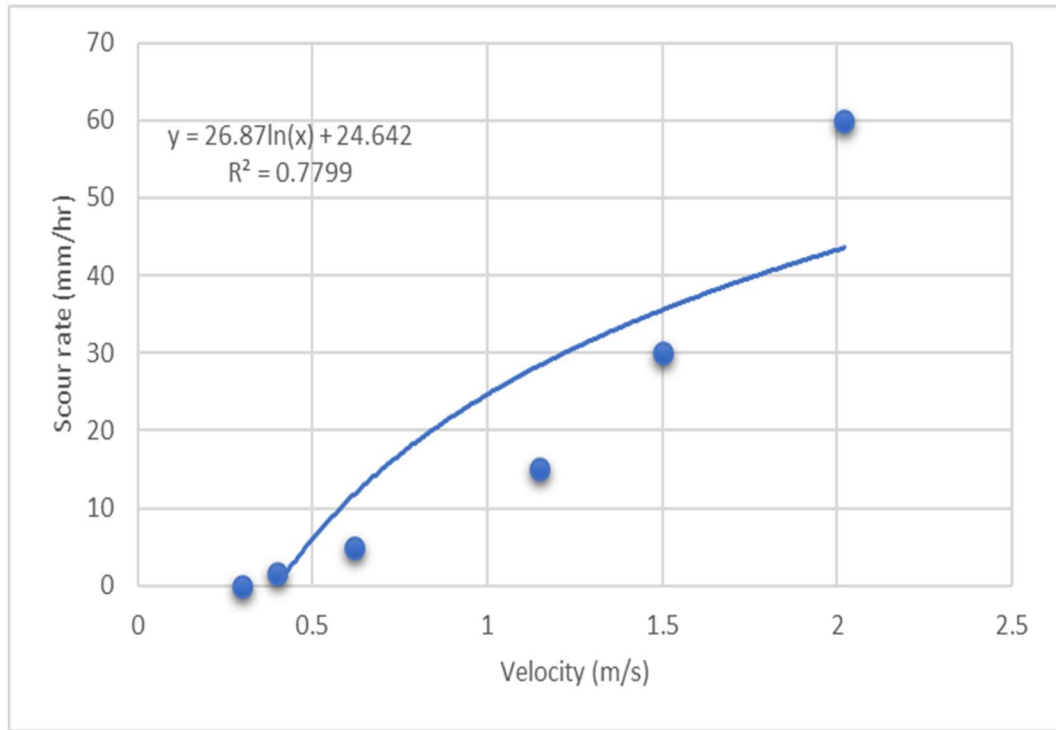


Figure B.8 Velocity-based erosion function for sample 1

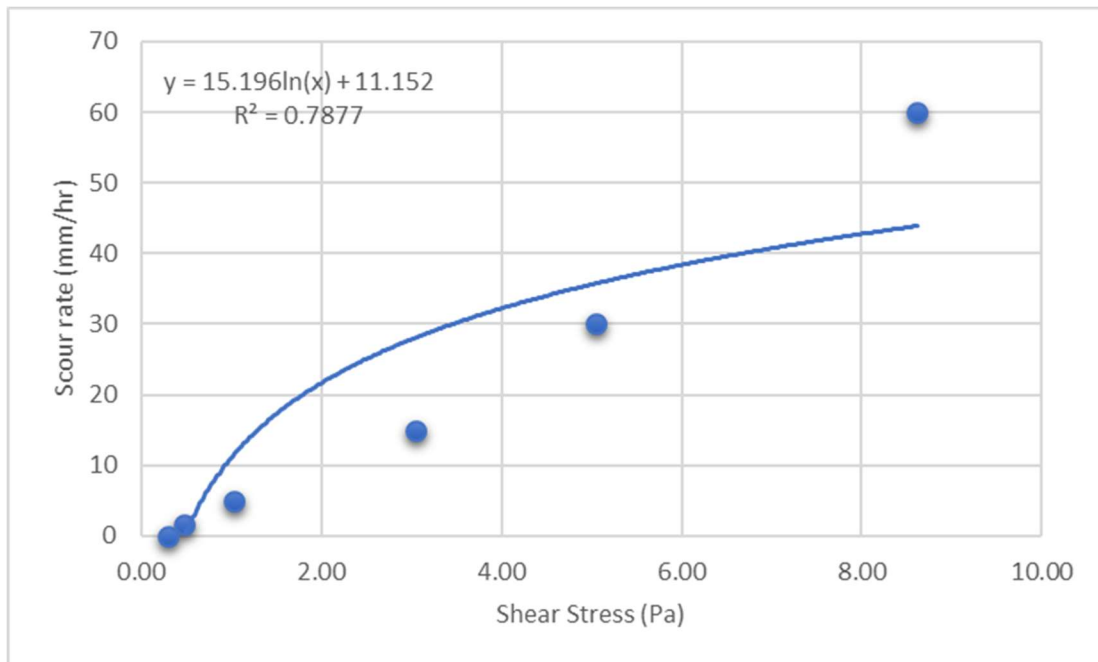


Figure B.9 Shear stress based erosion function for sample 1

Soil sample 2 test was started at 0.2 m/s velocity. There was no scour at that velocity. The velocity was increased to 0.35 m/s (average from the computer data). At this velocity scour occurred. So, it was decided to run the test in between 0.2 m/s and 0.35 m/s to find out the critical velocity. After doing several tests, the critical velocity was figured out as 0.29 m/s in average. The critical shear stress corresponding to critical velocity is 0.27 Pa. The velocity and calculated shear stress were used to draw a velocity based erosion function (Figure B.10) and shear stress erosion function (Figure B.11). The average of time and velocity was taken for calculating scour rate and shear stress (Table B.4)

The difference in scours rate calculated from observed time and recorded time in computer ranges from 0.02 to 1.75 mm/hr. The computer only records the time in an hour and minute so for the last velocity (3 m/s) it was not applicable as the scour occurred in less than a minute.

Table B.4 Calculation of shear stress and scour rate for the sample 2

Velocity (m/s)	Reynold number	friction factor (f)	Shear stress (pa)	elapsed time (computer) min	elapsed time (visual) min	Scour rate (mm/hr) (Computer)	scour rate (mm/hr) (visual)
0.35	26518	0.025	0.38	56	57	1.1	1.1
0.57	43186	0.022	0.89	6	5.96	10.0	10.1
1	75764	0.019	2.38	7	5.93	8.6	10.1
2	151529	0.016	8.26	1	1.03	60.0	58.3
3	227293	0.015	17.16	N/A	0.25	–	240.0

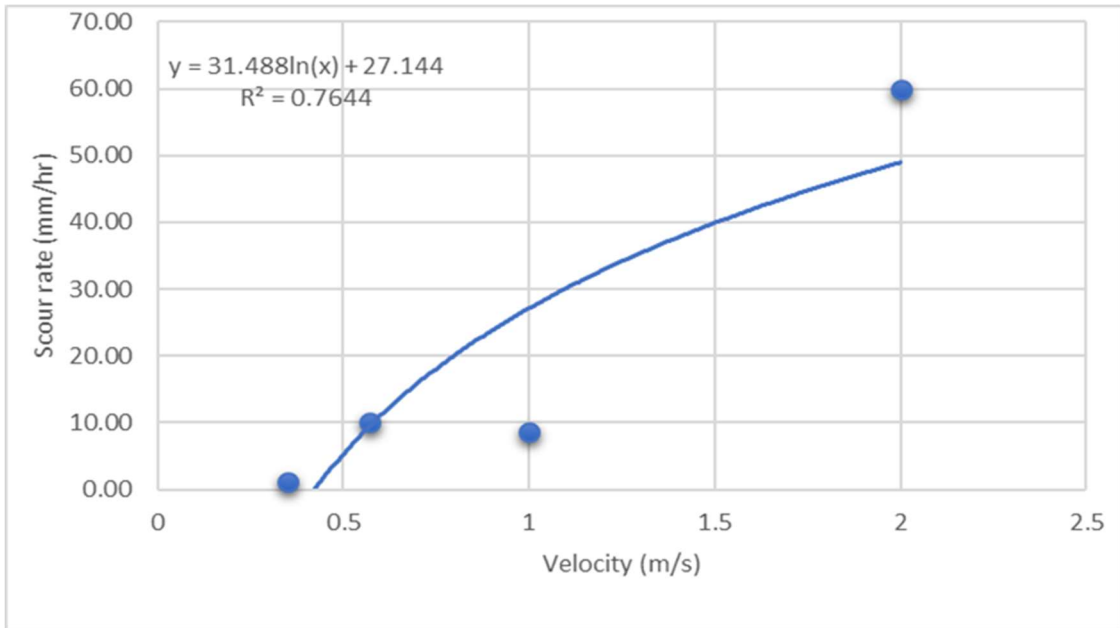


Figure B.10 Velocity based erosion function

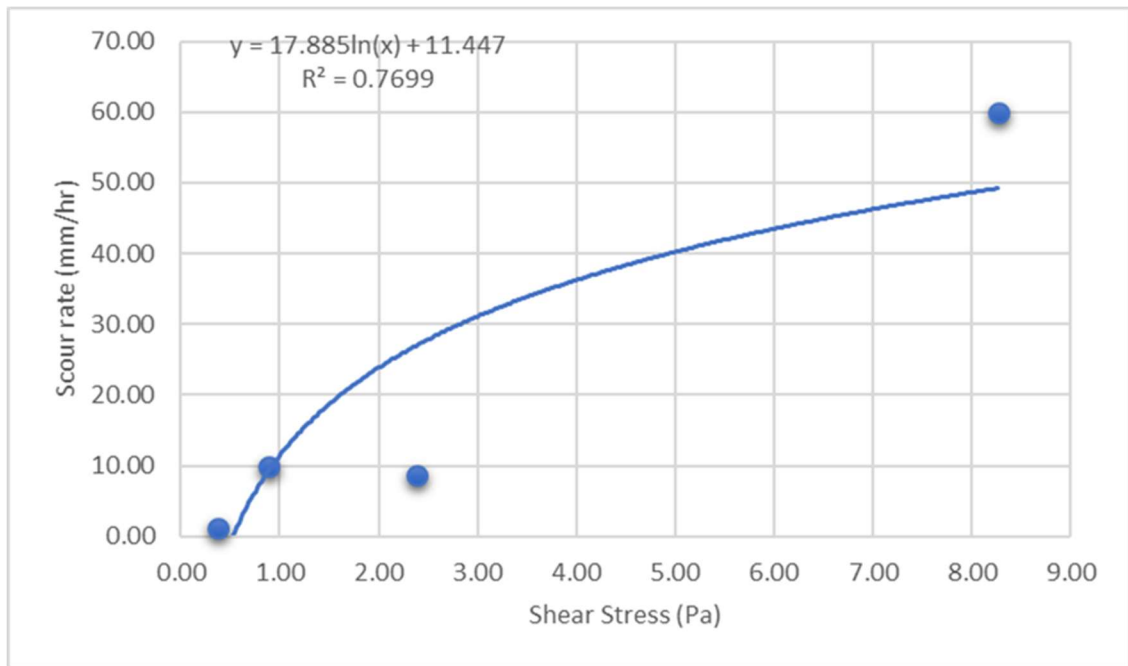


Figure B.11 Shear stress based erosion function

sampl1-0.3 - Notepad

File Edit Format View Help

wednesday, October 11, 2017 1:34 PM

SOIL PUSH: 1.0

Time	Temp	Flow
1:34 PM	80.301	0.324
1:34 PM	80.602	0.303
1:34 PM	80.000	0.320
1:34 PM	80.000	0.320
1:34 PM	80.301	0.311
1:34 PM	80.000	0.315
1:34 PM	80.301	0.320
1:34 PM	80.602	0.315
1:34 PM	80.301	0.307
1:34 PM	80.301	0.307
1:34 PM	80.602	0.307
1:34 PM	80.301	0.315
1:34 PM	80.301	0.299
1:34 PM	80.602	0.299
1:34 PM	80.602	0.320
1:34 PM	80.000	0.315
1:34 PM	80.602	0.315
1:34 PM	80.301	0.320
1:34 PM	80.000	0.324
1:34 PM	80.000	0.303
1:34 PM	80.602	0.315
1:34 PM	80.301	0.311
1:34 PM	80.000	0.315
1:34 PM	80.000	0.307
1:34 PM	80.301	0.290
1:34 PM	80.000	0.286

Figure B.12 Example of data recorded by computer during an EFA test

B.6 CRITICAL VELOCITY AND SHEAR STRESS FROM EFA AND HEC-18

The critical velocity and shear stress obtained from the EFA is compared to the HEC-18 critical velocity and shear stress as in section 3.2. The D_{50} values for the soil samples were obtained from the particle size distribution chart (Figure B.4). The D_{50} value, critical shear stress, and critical velocity obtained from the EFA test for soil samples are listed in Table B.5

Table B.5 Critical velocity and shear stress of two soil samples determined using EFA

Soil index	D_{50} (mm)	Critical velocity (m/s)	Critical shear stress (Pa)
Sample 1	0.20	0.29	0.27
Sample 2	0.27	0.32	0.33

The shear stress obtained from the EFA test was compared to the shear stress from the HEC-18 equation. In Table B.6, the critical shear stress obtained from EFA (τ_{c1}) is compared to the critical shear stress obtained from the HEC-18 (τ_{c2}) using D_{50} as input. The ratio ranges from 1.50 to 2.54 with an average of 2.02 and standard deviation of 0.52; therefore, it means for these soil samples the critical shear stress from HEC-18 is significantly smaller than the critical shear stress determined using EFA tests.

In Table B.7 the critical velocity calculated from HEC-18 and the critical velocity using τ_{c-EFA} and D_{50} are compared when the upstream water depth (y) is taken as constant equal to 4 m, which is close to the water depth in the main channel for Spear Creek under the 100-year flood (presented in Chapter 1). The critical velocity was also computed using $y = 1.5$ m that is close to the water depths in the overbank areas of Spear Creek. The ratios of the critical velocity using τ_{c-EFA} and D_{50} are 1.3 and 1.6. This means for the soil samples the critical velocities calculated from HEC-18 are significantly smaller than critical velocities calculated using τ_c of EFA and D_{50} .

Currently, ALDOT determines the scour depths under 100-year and 500-year flood event for the bridge design purpose. For example, for the bridge site in Spear Creek, the velocity at the upstream approach section (V_I) calculated using WSPRO and HEC-RAS ranges from 0.64 to 0.97 ft/s (0.19–0.29 m/s) in the overbank areas and 2.65 to 3.35 ft/s (0.81–1.02 m/s) in the main channel (from Table 5.9 presented in Chapter 4). Based on Table B.7 it would result in the live-bed scour in the main channel ($V_I > V_c$) and the clear-water scour in the overbank areas since ($V_I < V_c$) using either critical velocity. When overbank areas are heavily vegetated, only the clear-water scour is calculated using HEC-18 based on ALDOT’s practice. The particle size D_{50} has a direct impact on calculating the clear-water scour depth after the scour (Equation 1.3), i.e., proportion to $1/D_{50}^{2/7}$

Table B.6 Comparison of critical shear stress from EFA and HEC-18

Soil Type	D_{50} (mm)	Critical Shear Stress for HEC-18 (N/m^2) (τ_{c1})	EFA’s Critical Shear Stress τ_{c-EFA} (N/m^2) (τ_{c2})	Ratio (τ_{c2}/τ_{c1})
Sample 1	0.20	0.13	0.33	2.54
Sample 2	0.27	0.18	0.27	1.50

Note: critical shear stress from HEC-18: $\tau_c = k_s \gamma (s-1) D_{50}$ and $k_s = 0.039$, $S=2.72$ for sample 1 and 2.74 for sample 2.

Table B.7 Comparison of critical velocities for two soil sample from EFA and HEC-18

Soil Type	D_{50} (mm)	V_{c1} (HEC-18) Eqn. (3.5) (m/s)	V_{c2} using τ_{c-EFA} and D_{50} Eqn. (3.6) (m/s)	Ratio V_{c2}/V_{c1}
Sample 1	0.20	0.46 (0.39) ¹	0.73 (0.62)	1.6
Sample 2	0.27	0.50 (0.43)	0.63 (0.53)	1.3

Note: ¹ the water depth y in Equations (2.5) and (2.6) was assumed as 4.0 m for the comparison purpose. The critical velocity inside brackets was computed using $y = 1.5$ m.

B.7 ADVANTAGE AND LIMITATION OF EFA

EFA can be used to predict the scour depth both for cohesive and non-cohesive soil. It is a very useful tool when studying the scour characteristics of the soil. Shelby tube samples which are taken from the bridge site can be used in EFA to predict the scour depth. EFA could be used to figure out the scour of any soil at a range of velocities. The EFA test can be used to find the erosion function, critical shear stress, and the initial erodibility of a particular soil. The result from the EFA could be used to predict the scour depth that may be expected at a bridge site during any flood event. Also, EFA could be used to predict the scour depth for a soil sample taken at different depths. At different depths, soil samples may have different soil composition and would have a different scour rate. EFA could be one of the useful tools for predicting the scour rates of soils at different layers. The results from the EFA could be used within an associated scour prediction method like SRICOS-EFA (Briaud et al. 2005).

However, there was a limitation in this method too. Prior to the use of ultrasonic sensor installed in the EFA, only the operator decides the time taken for a 1 mm of soil to erode. Fine-grained soil erodes irregularly. The time could vary from one operator to another and that could change the scour rate calculation. For example, if the operator account 10 min to erode 1 mm of soil, the erosion rate would be 6 mm/hr, however, if the operator estimates 15 min to erode 1 mm of soil, the erosion rate would be 4 mm/hr. The difference in the erosion rate changes the resulting erosion plots. This limitation of EFA introduced was minimized by the use of the ultrasonic sensor designed by Seatek for Auburn University. The scan from the sensor contains time information, a distance measurement from all 16 transducers, and a voltage reading. The measured distance from the transducer would be converted finally to a volume of erosion at any given time. Also, it is very

difficult to maintain the lower velocities. The fluctuation of the velocity makes it very difficult to maintain the exact velocities.

Although, there is a use of ultrasonic sensor still the observer should observe the soil sample erosion from the observational window of the EFA to compare that with the ultrasonic sensor results. It could be very precise if an observation lenses (1 mm precise) could be added in the observational windows of the EFA so that the observer could easy visualize the scour of a soil. This could minimize the error to some extent. Also, a different velocity control mechanism could be installed so that there is less fluctuation of velocity while running an EFA test.